Electronic Supplementary Material (ESI) for ChemComm.
This journal is © The Royal Society of Chemistry 2017

Supporting Information

Selective Catalytic Synthesis of Amino-Silanes at Part-per Million Catalyst Loadings

Pablo Ríos,[a] Marta Roselló-Merino,[a] Orestes Rivada-Wheelaghan,[a] Javier Borge,[b] Joaquín López-Serrano,[a] Salvador Conejero*[a]

[a] *Instituto de Investigaciones Químicas (IIQ), Departamento de Química Inorgánica, Centro de Innovación en Química Avanzada (ORFEO-CINQA), CSIC / Universidad de Sevilla, Avda. Américo Vespucio 49, 41092 Sevilla (Spain).*

[b] *Departamento de Química Física y Analítica, Centro de Innovación en Química Avanzada (ORFEO-CINQA), Universidad de Oviedo, C/ Julián Clavería 8, 33006, Oviedo (Spain)*

* *Corresponding author: sconejero@iiq.csic.es*

Contents:

1. General. The NMR instruments were Bruker DRX-500, DRX-400 and DPX-300 spectrometers. Spectra were referenced to external $SiMe_4$ (δ 0 ppm) using the residual protio solvent peaks as internal standard (^{1}H NMR experiments) or the characteristic resonances of the solvent nuclei (^{13}C NMR experiments). ^{15}N NMR experiments were referenced against external NH_3. Spectral assignments were made by routine one- and two-dimensional NMR experiments where appropriate. Silanes were purchased from Aldrich, stored under argon and used as received. All manipulations were performed under dry, oxygen-free argon, following conventional Schlenk techniques. HR-MS spectra were recorded on a QExactive mass spectrometer with an APCI (Atmospheric Pressure Chemical Ionization) source in positive mode at the CITIUS central services of the University of Seville. Complexes $[Pt(I^tBu')(I^tBu)][BAr^F{}_4]$[1] and $[PtH(I^tBu)]_2[BAr^F{}_4]$[2] were obtained accordingly to published procedures.

H_2 evolution was measured using a Man on the Moon series X102 kit,[3] which monitors the variation of pressure and temperature of the gas phase inside a closed reaction flask.[1] The reaction flask is connected to a switchable 3-way valve via a Thorion screw through polyamide tubing. The valve can be switched between two positions, one of them connecting the reactor vessel to the exterior so that it can be used like a conventional Schlenk flask. The other position connects the flask to the pressure transducer, thus closing the system. The assembled device is depicted in Figure S1.

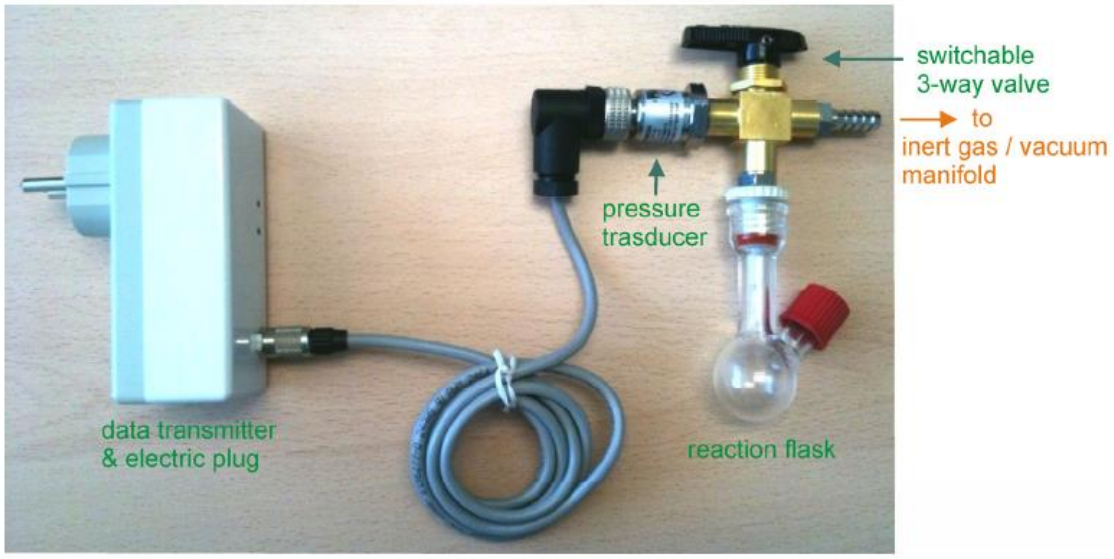

Figure S1. Man on the moon series X102 kit.

2. Synthesis and spectroscopic and analytical data for amino-silanes

2.1 Catalytic reactions leading to $RSiH_2(NR'R'')$ in a man-on-the-moon flask with ppm of complex 1a and $RSiH_3$ (R = Ph, ^{n}Bu).

In a typical procedure, a stock solution of complex **1a** (1.35 mg in 1 mL of CH_2Cl_2 or CD_2Cl_2) is prepared immediately before used. Then 10 μL of this solution (containing 9.5×10^{-6} mmol of **1a**, 0.005mol%) is placed, under argon, in a 35 mL flask containing the amount of CH_2Cl_2 (or CD_2Cl_2) required to reach a total amount of 0.25 mL of solvent. The amine (0.185 mmol) is then added and the pressure inside is allowed to stabilize. Thereafter, $PhSiH_3$ (23 μL, 0.185 mmol) or ^{n}BuSiH$_3$ (24 μL, 0.185 mmol) were injected and the pressure inside the flask measured at intervals of 1.38 s until no increase in the internal pressure is observed. Conversions and characterization of compounds were determined by ^{1}H NMR in reactions carried out in CD_2Cl_2.

2.2. Catalytic reactions leading to $RSiH(NR'R'')_2$ in a man-on-the-moon flask with complex 1a (0.2 mol%) and $RSiH_3$ (R = Ph, ^{n}Bu).

In a typical procedure, a stock solution of complex **1a** (0.52 mg, 3.7×10^{-4} mmol, in 0.25 mL of CH_2Cl_2 or CD_2Cl_2) prepared immediately before use is placed, under argon, in a 35 mL flask. The amine (0.37 mmol) is then added and the pressure inside is allowed to stabilize. Thereafter, $PhSiH_3$ (23 μL, 0.185 mmol) or ^{n}BuSiH$_3$ (24 μL, 0.185 mmol) is injected and the pressure inside the flask measured at intervals of 1.38 s. until no increase in the internal pressure is observed. Conversions and characterization of compounds were determined by ^{1}H NMR in reactions carried out in CD_2Cl_2.

2.3 Catalytic reactions leading to $PhSiH_2(NRR')$ (R = R' = ^{i}Pr; R = H, R' = Mes) and $R_2SiH(NR'R'')$ (R' = ^{t}Bu, R'' = H; R' = R'' Et; R' = R'' = $(CH_2)_4$) in a man-on-the-moon flask with complex 1a (0.1mol%) and silanes $PhSiH_3$ and R_2SiH_2 (R = Ph, Et).

In a typical procedure, 0.25 mL of a stock solution of complex **1a** (0.52 mg, 3.7×10^{-4} mmol, in 0.5 mL of CH_2Cl_2 or CD_2Cl_2) prepared immediately before use is placed, under argon, in a 35 mL flask. The amine (0.185 mmol) is then added and the pressure inside is allowed to stabilize. Thereafter, $PhSiH_3$ (23 μL, 0.185 mmol), or Ph_2SiH_2 (36 μL, 0.185 mmol), or Et_2SiH_2 (24 μL, 0.185 mmol) is injected and the pressure inside the

flask measured at intervals of 1.38 s until no increase in the internal pressure is observed. Conversions and characterization of compounds were determined by ^{1}H NMR in reactions carried out in CD_2Cl_2.

2.4. Catalytic reactions at 1 mmol scale: synthesis of monoaminosilanes $PhSiH_2(N^tBuH)$, $PhSiH_2(NEt_2)$, $PhSiH_2(NMesH)$ and $PhSiH_2[N(CH_2)_4]$ at ppm catalytic loadings.

0.75 mg (5.3 x 10^{-4} mmol) of complex **1a** are dissolved in 0.5 mL of CH_2Cl_2 under argon. Thereafter, 47 µL of this solution (containing 5 x10^{-5} mmol of **1a**, 0.005 mol%)) are diluted in 1 mL of CH_2Cl_2 in a Young tube. Then, the amine (1 mmol) and the silane (1 mmol) are added sequentially (in this order), and the reaction is stirred at r.t. until gas evolution ceased. The solvent was then evaporated to dryness and the aminosilane was extracted with pentane (4 mL) filtering with a cannula. Evaporation of the solvent led to the corresponding aminosilanes. Compounds $PhSiH_2[N(CH_2)_4]$ and $PhSiH_2(NMesH)$ proved too sensitive and have not been isolated. NMR data has been obtained from the crude reaction mixture in CD_2Cl_2 (see Figures S22-24, and S35-37).

2.5. Catalytic reactions at 1 mmol scale: synthesis of monoaminosilanes $^n BuSiH_2(N^tBuH)$, $^n BuSiH_2(NEt_2)$ and $^n BuSiH_2[N(CH_2)_4]$, at ppm catalytic loadings.

0.75 mg (5.3 x 10^{-4} mmol) of complex **1a** are dissolved in 0.5 mL of CH_2Cl_2 under argon. Thereafter, 47 µL of this solution (containing 5 x10^{-5} mmol of **1a**, 0.005 mol%) are diluted in 1 mL of CH_2Cl_2 in a Young tube. Then, the amine (1 mmol) and the silane (1 mmol) are sequentially added (in this order), and the reaction is stirred at r.t. until gas evolution ceased. Both the solvent and the product were then transferred by trap-to-trap into a young tube under high vacuum (*ca.* 5 x 10^{-4} mbar). Removal of the solvent at -25 °C led to a colorless liquid analytically pure.

We have noticed that compound $^n BuSiH_2[N(CH_2)_4]$ is unstable due to a disproportion reaction leading to $^n BuSiH_3$ and $^n BuSiH[N(CH_2)_4]_2$. This process takes place slowly in CD_2Cl_2 solutions both in the presence or absence of catalyst **1a**. Exposure to vacuum favors the formation of the diaminosilane $^n BuSiH[N(CH_2)_4]_2$ through removal of the volatile $^n BuSiH_3$. Thus, no pure $^n BuSiH_2[N(CH_2)_4]$ could be isolated, although reactions carried out in NMR tubes in CD_2Cl_2 indicated that $^n BuSiH_2[N(CH_2)_4]$ is the major product *ca.* 95%) contaminated with *ca.* 5% of $^n BuSiH\ [N(CH_2)_4]_2$.

2.6. Catalytic reactions at 1 mmol scale: synthesis of monoaminosilanes $PhSiH_2(N^iPr_2)$, $^nBuSiH_2(N^iPr_2)$, $Ph_2SiH(N^tBuH)$, $Ph_2SiH(NEt_2)$ and $Ph_2SiH[N(CH_2)_4]$, using 0.1 mol% of complex 1a.

1.4 mg (0.001 mmol) of complex **1a** are dissolved in 1.4 mL of CH_2Cl_2 under argon. Then, the amine (1 mmol) and the silane (1 mmol) are sequentially added (in this order), and the reaction is stirred at r.t. until gas evolution ceased. The solvent was then evaporated to dryness and the aminosilane was extracted with pentane (4 mL) filtering with a cannula. Evaporation of the solvent led to the corresponding aminosilanes as colorless liquids.

2.7. Catalytic reactions at 1 mmol scale: synthesis of monoaminosilanes $Et_2SiH(N^tBuH)$, $Et_2SiH(NEt_2)$ and $Et_2SiH[N(CH_2)_4]$, using 0.1 mol% of complex 1a.

1.4 mg (0.001 mmol) of complex **1a** are dissolved in 1.4 mL of CH_2Cl_2 under argon. Then, the amine (1 mmol) and the silane (1 mmol) are sequentially added (in this order), and the reaction is stirred at r.t. until gas evolution ceased. Both the solvent and the product were then transferred by trap-to-trap into a young tube under high vacuum (*ca.* 5 x 10^{-4} mbar). Removal of the solvent at -25 °C led to a colorless liquid analytically pure.

2.8. Catalytic reactions at 1 mmol scale: synthesis of diaminosilanes $PhSiH(N^tBuH)_2$, $PhSiH(NEt_2)_2$, $PhSiH[N(CH_2)_4]_2$, $^nBuSiH(N^tBuH)_2$, $^nBuSiH(NEt_2)_2$ and $^nBuSiH[N(CH_2)_4]_2$ using 0.2 mol% of complex 1a.

2.8 mg (0.002 mmol with respect to the silane) of complex **1a** are dissolved in 1.4 mL of CH_2Cl_2 under argon. Then, the amine (2 mmol) and the silane (1 mmol) are sequentially added (in this order), and the reaction is stirred at r.t. until gas evolution ceased. The solvent was then evaporated to dryness and the aminosilane was extracted with pentane (4 mL) filtering with a cannula. Evaporation of the solvent led to the corresponding aminosilanes as colorless liquids.

$PhSiH_2(NH^tBu)$. ^{1}H NMR (300 MHz, CD_2Cl_2, 298 K): δ 7.69-7.66 (m, 2H, Ph) 7.42-7.39 (m, 3H, Ph), 4.88 (d, 2H, $^3J_{HH}$ = 3.0 Hz, SiH), 1.22 (s, 9H, ^{t}Bu), 1.06 (br, 1H, NH). $^{13}C\{^1H\}$ (125 MHz, CD_2Cl_2, 298 K): δ 136.6, 135.0, 130.2, 128.3 (s, Ph), 49.8 (s, **C**Me_3), 33.1 (s, C**Me**$_3$). ^{29}Si (79 MHz, CD_2Cl_2, 298 K): δ -38.2 (t, $J_{Si,H}$ = 205 Hz).

PhSiH(NH^{t}Bu)$_2$. ^{1}H NMR (400 MHz, CD_2Cl_2, 298 K): δ 7.70-7.68 (m, 2H, Ph) 7.39-7.37 (m, 3H, Ph), 5.22 (t, 1H, $^3J_{HH}$ = 2.9 Hz, SiH), 1.26 (s, 18H, ^{t}Bu), 0.98 (br, 2H, NH). $^{13}C\{^1H\}$ (100 MHz, CD_2Cl_2, 298 K): δ 140.7, 134.5, 129.5, 128.0 (s, Ph), 49.7 (s, **C**Me_3), 33.7 (s, C**Me$_3$**). ^{29}Si (79 MHz, CD_2Cl_2, 298 K): δ -37.5 (d, $J_{Si,H}$ = 214 Hz).

PhSiH$_2$(NEt$_2$). ^{1}H NMR (300 MHz, CD_2Cl_2, 298 K): δ 7.64-7.63 (m, 2H, Ph) 7.43-7.41 (m, 3H, Ph), 4.91 (s, 2H, SiH), 2.96 (q, 4H, $^3J_{HH}$ = 7 Hz, NC**H**$_2$CH$_3$), 1.08 (t, 6H, $^3J_{HH}$ = 7 Hz, NCH$_2$C**H**$_3$). $^{13}C\{^1H\}$ (100 MHz, CD_2Cl_2, 298 K): δ 136.0, 135.0, 130.2, 128.3 (s, Ph), 42.9 (s, N**C**H$_2$CH$_3$), 15.6 (s, NCH$_2$**C**H$_3$). ^{29}Si (79 MHz, CD_2Cl_2, 298 K): δ -25.5 (t, $J_{Si,H}$ = 204 Hz).

PhSiH(NEt$_2$)$_2$. ^{1}H NMR (400 MHz, CD_2Cl_2, 298 K): δ 7.67-7.66 (m, 2H, Ph) 7.44-7.43 (m, 3H, Ph), 4.91 (s, 2H, SiH), 3.00 (q, 8H, $^3J_{HH}$ = 7 Hz, NC**H**$_2$CH$_3$), 1.10 (t, 12H, $^3J_{HH}$ = 7 Hz, NCH$_2$C**H**$_3$). $^{13}C\{^1H\}$ (100 MHz, CD_2Cl_2, 298 K): δ 138.1, 135.0, 129.7, 128.1 (s, Ph), 40.0 (s, N**C**H$_2$CH$_3$), 15.4 (s, NCH$_2$**C**H$_3$). ^{29}Si (79 MHz, CD_2Cl_2, 298 K): δ -19.5 (d, $J_{Si,H}$ = 214 Hz).

PhSiH$_2$[N(CH$_2$)$_4$]. ^{1}H NMR (300 MHz, CD_2Cl_2, 298 K): δ 7.65-7.61 (m, 2H, Ph) 7.43-7.41 (m, 3H, Ph), 4.93 (s, 2H, SiH), 3.06 (m, 4H, NC**H**$_2$CH$_2$), 1.79 (m, 4H, NCH$_2$C**H**$_2$). $^{13}C\{^1H\}$ (100 MHz, CD_2Cl_2, 298 K): δ 135.1, 130.2, 128.4 (s, Ph), 49.1 (s, N**C**H$_2$CH$_2$), 27.5 (s, NCH$_2$**C**H$_2$). ^{29}Si (79 MHz, CD_2Cl_2, 298 K): δ -29.8.

PhSiH[N(CH$_2$)$_4$]$_2$. ^{1}H NMR (300 MHz, CD_2Cl_2, 298 K): δ 7.75-7.72 (m, 2H, Ph) 7.50-7.48 (m, 3H, Ph), 5.13 (s, 2H, SiH), 3.18 (m, 8H, NC**H**$_2$CH$_2$), 1.86 (m, 8H, NCH$_2$C**H**$_2$). $^{13}C\{^1H\}$ (100 MHz, CD_2Cl_2, 298 K): δ 137.4, 134.8, 129.8, 128.2 (s, Ph), 47.5 (s, N**C**H$_2$CH$_2$), 27.2 (s, NCH$_2$**C**H$_2$). ^{29}Si (79 MHz, CD_2Cl_2, 298 K): δ -25.8 (d, $J_{Si,H}$ = 213 Hz).

PhSiH$_2$(N^{i}Pr$_2$). ^{1}H NMR (300 MHz, CD_2Cl_2, 298 K): δ 7.67-7.66 (m, 2H, Ph) 7.42-7.39 (m, 3H, Ph), 4.95 (s, 2H, SiH), 3.25 (sept, 2H, $^3J_{HH}$ = 6.8 Hz, NC**H**CH$_3$), 1.18 (d, 12H, $^3J_{HH}$ = 6.8 Hz, NCHC**H**$_3$). $^{13}C\{^1H\}$ (100 MHz, CD_2Cl_2, 298 K): δ 137.2, 135.0, 129.9, 128.3 (s, Ph), 47.9 (s, N**C**HCH$_3$), 24.5 (s, NCH**C**H$_3$). ^{29}Si (79 MHz, CD_2Cl_2, 298 K): δ -39.0.

PhSiH$_2$(NHMes). ^{1}H NMR (400 MHz, CD_2Cl_2, 298 K): δ 7.74-7.71 (m, 2 H, Ph), 7.50-7.43 (m, 3H, Ph), 6.86 (s, 2H, Mes), 5.14 (d, 2 H, $^3J_{HH}$ = 3.1 Hz, SiH), 2.94 (br, 1H, NH), 2.33 (s, 6H, Mes), 2.26 (s, 3H, Mes). $^{13}C\{^1H\}$ (100 MHz, CD_2Cl_2, 298 K): δ

140.2, 131.2, 130.3, 129.6 (Mes), 135.1, 134.3, 130.8, 128.6 (s, Ph), 20.7, 19.7 (s, Mes). ^{29}Si (79 MHz, CD_2Cl_2, 298 K): δ -31.2.

$Ph_2SiH(NH^tBu)$. ^{1}H NMR (300 MHz, CD_2Cl_2, 298 K): δ 7.68-7.66 (m, 4H, Ph) 7.42-7.40 (m, 6H, Ph), 5.48 (d, 1H, $^3J_{HH}$ = 3.3 Hz, SiH), 1.26 (s, 10H, ^{t}Bu + NH). ^{13}C{^{1}H} (125 MHz, CD_2Cl_2, 298 K): δ 137.6, 135.0, 130.0, 128.3 (s, Ph), 50.0 (s, **C**Me_3), 33.5 (s, C**Me**$_3$). ^{29}Si (79 MHz, CD_2Cl_2, 298 K): δ -24.9 (d, $J_{Si,H}$ = 205 Hz).

$Ph_2SiH(NEt_2)$. ^{1}H NMR (400 MHz, CD_2Cl_2, 298 K): δ 7.69-7.67 (m, 4H, Ph) 7.47-7.42 (m, 6H, Ph), 5.38 (s, 1H, SiH), 3.03 (q, 4H, $^3J_{HH}$ = 7 Hz, NC**H**$_2$$CH_3$), 1.10 (t, 6H, $^3J_{HH}$ = 7 Hz, NCH_2C**H**$_3$). ^{13}C{^{1}H} (100 MHz, CD_2Cl_2, 298 K): δ 136.3, 135.5, 130.1, 128.3 (s, Ph), 41.4 (s, N**C**H_2CH_3), 15.6 (s, NCH_2**C**H_3). ^{29}Si (79 MHz, CD_2Cl_2, 298 K): δ -14.8.

$Ph_2SiH[N(CH_2)_4]$. ^{1}H NMR (400 MHz, CD_2Cl_2, 298 K): δ 7.68-7.66 (m, 4H, Ph) 7.47-7.44 (m, 6H, Ph), 5.40 (s, 1H, SiH), 3.12 (m, 4H, NC**H**$_2$$CH_2$), 1.82 (m, 4H, NCH_2C**H**$_2$). ^{13}C{^{1}H} (100 MHz, CD_2Cl_2, 298 K): δ 135.9, 135.4, 130.1, 128.4 (s, Ph), 48.5 (s, N**C**H_2CH_2), 27.4 (s, NCH_2**C**H_2). ^{29}Si (79 MHz, CD_2Cl_2, 298 K): δ -17. 9 (d, $J_{Si,H}$ = 203 Hz).

^{n}BuSiH_2(NH^tBu). ^{1}H NMR (300 MHz, CD_2Cl_2, 298 K): δ 4.31 (m, 2H, SiH_2), 1.37 (m, 4H, $2CH_2$), 1.17 (s, 9H, ^{t}Bu), 0.90 (t, $^3J_{HH}$ = 7 Hz, 3H, CH_3), 0.69 (m, 2H, CH_2), 0.62 (br, 1H, NH). ^{13}C{^{1}H} (100 MHz, CD_2Cl_2, 298 K): 49.5 (s, **C**Me_3), 33.2 (s, C**Me**$_3$), 26.9, 26.6, 14.3 and 14.2 (s, ^{n}Bu). ^{29}Si (79 MHz, CD_2Cl_2, 298 K): δ -33.2 ($^1J_{Si,H}$ = 195 Hz). APCI HR-MS (+): $[M+H]^+$, *m/z* theoretical 160.1516, found 160.1515.

^{n}BuSiH(NH^tBu)$_2$. ^{1}H NMR (400 MHz, CD_2Cl_2, 298 K): δ 4.62 (m, H, SiH), 1.37 (m, 4H, $2CH_2$), 1.22 (s, 18H, ^{t}Bu), 0.92 (m, 3H, CH_3), 0.68 (br, 2H, NH), 0.55 (m, 2H, CH_2). ^{13}C{^{1}H} (100 MHz, CD_2Cl_2, 298 K): 49.7 (s, **C**Me_3), 34.0 (s, C**Me**$_3$), 27.0, 26.9, 18.1 and 14.4 (s, ^{n}Bu). ^{29}Si (79 MHz, CD_2Cl_2, 298 K): δ -30.1 (d, $^1J_{Si,H}$ = 205 Hz). All attempts to obtain spectroscopic data by APCI, FAB or ESI experiments failed due to decomposition of the sample under the experimental conditions.

^{n}BuSiH_2(NEt_2). ^{1}H NMR (300 MHz, CD_2Cl_2, 298 K): δ. 4.36 (m, 2H, SiH_2), 2.87 (q, 4H, $^3J_{HH}$ = 7 Hz, NC**H**$_2$$CH_3$), 1.41 (m, 4H, CH_2), 1.05 (t, 6H, $^3J_{HH}$ = 7 Hz, NCH_2C**H**$_3$), 0.94 (t, $^3J_{HH}$ = 6.5 Hz, 3H, CH_3), 0.73 (m, 2H, CH_2). ^{13}C{^{1}H} (100 MHz, CD_2Cl_2, 298 K): 43.2 (s, N**C**H_2CH_3), 26.9 and 26.7 (s, ^{n}Bu), 15.9 (s, NCH_2**C**H_3), 14.3 and 14.1 (s, ^{n}Bu). ^{29}Si (79 MHz, CD_2Cl_2, 298 K): δ -20.0 (t, $^1J_{Si,H}$ = 194 Hz). APCI HR-MS (+): $[M+H]^+$, *m/z* theoretical 160.1516, found 160.1516.

^{n}BuSiH(NEt$_2$)$_2$. ^{1}H NMR (300 MHz, CD_2Cl_2, 298 K): δ 4.33 (t, 1H, $^3J_{HH}$ = 2.6 Hz, SiH), 2.87 (q, 8H, $^3J_{HH}$ = 7 Hz, NC**H**$_2$CH$_3$), 1.38 (m, 4H, CH_2), 1.03 (t, 12H, $^3J_{HH}$ = 7 Hz, NCH$_2$C**H**$_3$), 0.93 (t, $^3J_{HH}$ = 7.0 Hz, 3H, CH_3), 0.67 (m, 2H, CH_2). ^{13}C{^{1}H} (100 MHz, CD_2Cl_2, 298 K): 40.6 (s, N**C**H$_2$CH$_3$), 27.0 and 26.6 (s, ^{n}Bu), 15.9 (s, NCH$_2$**C**H$_3$), 14.3 and 14.1 (s, ^{n}Bu). ^{29}Si (79 MHz, CD_2Cl_2, 298 K): δ -11.8 (d, $^1J_{Si,H}$ = 203 Hz). All attempts to obtain spectroscopic data by APCI, FAB or ESI experiments failed due to decomposition of the sample under the experimental conditions.

^{n}BuSiH$_2$[N(CH$_2$)$_4$]. ^{1}H NMR (300 MHz, CD_2Cl_2, 298 K): δ 4.32 (t, 1H, $^3J_{HH}$ = 2.8 Hz, SiH), 2.94 (m, 4H, NC**H**$_2$CH$_2$), 1.72 (m, 4H, NCH$_2$C**H**$_2$), 1.39 (m, 4H, CH_2), 0.90 (m, 3H, CH_3), 0.75 (m, 2H, CH_2). ^{13}C{^{1}H} (100 MHz, CD_2Cl_2, 298 K): δ 49.1 (s, N**C**H$_2$CH$_2$), 27.4 (s, NCH$_2$**C**H$_2$), 26.8, 26.4, 14.0 and 12.4 (s, ^{n}Bu). ^{29}Si (79 MHz, CD_2Cl_2, 298 K): δ -23.1 (t, $^1J_{Si,H}$ = 192 Hz).

^{n}BuSiH[N(CH$_2$)$_4$]$_2$. ^{1}H NMR (400 MHz, CD_2Cl_2, 298 K): δ 4.48 (br, 1H, SiH), 3.00 (m, 8H, NC**H**$_2$CH$_2$), 1.72 (m, 8H, NCH$_2$C**H**$_2$), 1.39 (m, 4H, CH_2), 0.94 (m, 3H, CH_3), 0.72 (m, 2H, CH_2). ^{13}C{^{1}H} (100 MHz, CD_2Cl_2, 298 K): δ 47.7 (s, N**C**H$_2$CH$_2$), 27.5 (s, NCH$_2$**C**H$_2$), 27.0, 26.5, 14.4 and 13.8 (s, ^{n}Bu). ^{29}Si (79 MHz, CD_2Cl_2, 298 K): δ -17.9 (d, $^1J_{Si,H}$ = 203 Hz). All attempts to obtain spectroscopic data by APCI, FAB or ESI experiments failed due to decomposition of the sample under the experimental conditions.

^{n}BuSiH$_2$(N^{i}Pr$_2$). ^{1}H NMR (400 MHz, CD_2Cl_2, 298 K): δ 4.37 (t, 2H, $^3J_{HH}$ = 2.5 Hz, SiH_2), 3.17 (sept, 2H, $^3J_{HH}$ = 6.6 Hz, NC**H**(CH$_3$)$_2$), 1.39 (m, 4H, CH_2), 1.13 (d, 12H, $^3J_{HH}$ = 6.6 Hz, NCH(C**H**$_3$)$_2$), 0.93 (t, 3H, $^3J_{HH}$ = 7.0 Hz, CH_3), 0.69 (m, 2H, CH_2). ^{13}C{^{1}H} (100 MHz, CD_2Cl_2, 298 K): δ 47.9 (s, N**C**H(CH$_3$)$_2$), 27.5 (s, NCH$_2$**C**H$_2$), 26.8 and 26.6 (s, ^{n}Bu), 24.7 (s, NCH(**C**H$_3$)$_2$), 15.4 and 14.3 (s, ^{n}Bu) . ^{29}Si (79 MHz, CD_2Cl_2, 298 K): δ -33.2 (d, $^1J_{Si,H}$ = 196 Hz). APCI HR-MS (+): $[M+H]^+$, *m/z* theoretical 188.1831, found 188.1829.

Et$_2$SiH(NEt$_2$). ^{1}H NMR (400 MHz, CD_2Cl_2, 298 K): δ. 4.19 (m, 1H, SiH), 2.87 (q, 4H, $^3J_{HH}$ = 7 Hz, NC**H**$_2$CH$_3$), 1.03 (t, 6H, $^3J_{HH}$ = 7.0 Hz, NCH$_2$C**H**$_3$), 1.00 (t, 6H, $^3J_{HH}$ = 8.0 Hz, SiCH$_2$C**H**$_3$), 0.63 (t, 4H, $^3J_{HH}$ = 7.2 Hz, SiC**H**$_2$CH$_3$). ^{13}C{^{1}H} (100 MHz, CD_2Cl_2, 298 K): 41.9 (s, N**C**H$_2$CH$_3$), 16.1 (s, NCH$_2$**C**H$_3$), 8.0 (s, Si**C**H$_2$CH$_3$), 6.2 (s, SiCH$_2$**C**H$_3$). ^{29}Si (79 MHz, CD_2Cl_2, 298 K): δ 3.0 (d, $^1J_{Si,H}$ = 204 Hz). APCI HR-MS (+): $[M+H]^+$, *m/z* theoretical 160.1516, found 160.1517.

$Et_2SiH(NH^tBu)$. ^1H NMR (400 MHz, CD_2Cl_2, 298 K): δ. 4.32 (m, 1H, SiH), 1.19 (s, 9H, ^{t}Bu), 0.99 (t, 6H, $^3J_{HH}$ = 8.1 Hz, $SiCH_2C\underline{\mathbf{H}}_3$), 0.59 (t, 4H, $^3J_{HH}$ = 8.1 Hz, $SiC\underline{\mathbf{H}}_2CH_3$). $^{13}C\{^1H\}$ (100 MHz, CD_2Cl_2, 298 K): 49.5 (s, $\underline{\mathbf{C}}Me_3$), 33.8 (s, $C\underline{\mathbf{Me}}_3$), 7.8 (s, $Si\underline{\mathbf{C}}H_2CH_3$), 7.1 (s, $SiCH_2\underline{\mathbf{C}}H_3$). ^{29}Si (79 MHz, CD_2Cl_2, 298 K): δ -8.9 (t, $^1J_{Si,H}$ = 189 Hz). APCI HR-MS (+): $[M+H]^+$, *m/z* theoretical 160.1516, found 160.1517.

$Et_2SiH[N(CH_2)_4]$. ^1H NMR (400 MHz, CD_2Cl_2, 298 K): δ. 4.24 (quint, 1H, $^3J_{HH}$ = 2.5 Hz, SiH), 2.98 (m, 4H, $NC\underline{\mathbf{H}}_2CH_2$), 1.72 (m, 4H, $NCH_2C\underline{\mathbf{H}}_2$), 1.00 (t, 6H, $^3J_{HH}$ = 8.0 Hz, $SiCH_2C\underline{\mathbf{H}}_3$), 0.66 (m, 4H, $SiC\underline{\mathbf{H}}_2CH_3$). $^{13}C\{^1H\}$ (100 MHz, CD_2Cl_2, 298 K): 48.4 (s, $N\underline{\mathbf{C}}H_2CH_2$), 27.4 (s, $NCH_2\underline{\mathbf{C}}H_2$), 7.9 (s, $Si\underline{\mathbf{C}}H_2CH_3$), 5.2 (s, $SiCH_2\underline{\mathbf{C}}H_3$). ^{29}Si (79 MHz, CD_2Cl_2, 298 K): δ -1.1 (t, $^1J_{Si,H}$ = 188 Hz). APCI HR-MS (+): $[M+H]^+$, *m/z* theoretical 158.1360, found 158.1361.

$PhSiH_2(NH^tBu)$

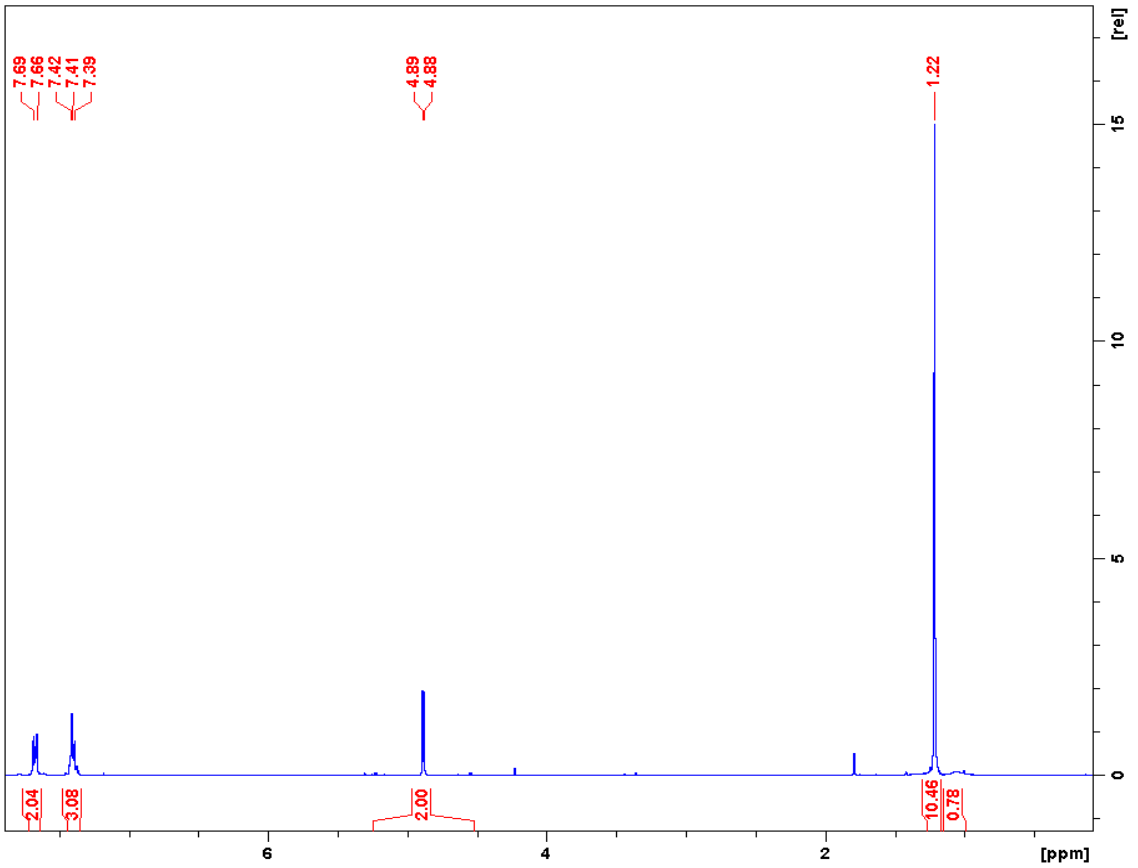

Figure S2. ^1H NMR (300 MHz) of $PhSiH_2(NH^tBu)$ in CD_2Cl_2.

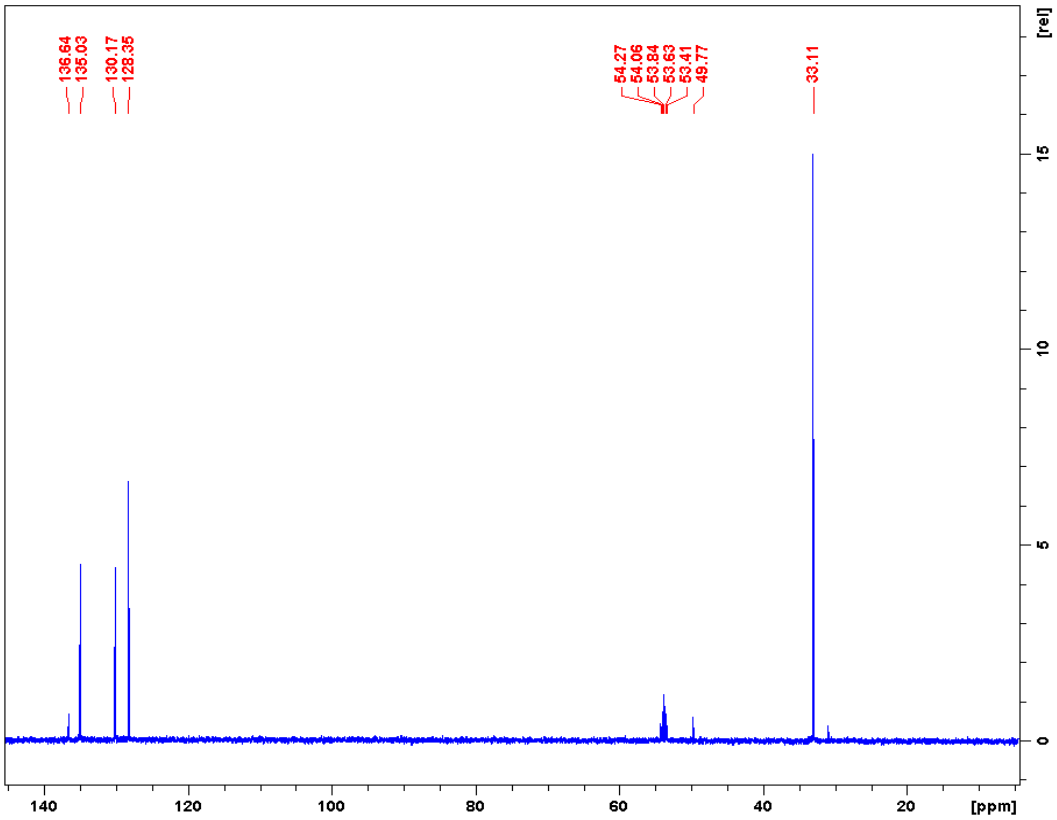

Figure S3. $^{13}C\{^{1}H\}$ NMR (125 MHz) of $PhSiH_2(NH^tBu)$ in CD_2Cl_2.

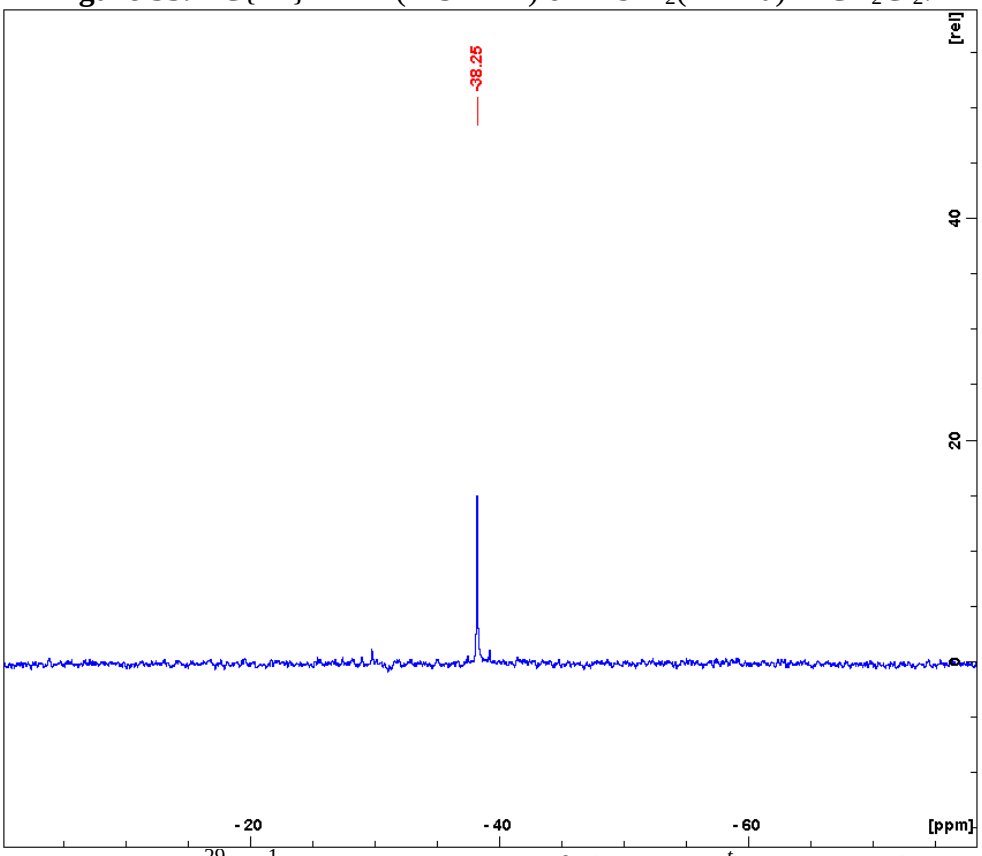

Figure S4. $^{29}Si\{^{1}H\}$ NMR (79 MHz) of $PhSiH_2(NH^tBu)$ in CD_2Cl_2.

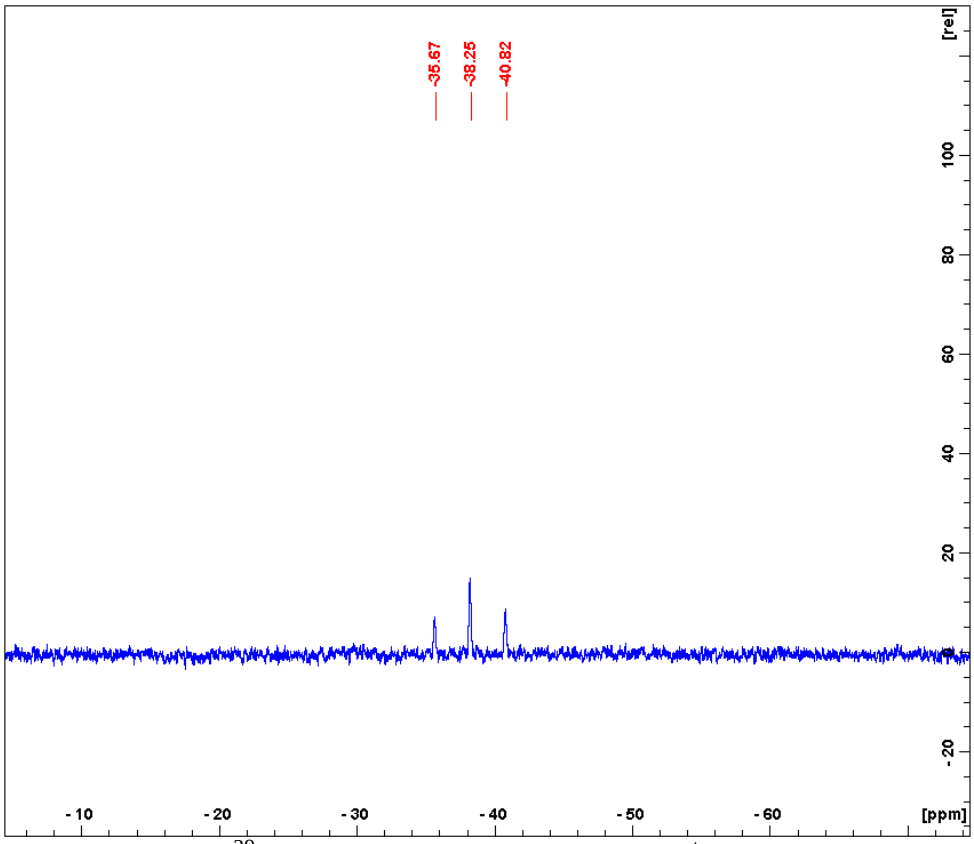

Figure S5. ^{29}Si NMR (79 MHz) of $PhSiH_2(NH^tBu)$ in CD_2Cl_2.

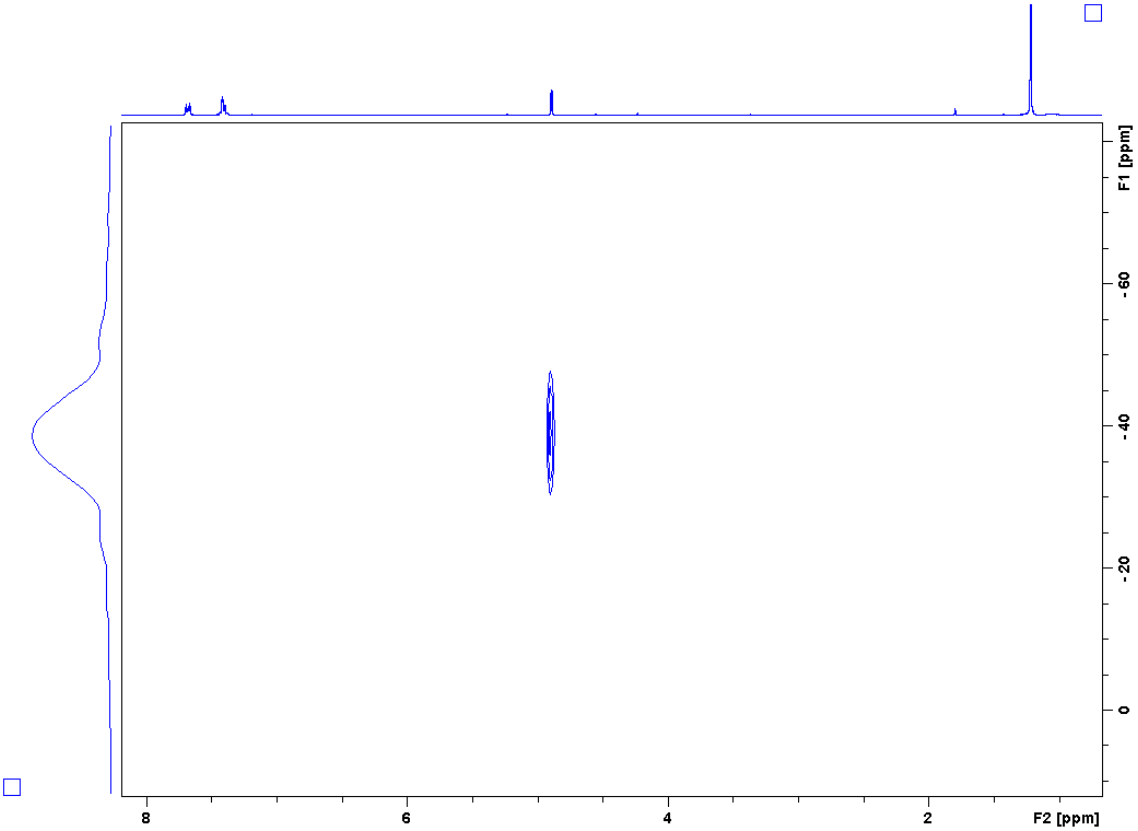

Figure S6. ^{1}H- ^{29}Si HMQC NMR of $PhSiH_2(NH^tBu)$ in CD_2Cl_2.

PhSiH(NH^{t}Bu)$_2$

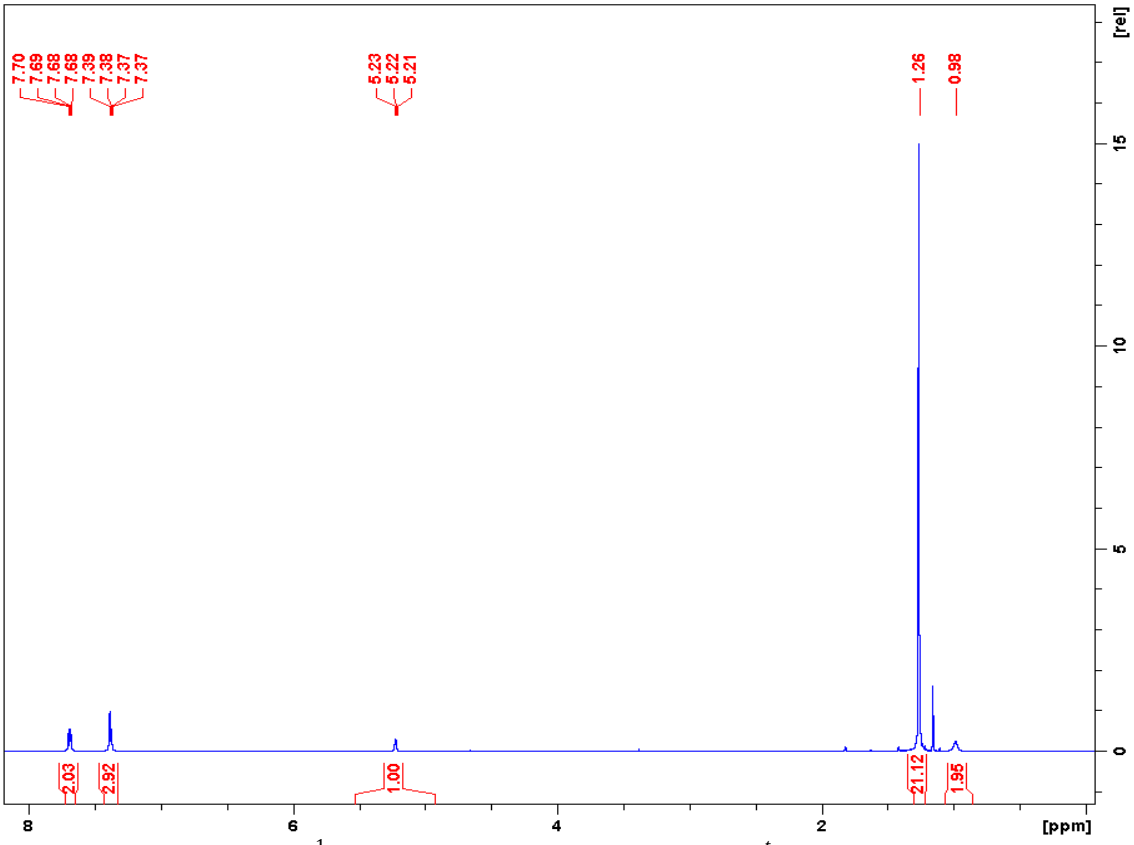

Figure S7. ^{1}H NMR (400 MHz) of PhSiH(NH^{t}Bu)$_2$ in CD_2Cl_2.

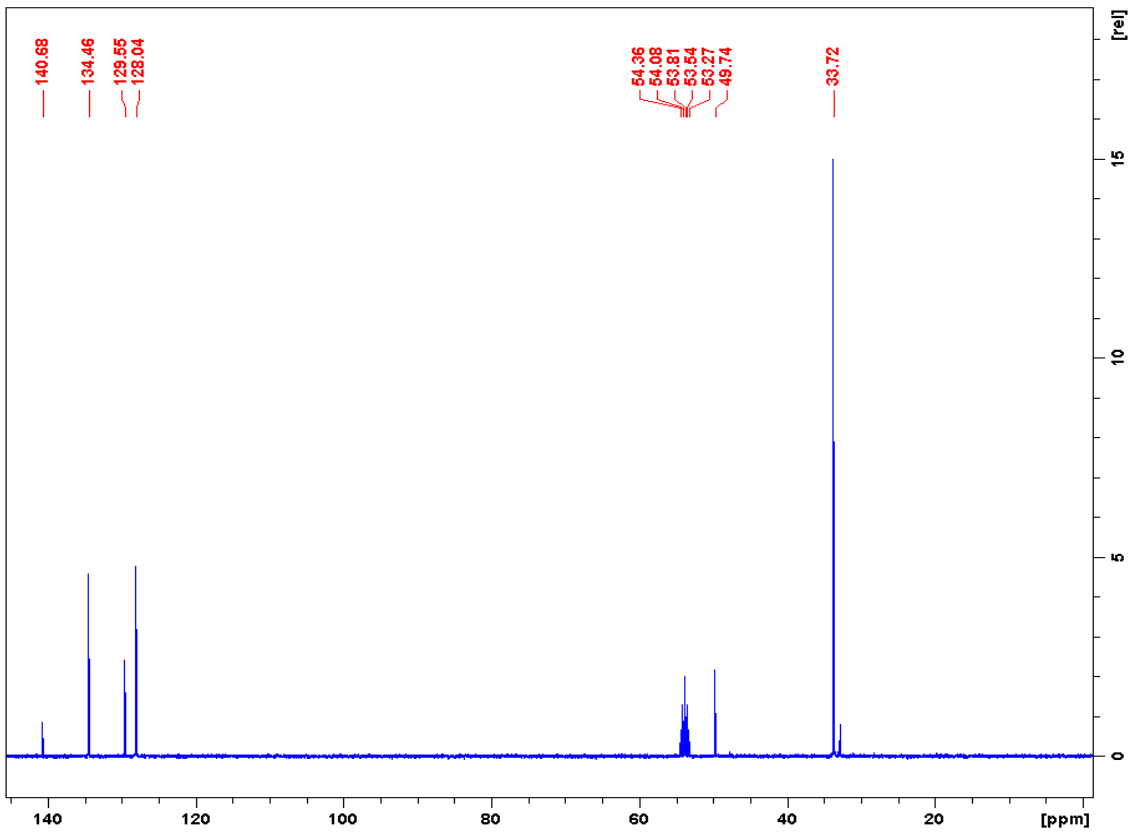

Figure S8. ^{13}C{^{1}H} NMR (100 MHz) of PhSiH(NH^{t}Bu)$_2$ in CD_2Cl_2.

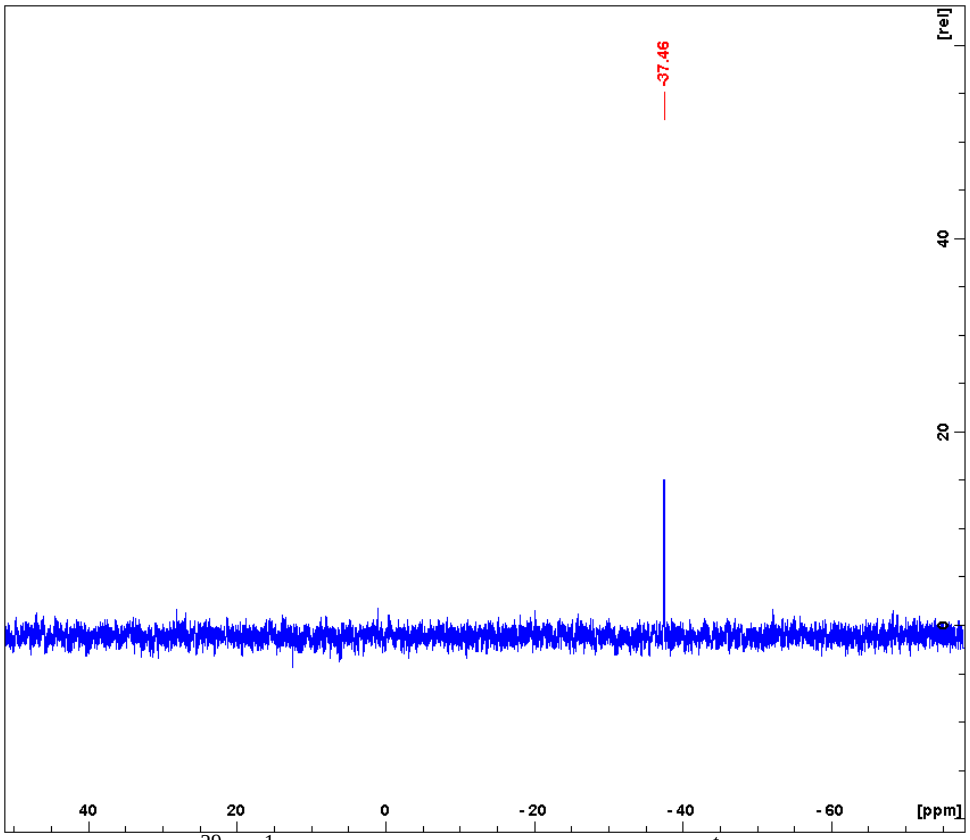

Figure S9. $^{29}Si\{^{1}H\}$ NMR (79 MHz) of $PhSiH(NH^{t}Bu)_2$ in CD_2Cl_2.

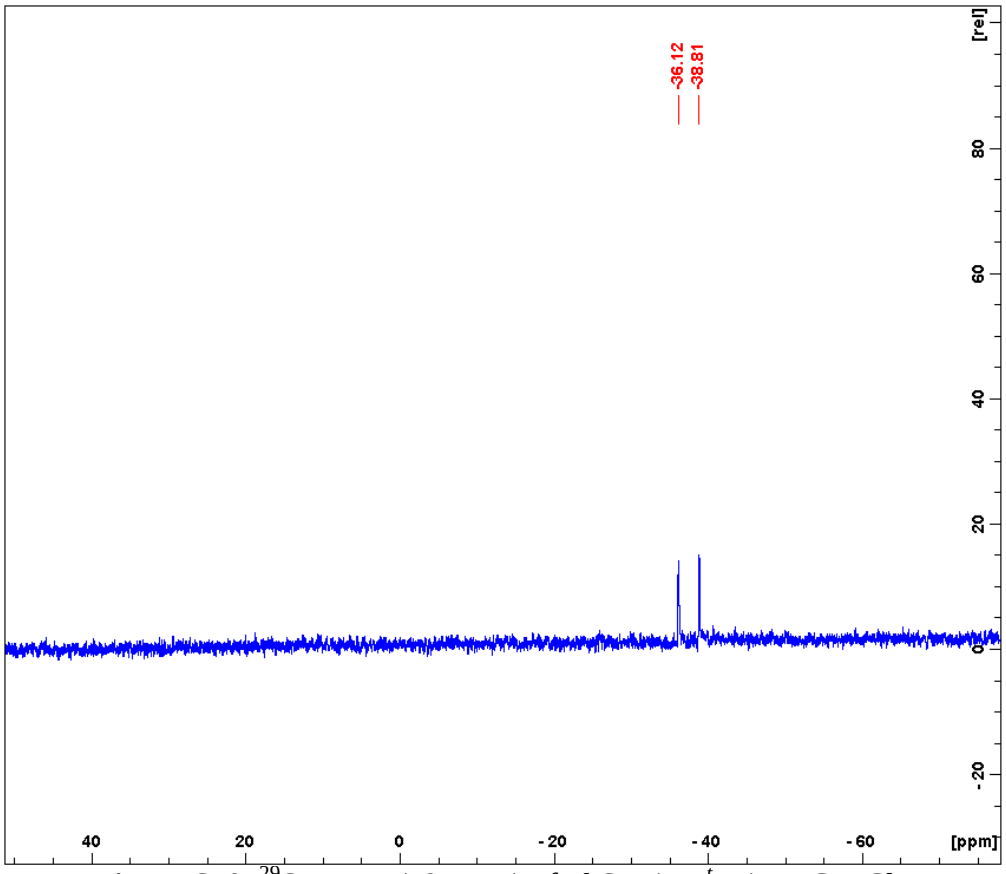

Figure S10. ^{29}Si NMR (79 MHz) of $PhSiH(NH^{t}Bu)_2$ in CD_2Cl_2.

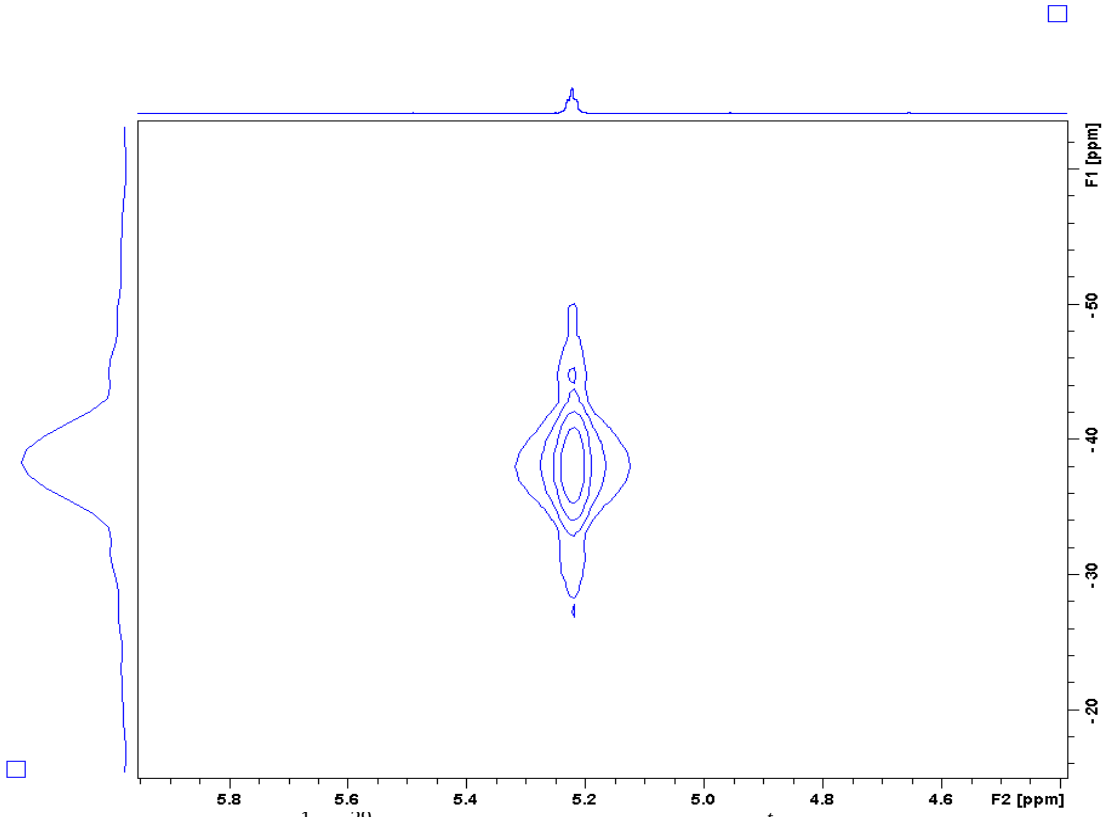

Figure S11. ^{1}H-^{29}Si HMQC NMR of PhSiH(NH^{t}Bu)$_2$ in CD_2Cl_2.

PhSiH$_2$(NEt$_2$)

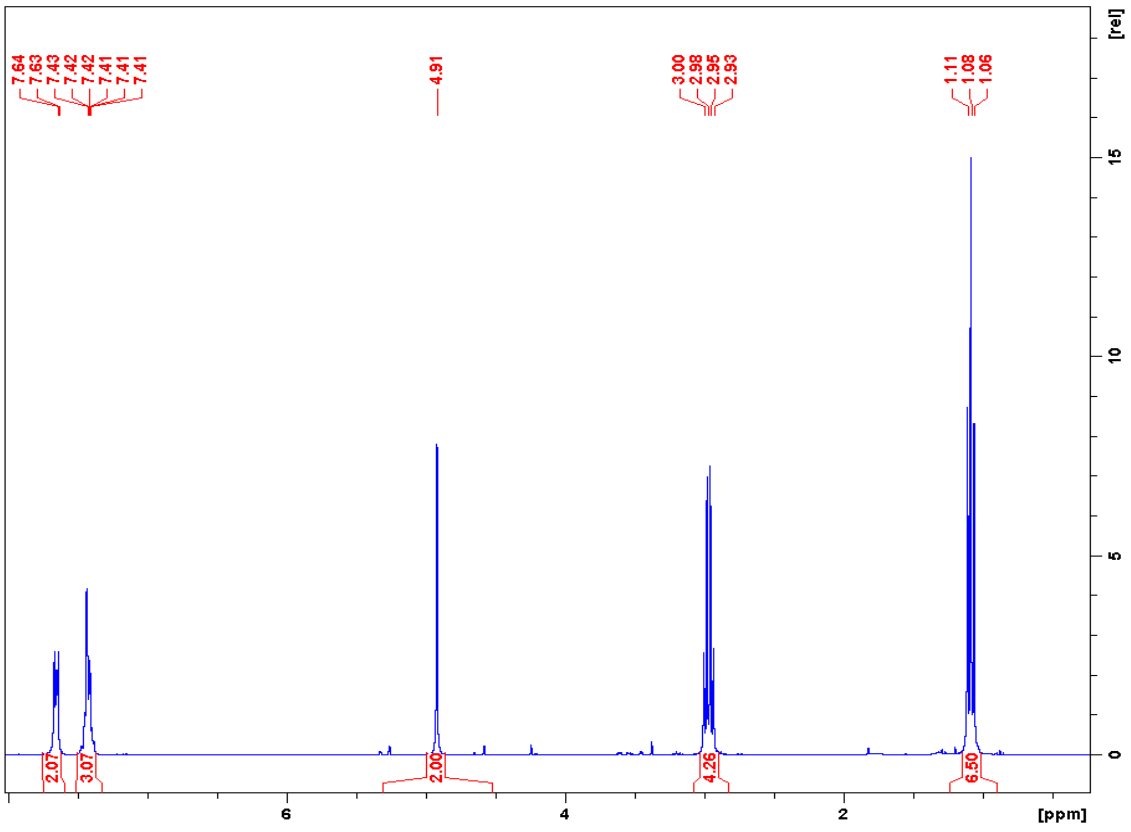

Figure S12. ^{1}H NMR (300 MHz) of PhSiH$_2$(NEt$_2$) in CD_2Cl_2.

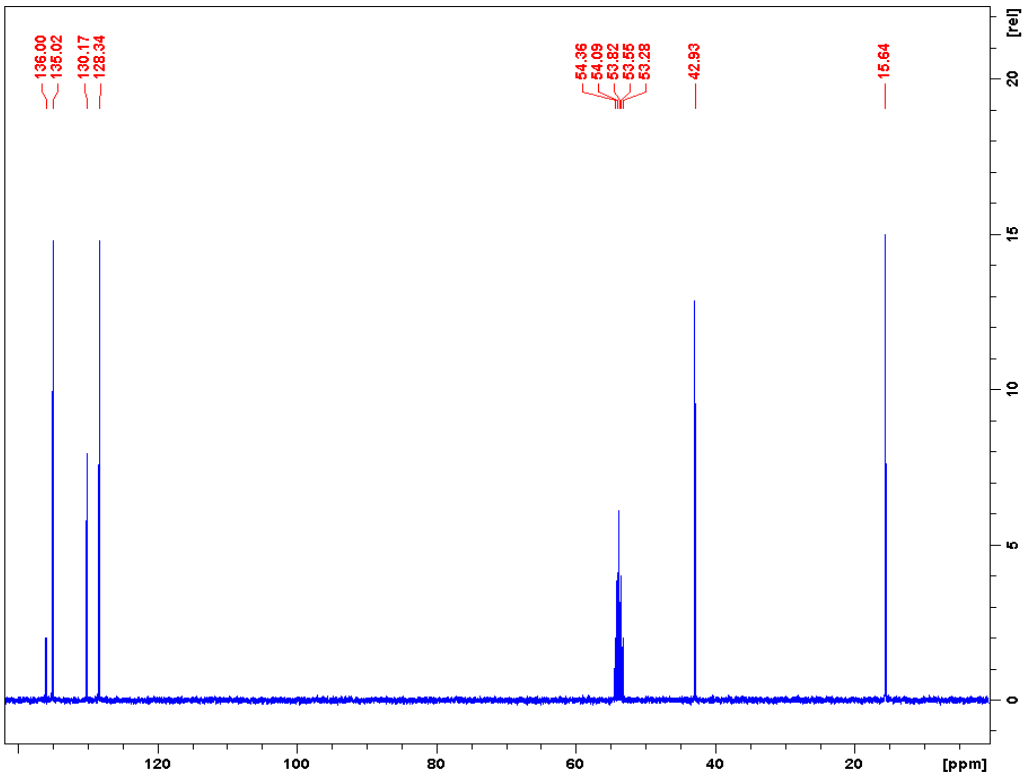

Figure S13. $^{13}C\{^{1}H\}$ NMR (100 MHz) of $PhSiH_2(NEt_2)$ in CD_2Cl_2.

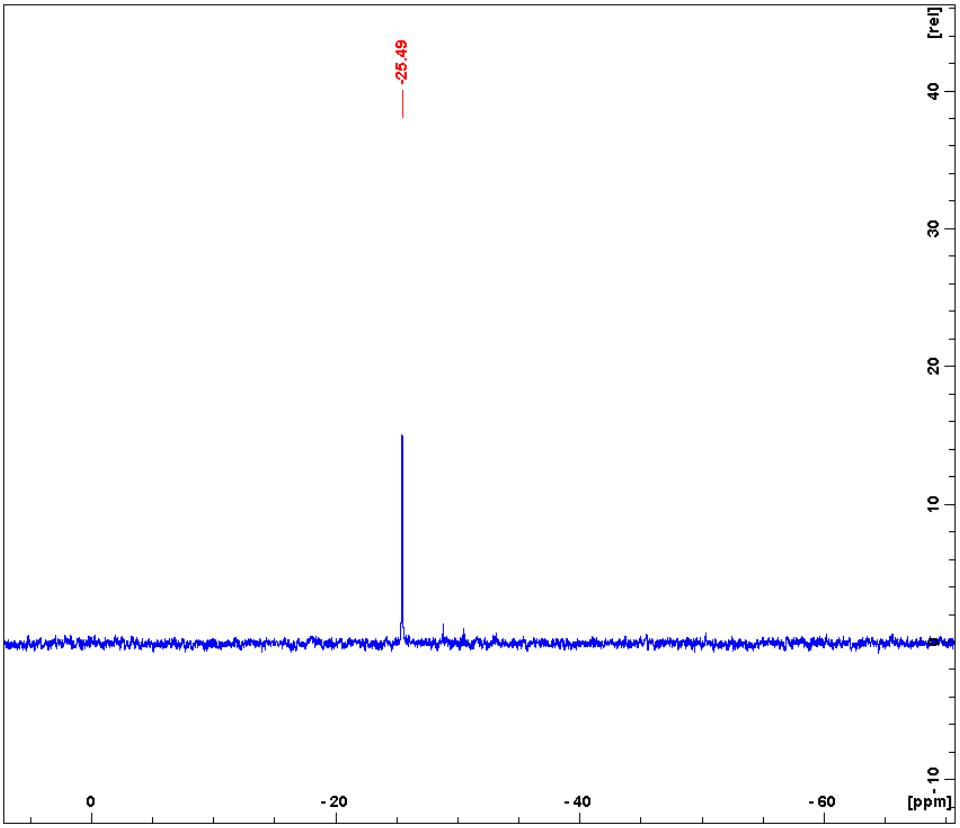

Figure S14. $^{29}Si\{^{1}H\}$ NMR (79 MHz) of $PhSiH_2(NEt_2)$ in CD_2Cl_2.

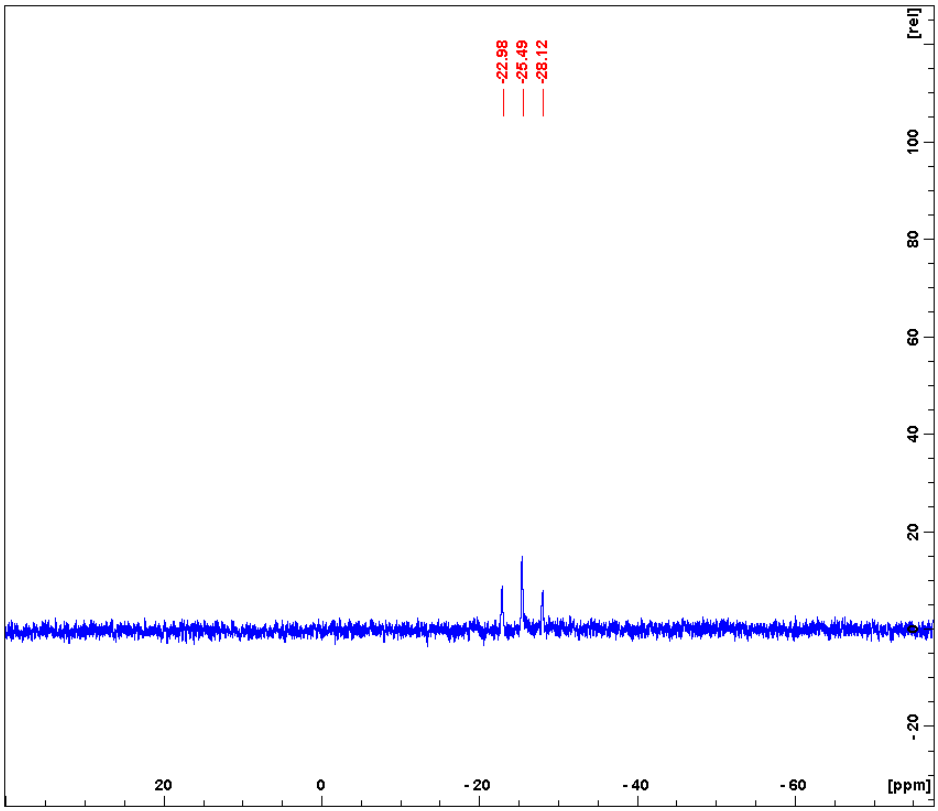

Figure S15. ^{29}Si NMR (79 MHz) of $PhSiH_2(NEt_2)$ in CD_2Cl_2.

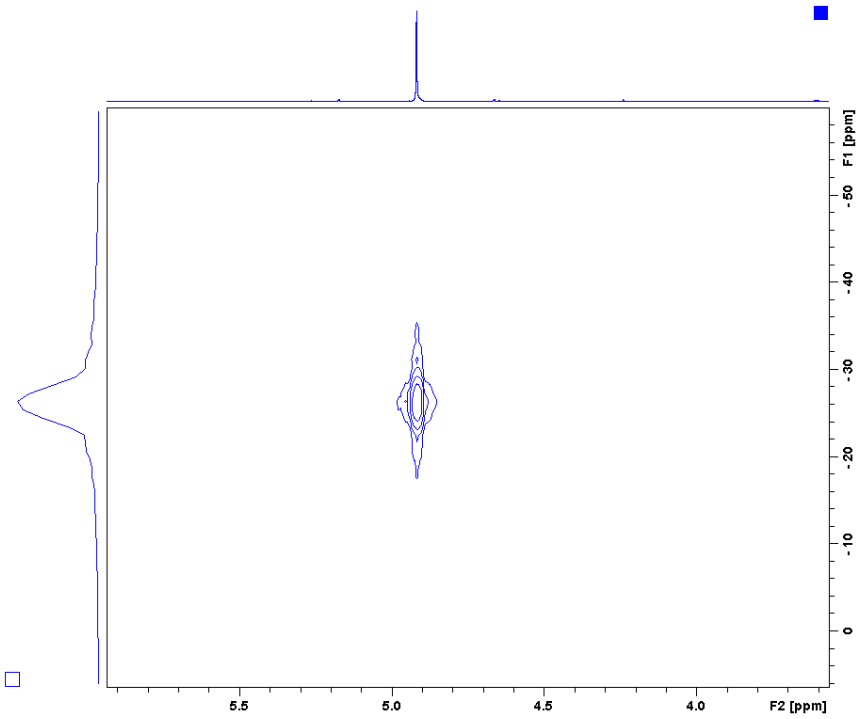

Figure S16. ^{1}H-^{29}Si HMQC NMR of $PhSiH_2(NEt_2)$ in CD_2Cl_2.

PhSiH(NEt$_2$)$_2$

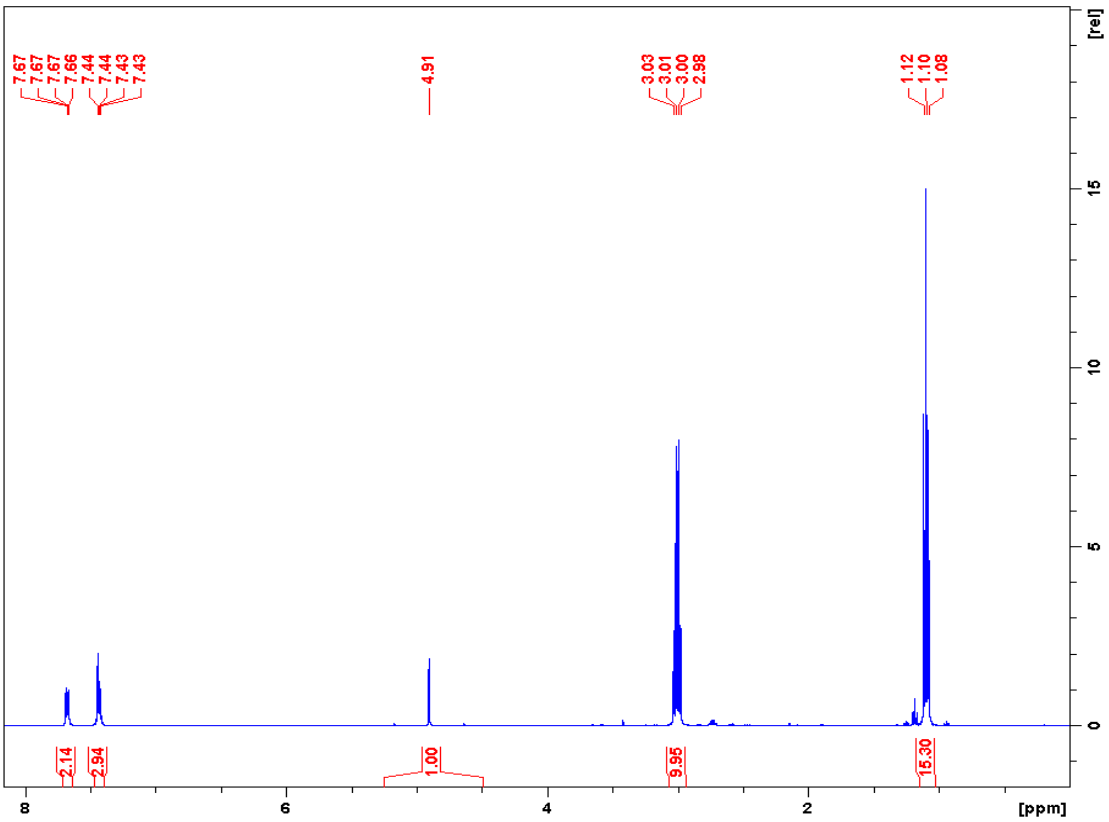

Figure S17. ^{1}H NMR (400 MHz) of PhSiH(NEt$_2$)$_2$ in CD_2Cl_2.

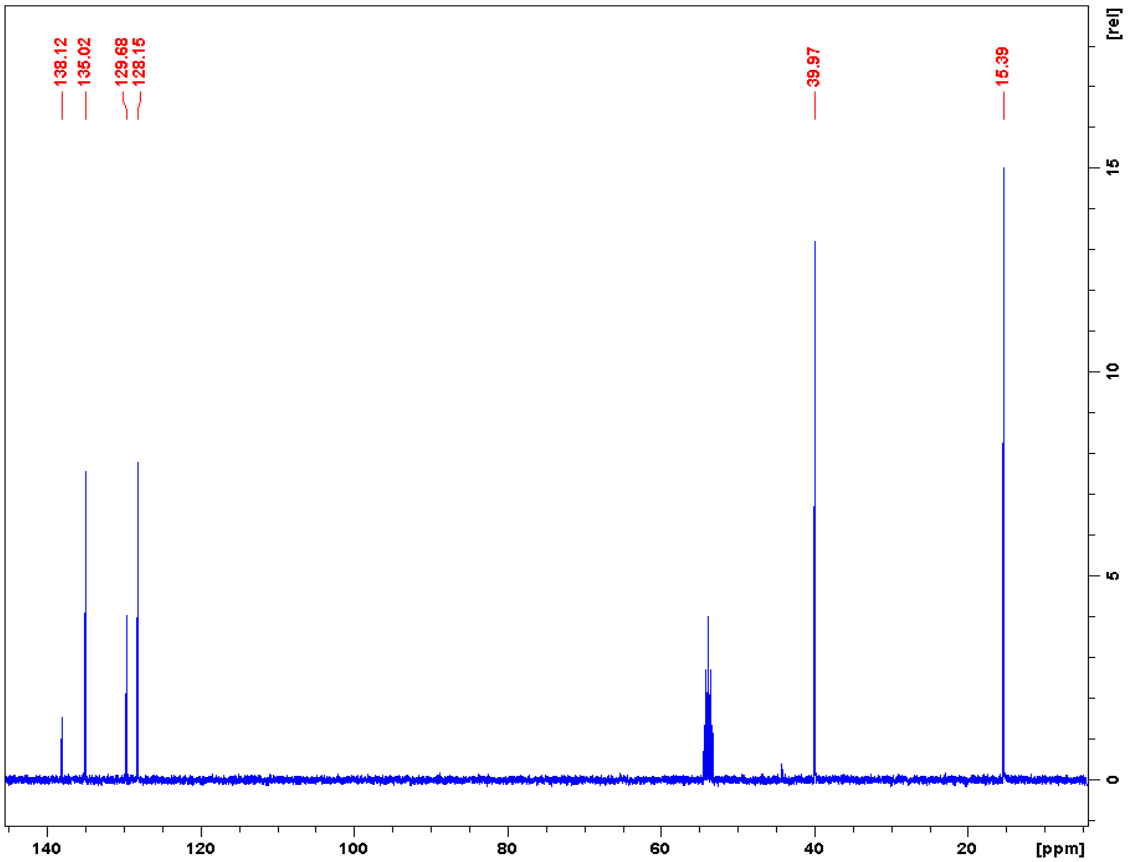

Figure S18. ^{13}C{^{1}H} NMR (100 MHz) of PhSiH(NEt$_2$)$_2$ in CD_2Cl_2.

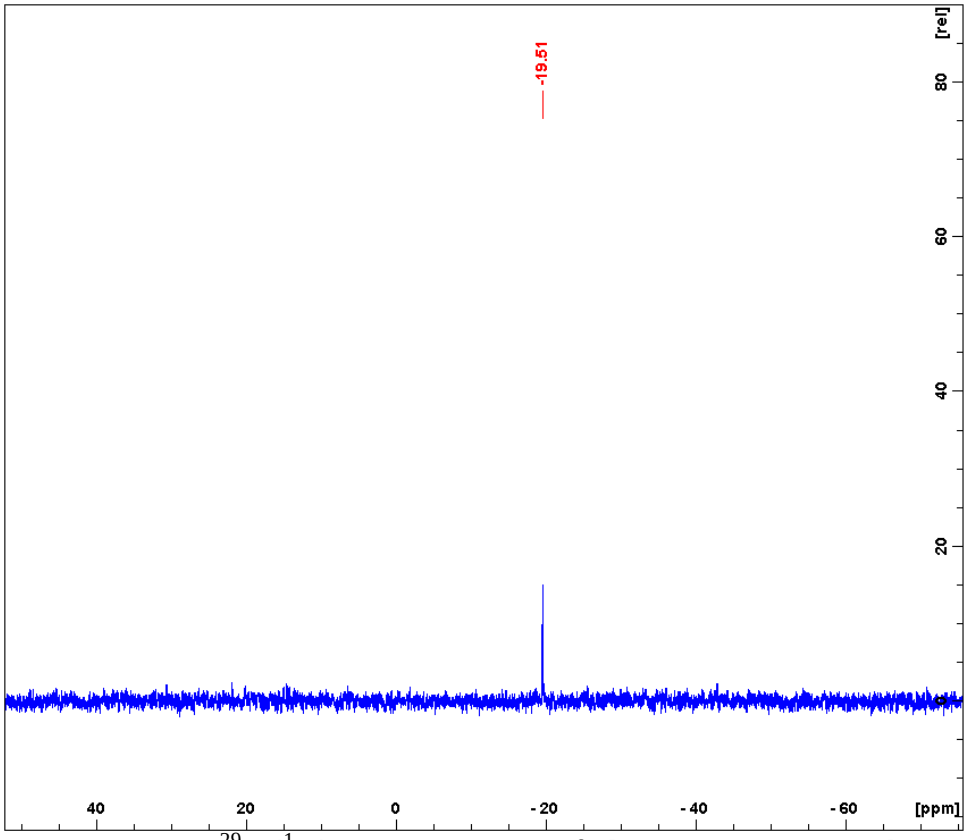

Figure S19. $^{29}Si\{^{1}H\}$ NMR (79 MHz) of $PhSiH(NEt_2)_2$ in CD_2Cl_2.

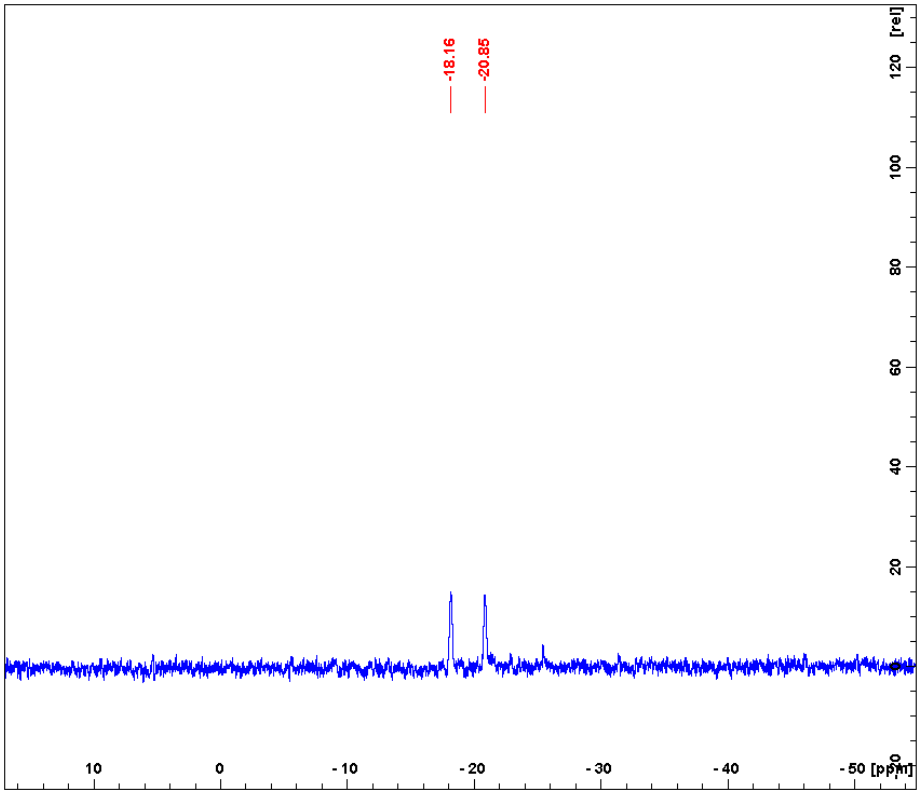

Figure S20. ^{29}Si NMR (79 MHz) of $PhSiH(NEt_2)_2$ in CD_2Cl_2.

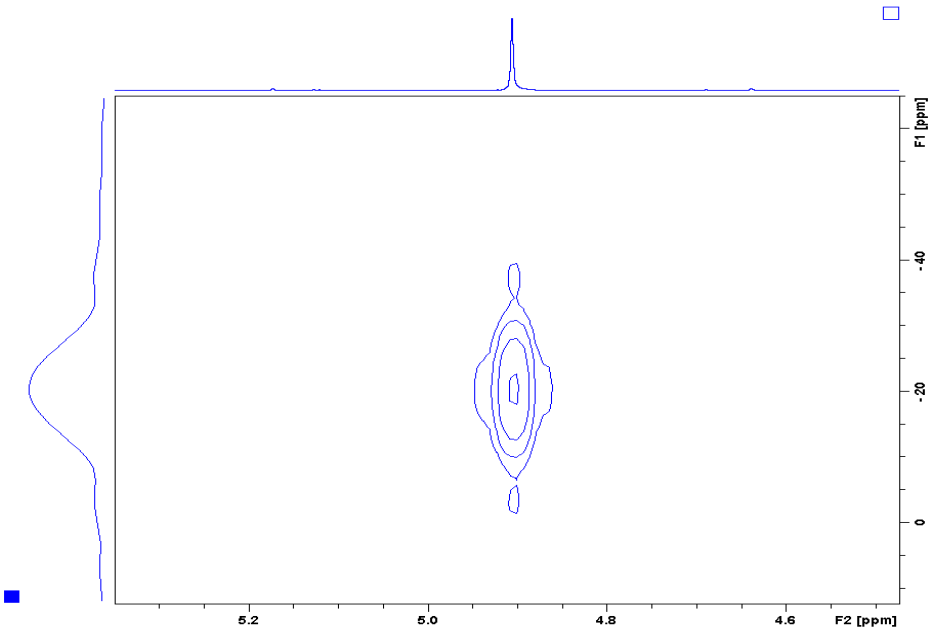

Figure S21. ^{1}H- ^{29}Si HMQC NMR of $PhSiH(NEt_2)_2$ in CD_2Cl_2.

$PhSiH_2[N(CH_2)_4]$

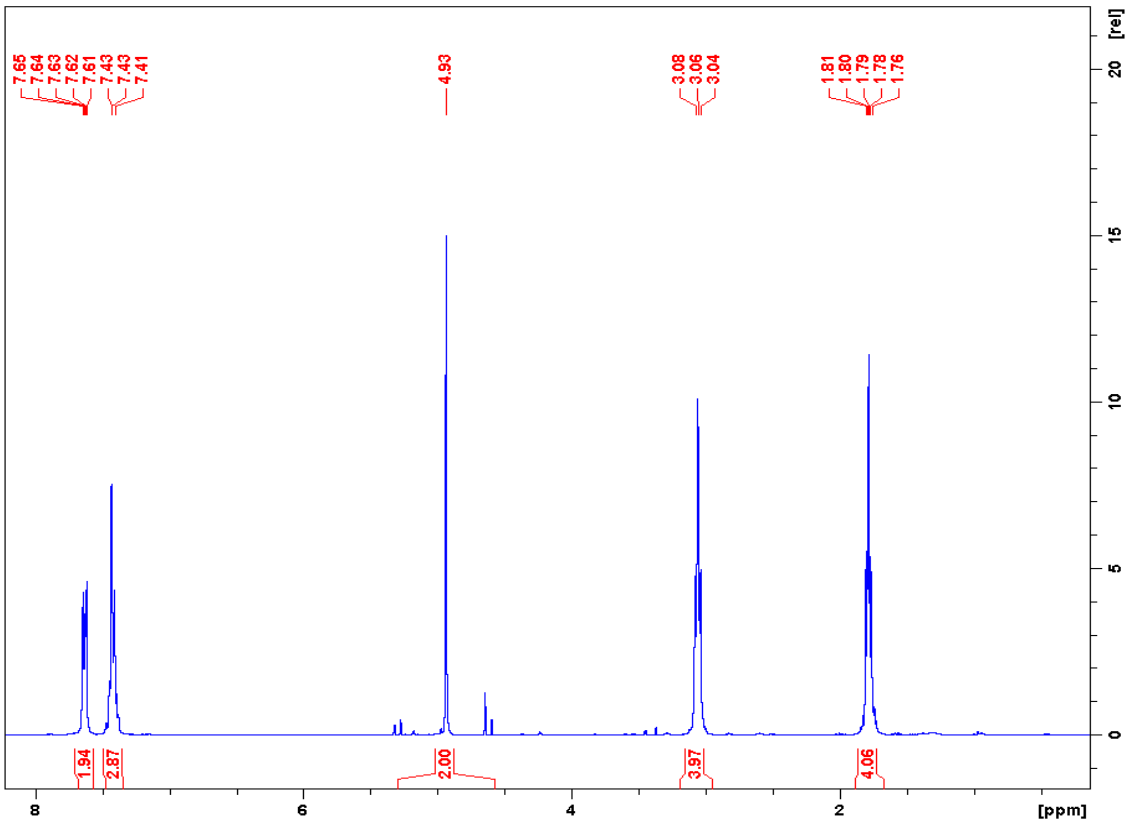

Figure S22. ^{1}H NMR (300 MHz) of $PhSiH_2[N(CH_2)_4]$ in CD_2Cl_2.

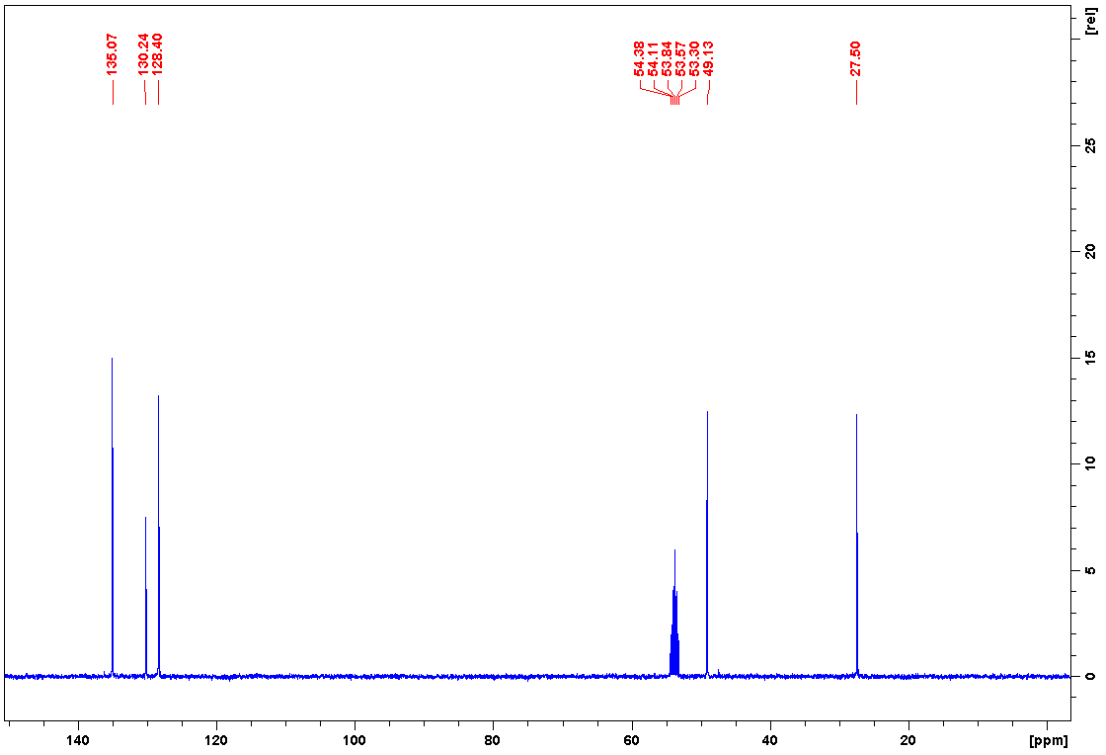

Figure S23. $^{13}C\{^{1}H\}$ NMR (100 MHz) of $PhSiH_2[N(CH_2)_4]$ in CD_2Cl_2.

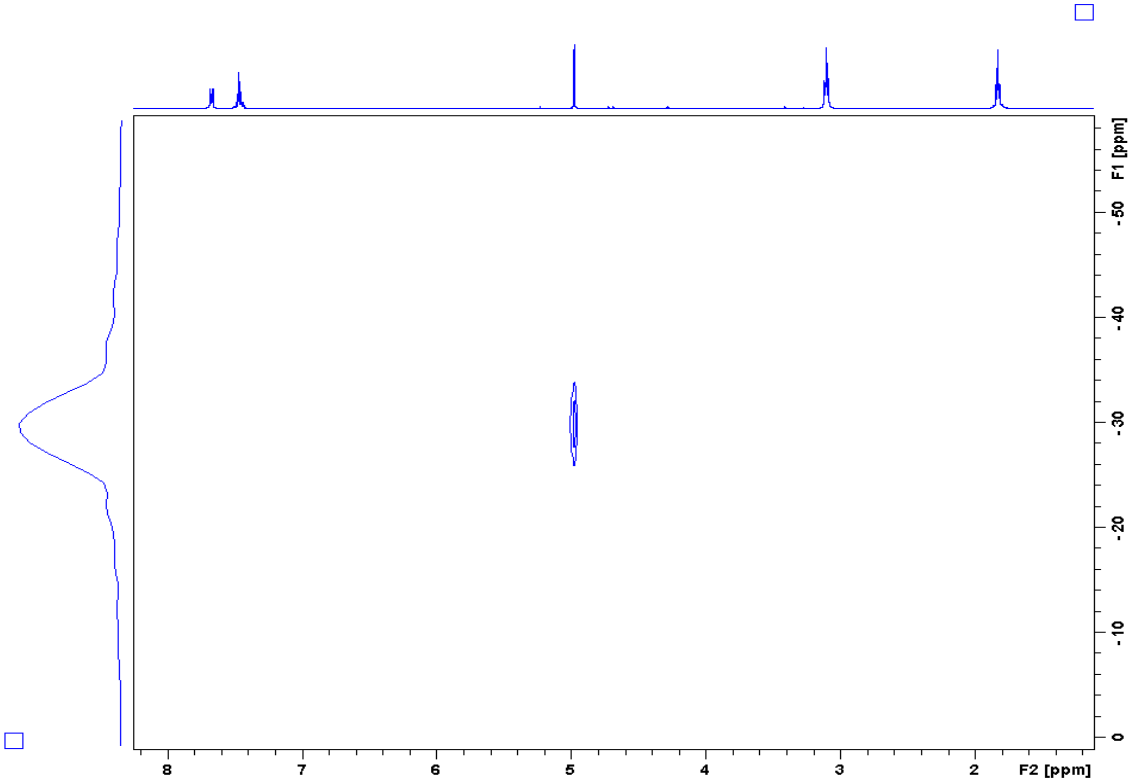

Figure S24. ^{1}H- ^{29}Si HMQC NMR of $PhSiH_2[N(CH_2)_4]$ in CD_2Cl_2.

PhSiH[N(CH$_2$)$_4$]$_2$

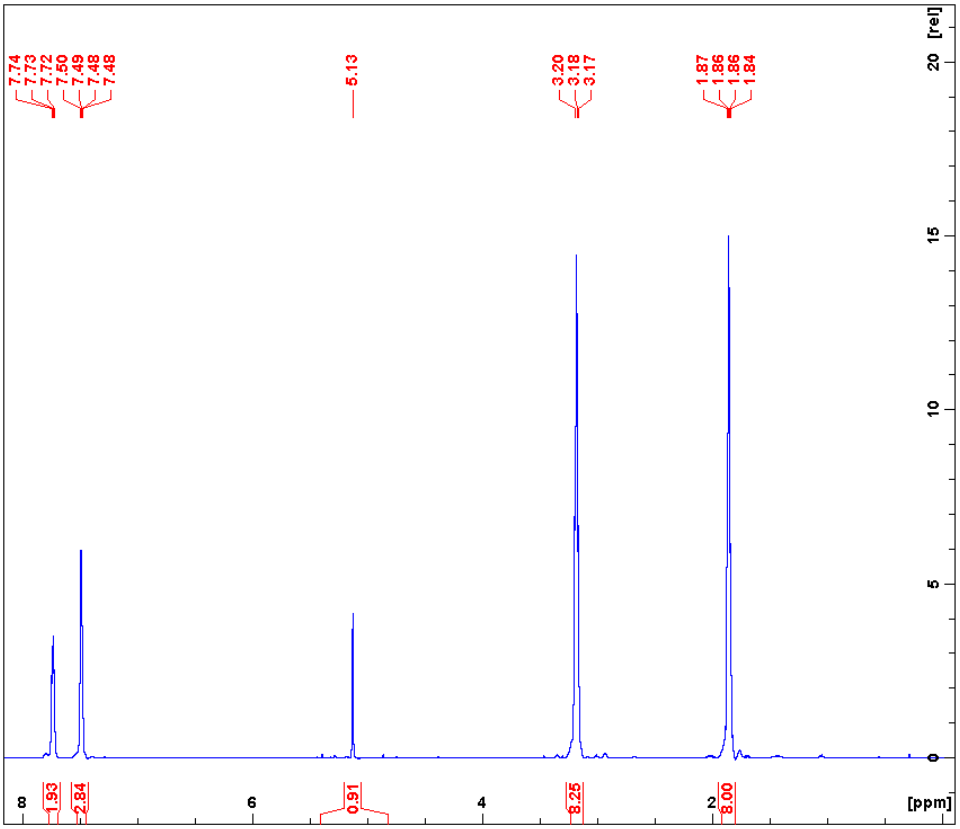

Figure S25. ^{1}H NMR (300 MHz) of PhSiH[N(CH$_2$)$_4$]$_2$ in CD_2Cl_2.

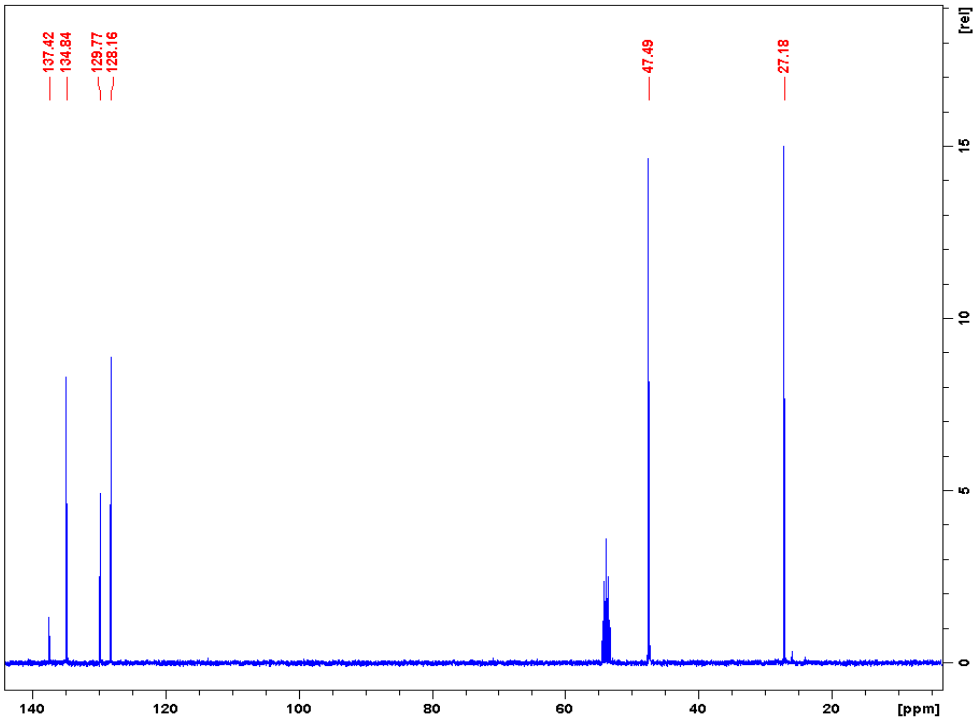

Figure S26. ^{13}C{^{1}H} NMR (100 MHz) of PhSiH[N(CH$_2$)$_4$]$_2$ in CD_2Cl_2.

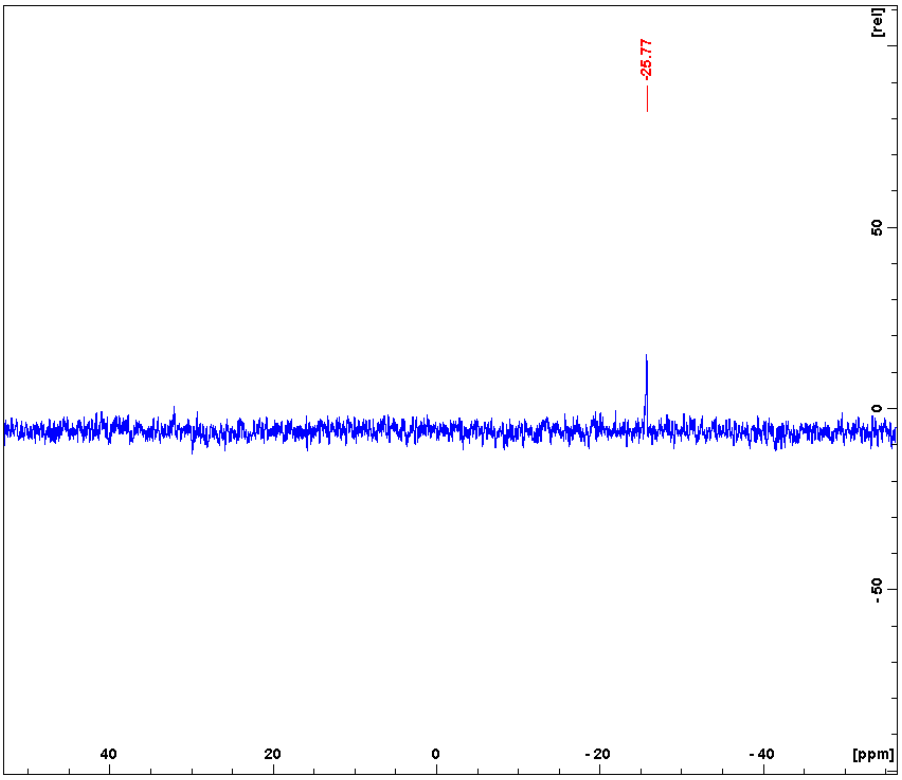

Figure S27. $^{29}Si\{^{1}H\}$ NMR (79 MHz) of $PhSiH[N(CH_2)_4]_2$ in CD_2Cl_2.

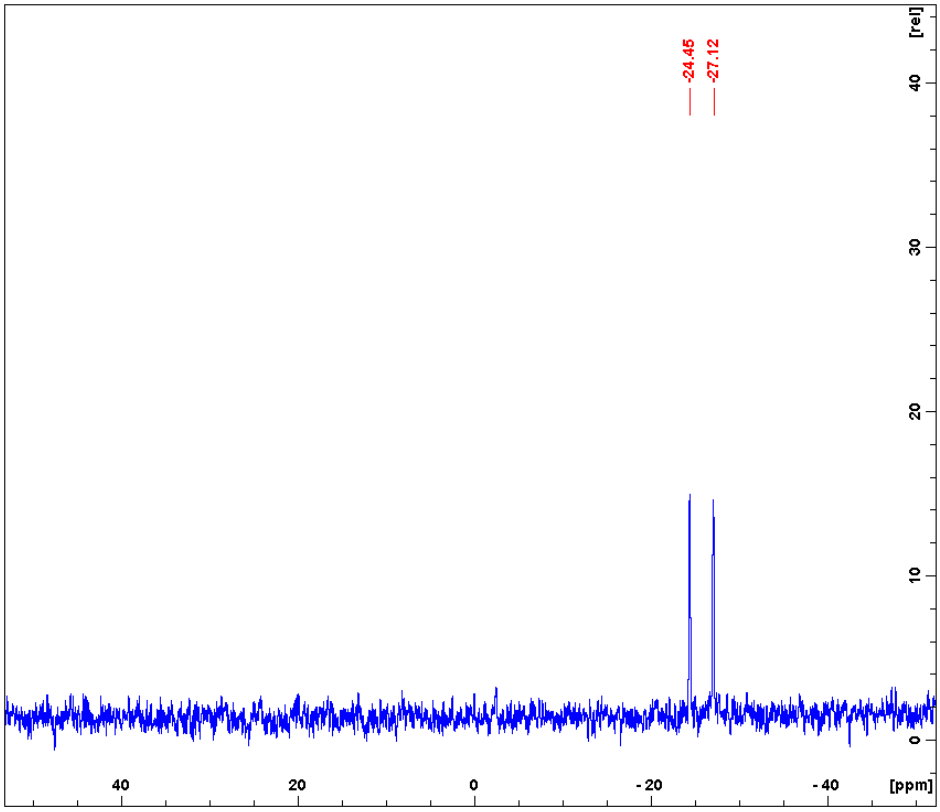

Figure S28. ^{29}Si NMR (79 MHz) of $PhSiH[N(CH_2)_4]_2$ in CD_2Cl_2.

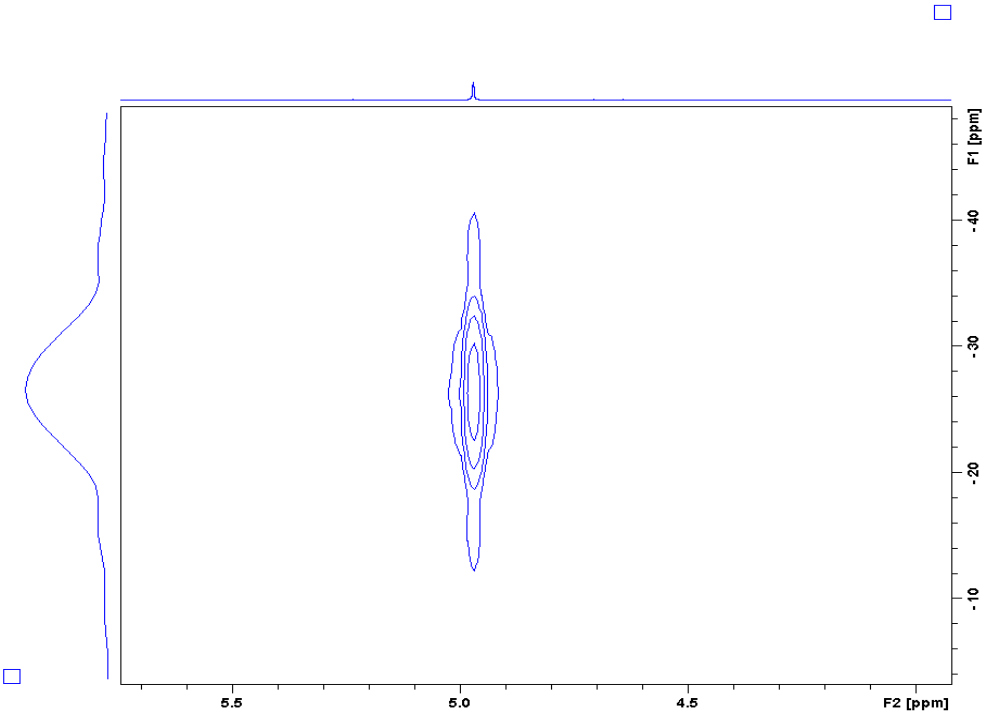

Figure S29. ^{1}H- ^{29}Si HMQC NMR of PhSiH[N(CH$_2$)$_4$]$_2$ in CD_2Cl_2.

PhSiH$_2$(N^{i}Pr$_2$)

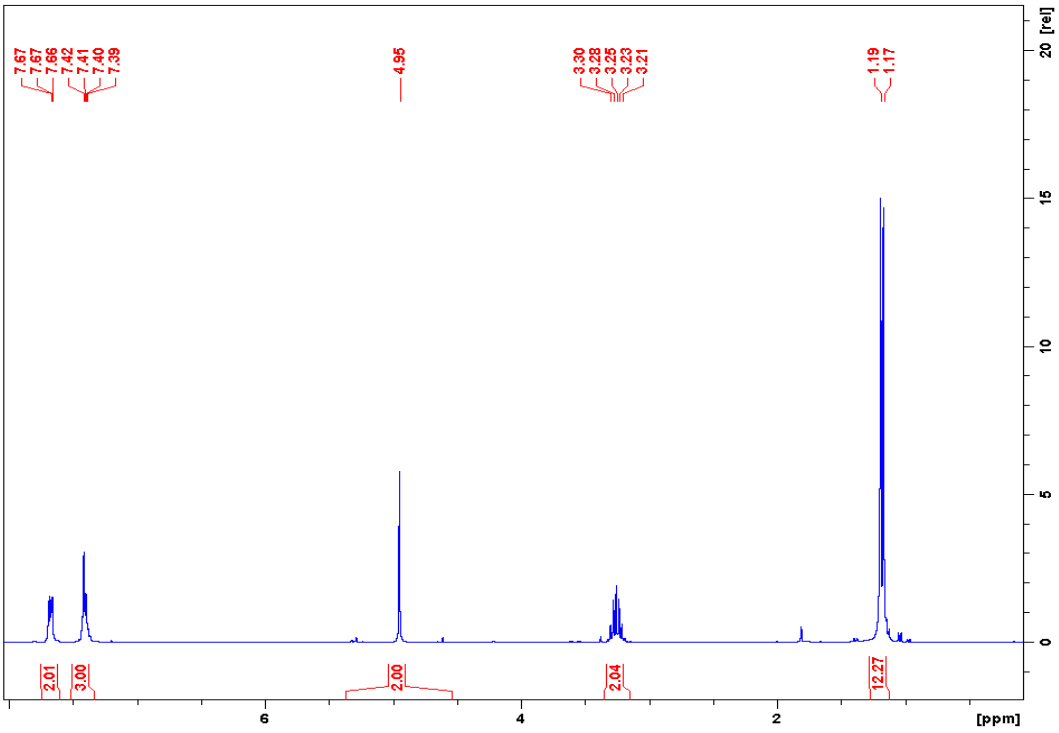

Figure S30. ^{1}H NMR (300 MHz) of PhSiH$_2$(N^{i}Pr$_2$) in CD_2Cl_2.

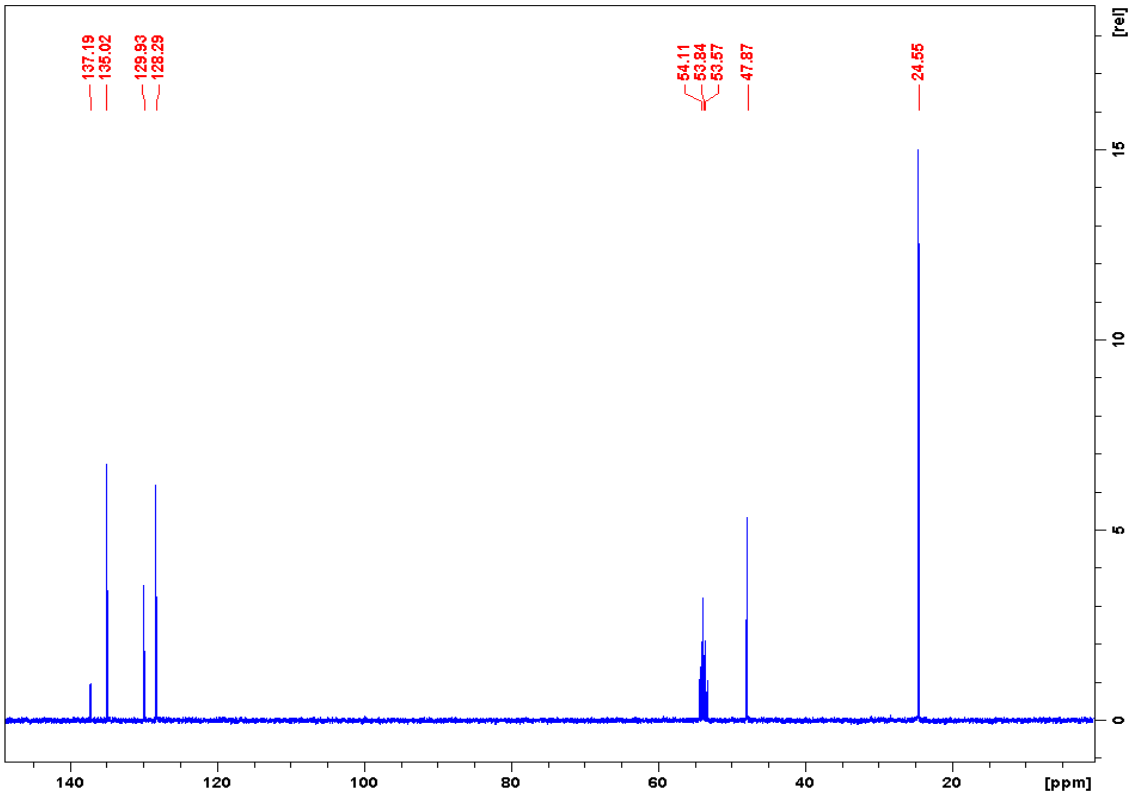

Figure S31. $^{13}C\{^{1}H\}$ NMR (100 MHz) of $PhSiH_2(N^iPr_2)$ in CD_2Cl_2.

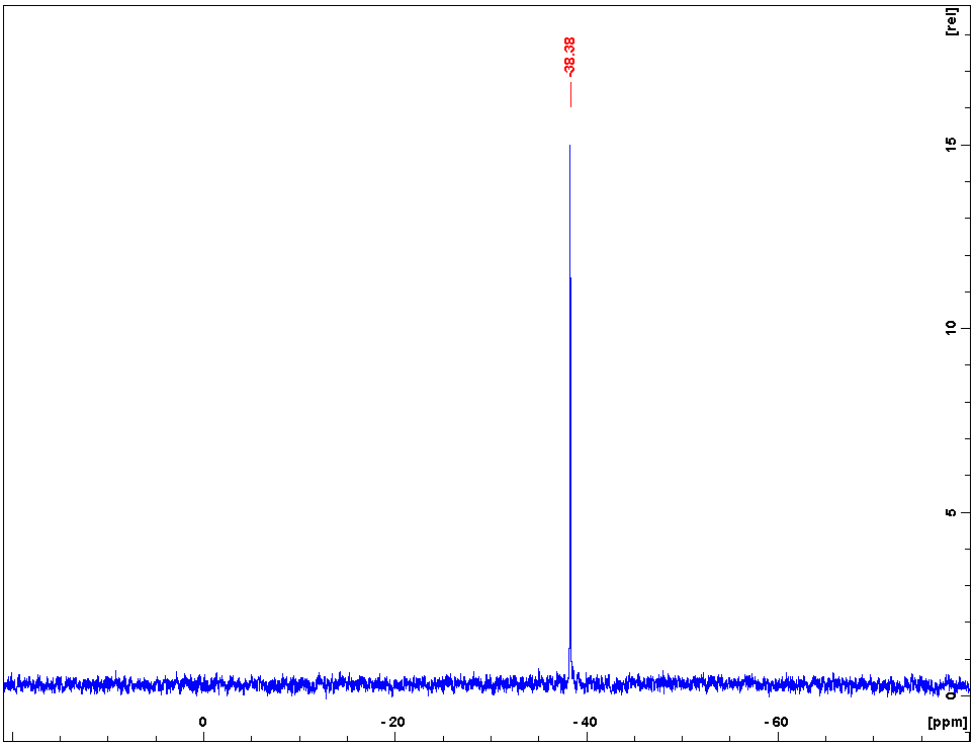

Figure S32. $^{29}Si\{^{1}H\}$ NMR (79 MHz) of $PhSiH_2(N^iPr_2)$ in CD_2Cl_2.

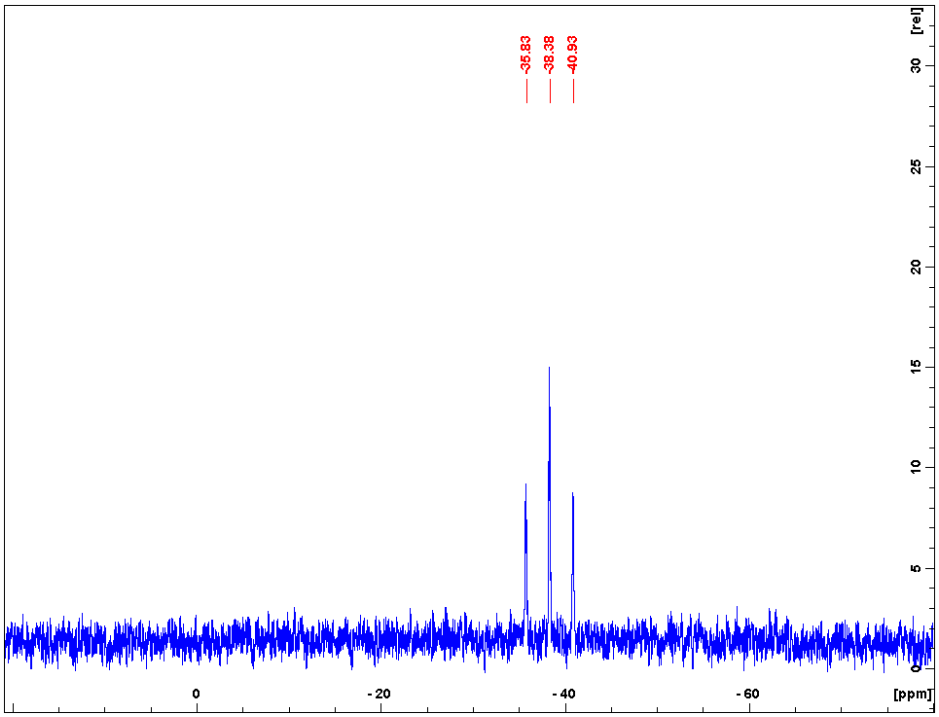

Figure S33. ^{29}Si NMR (79 MHz) of $PhSiH_2(N^iPr_2)$ in CD_2Cl_2.

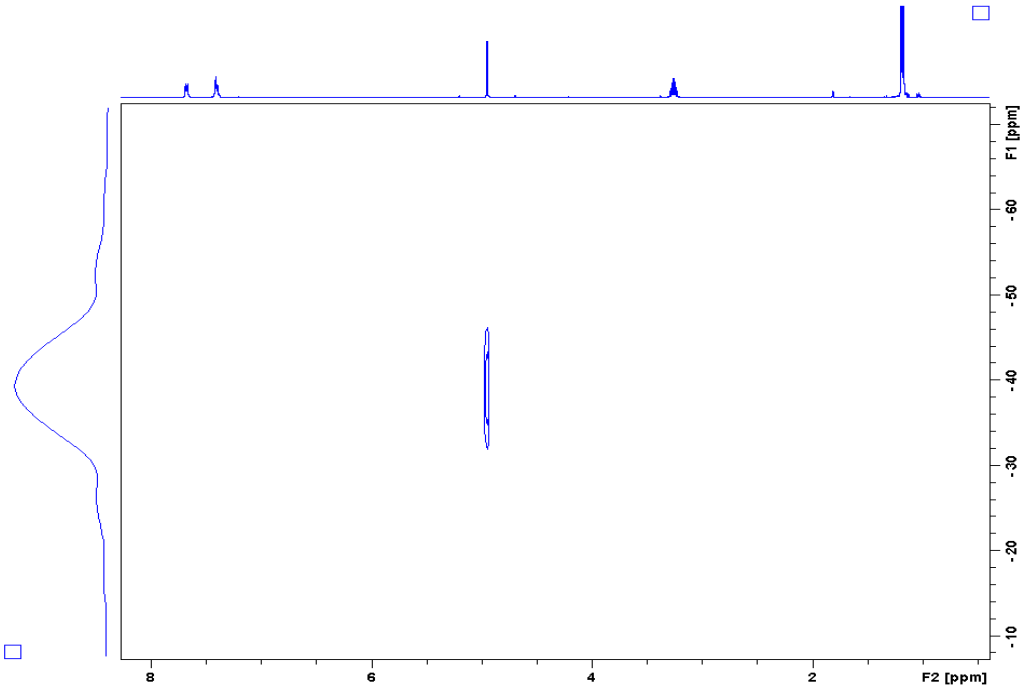

Figure S34. ^{1}H- ^{29}Si HMQC NMR of $PhSiH_2(N^iPr_2)$ in CD_2Cl_2.

$PhSiH_2$(NMesH)

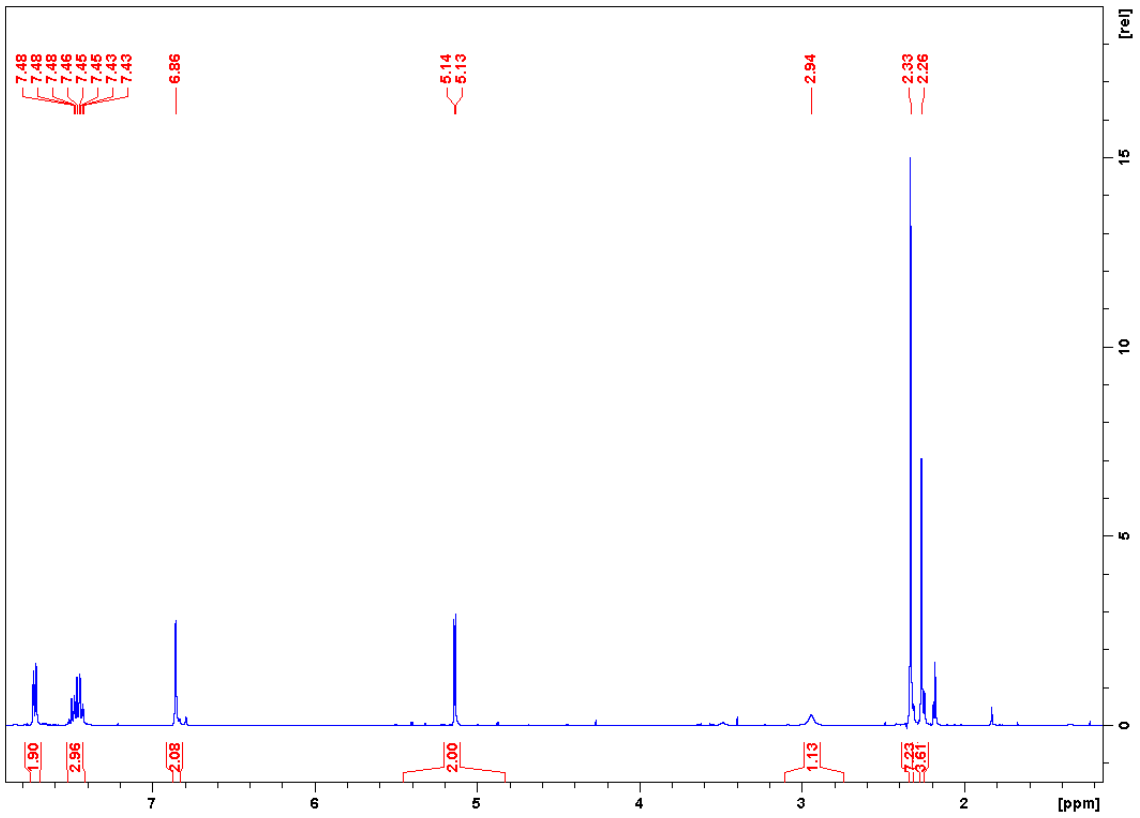

Figure S35. ^{1}H NMR (400 MHz) of $PhSiH_2$(NMesH) in CD_2Cl_2.

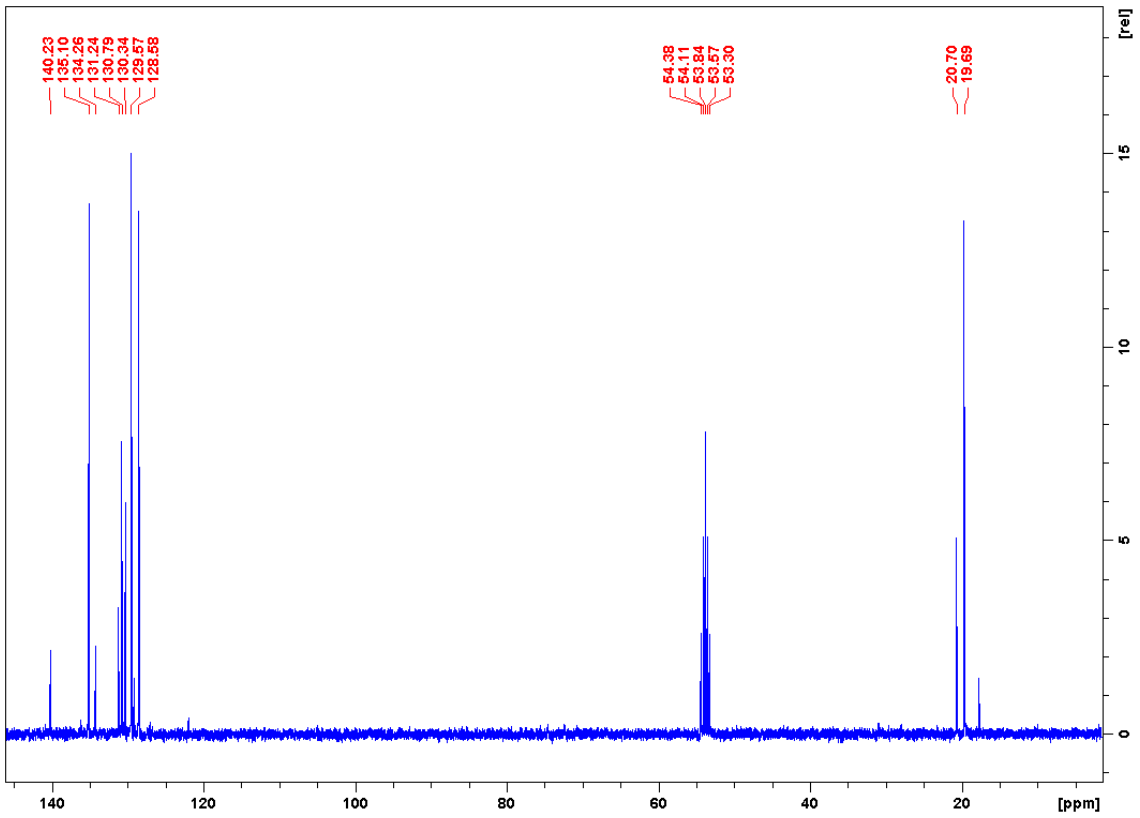

Figure S36. $^{13}C\{^{1}H\}$ NMR (100 MHz) of $PhSiH_2$(NMesH) in CD_2Cl_2.

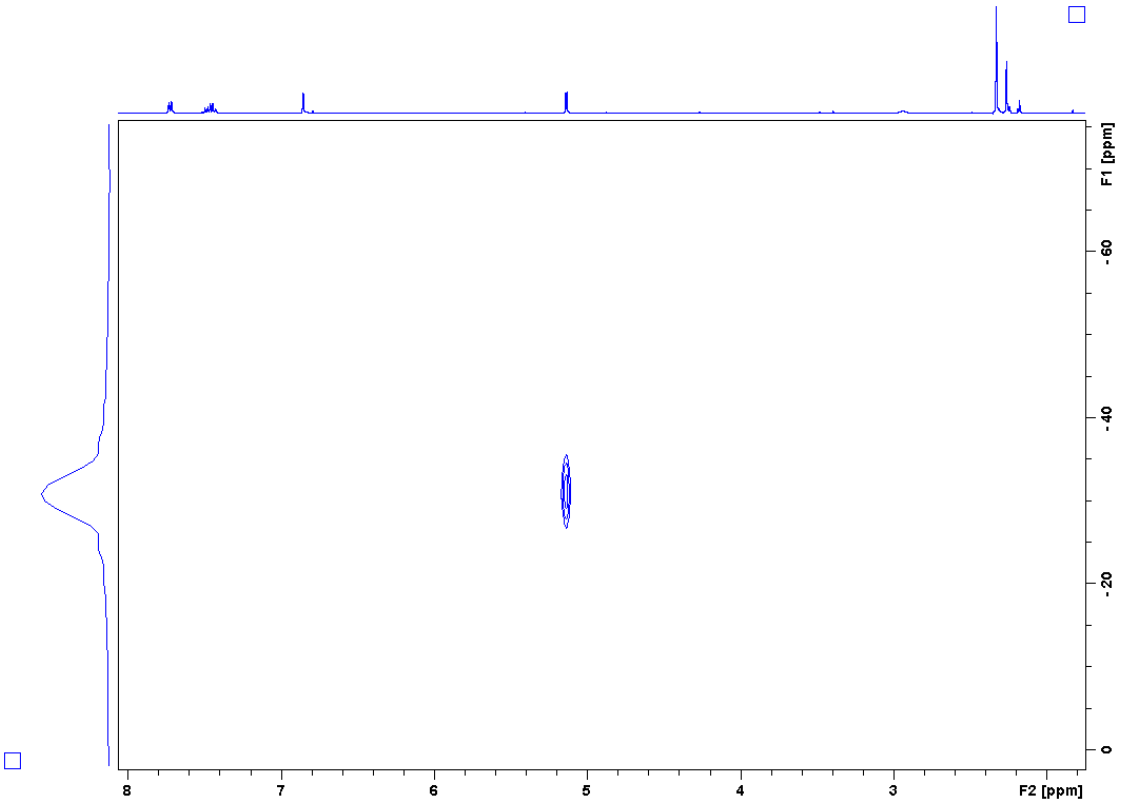

Figure S37. ^{1}H- ^{29}Si HMQC NMR of $PhSiH_2(NMesH)$ in CD_2Cl_2.

$Ph_2SiH(NH^tBu)$

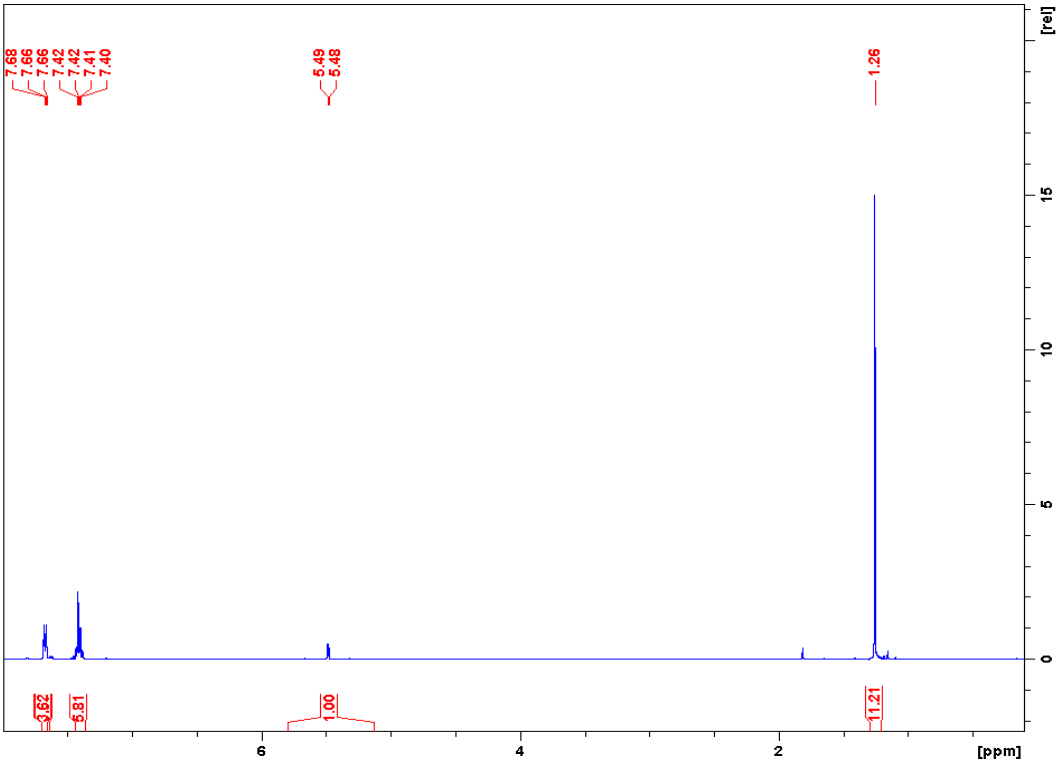

Figure S38. ^{1}H NMR (300 MHz) of $Ph_2SiH(NH^tBu)$ in CD_2Cl_2.

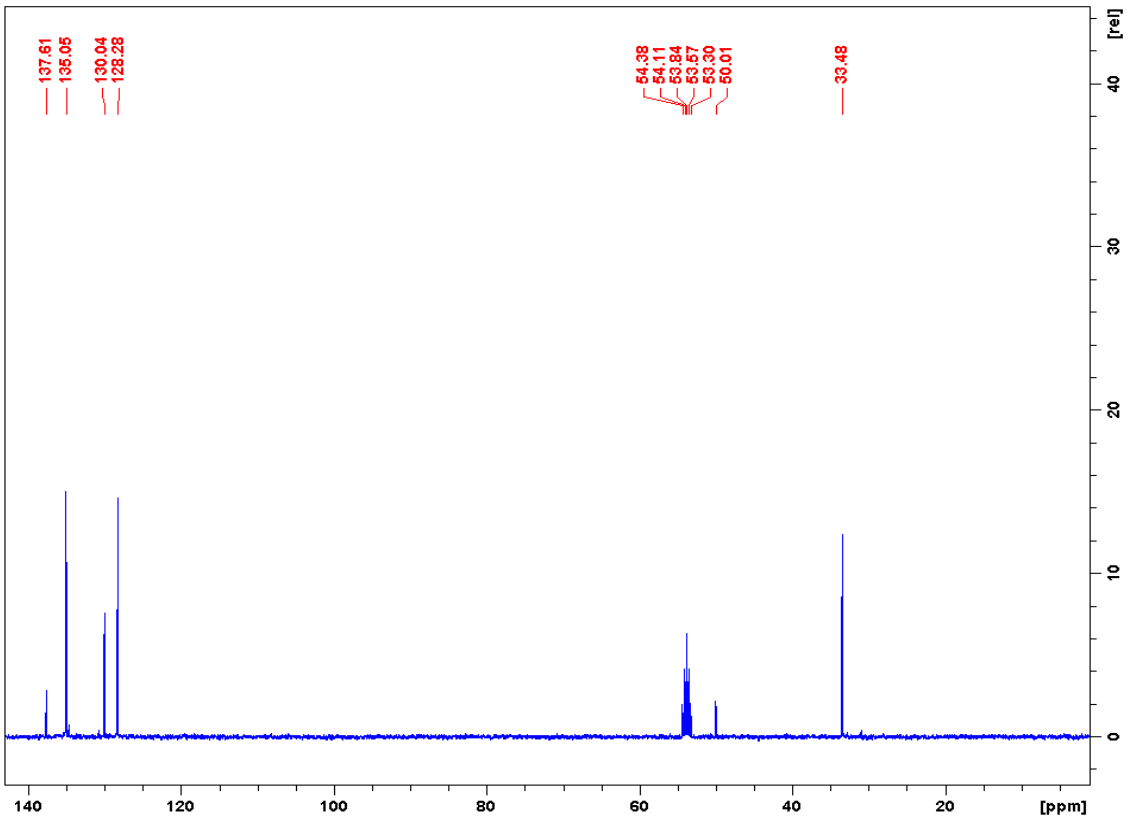

Figure S39. $^{13}C\{^{1}H\}$ NMR (125 MHz) of $Ph_2SiH(NH^tBu)$ in CD_2Cl_2.

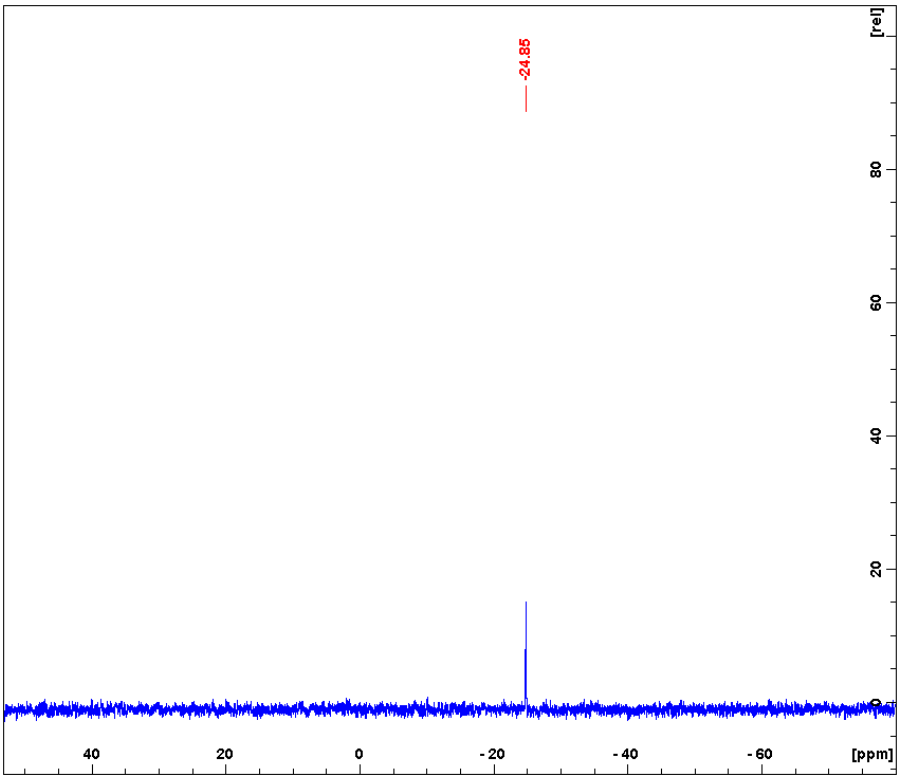

Figure S40. $^{29}Si\{^{1}H\}$ NMR (79 MHz) of $Ph_2SiH(NH^tBu)$ in CD_2Cl_2.

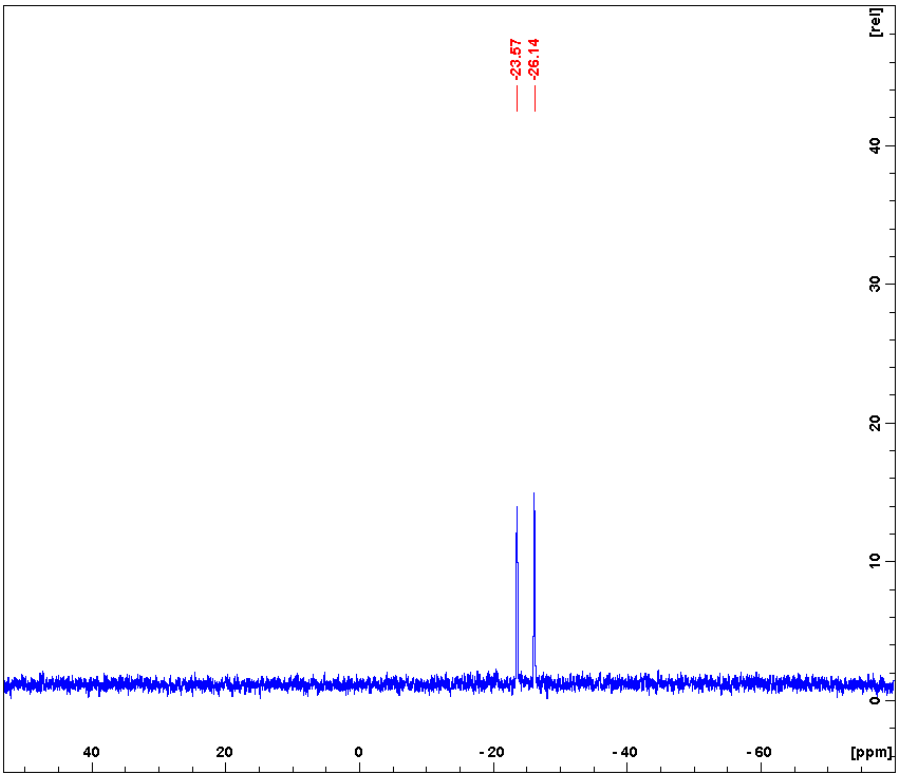

Figure S41. ^{29}Si NMR (79 MHz) of $Ph_2SiH(NH^tBu)$ in CD_2Cl_2.

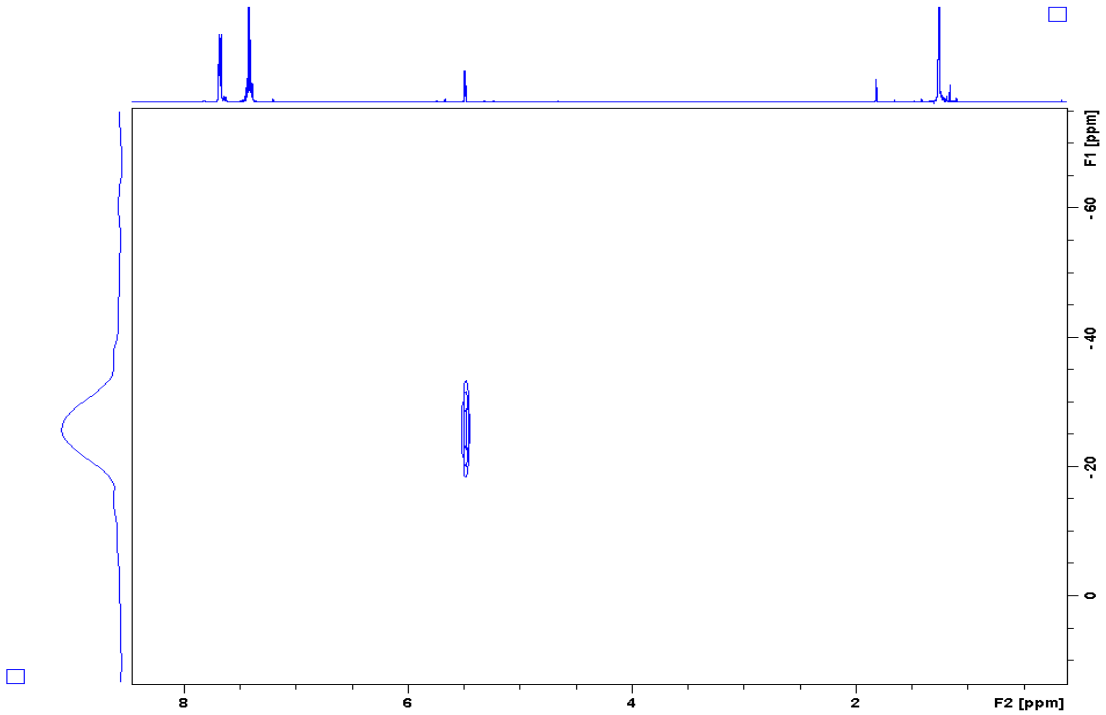

Figure S42. ^{1}H- ^{29}Si HMQC NMR of $Ph_2SiH(NH^tBu)$ in CD_2Cl_2.

$Ph_2SiH(NEt_2)$

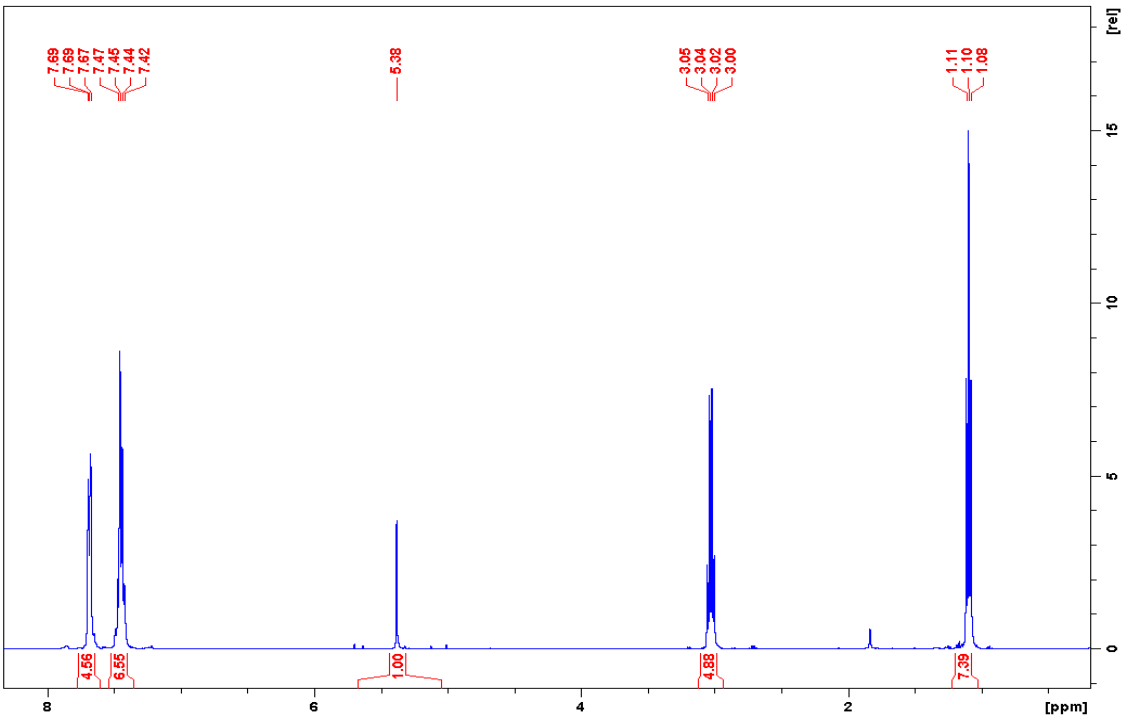

Figure S43. ^{1}H NMR (400 MHz) of $Ph_2SiH(NEt_2)$ in CD_2Cl_2.

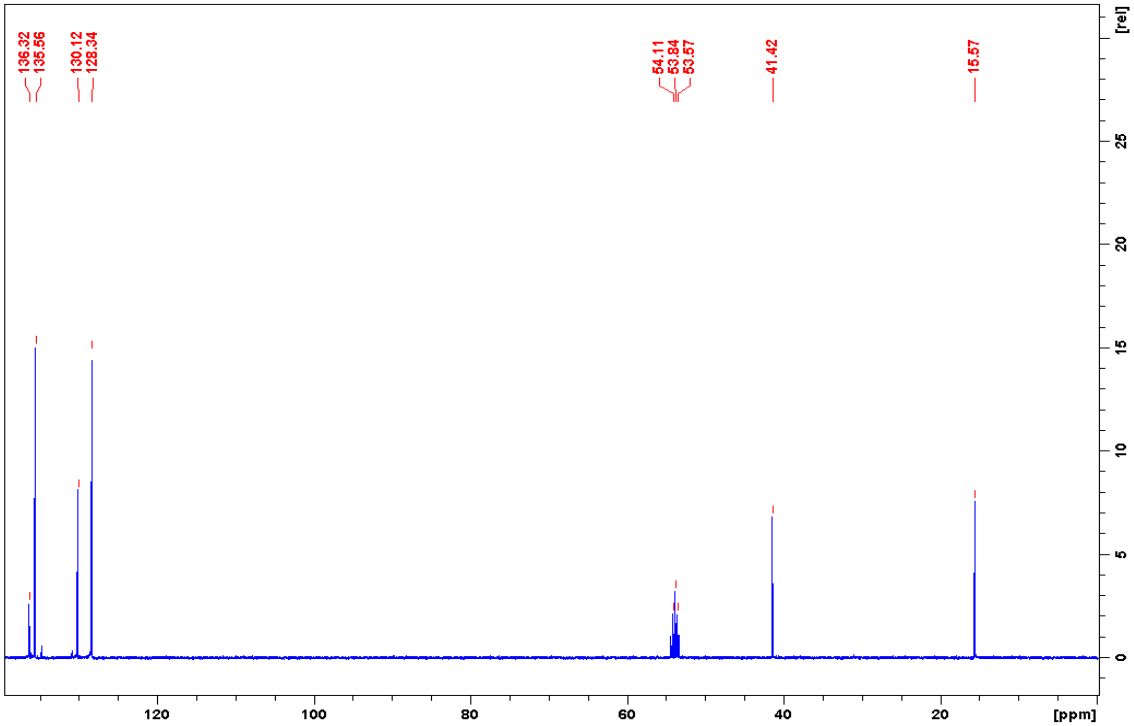

Figure S44. $^{13}C\{^{1}H\}$ NMR (100 Hz) of $Ph_2SiH(NEt_2)$ in CD_2Cl_2.

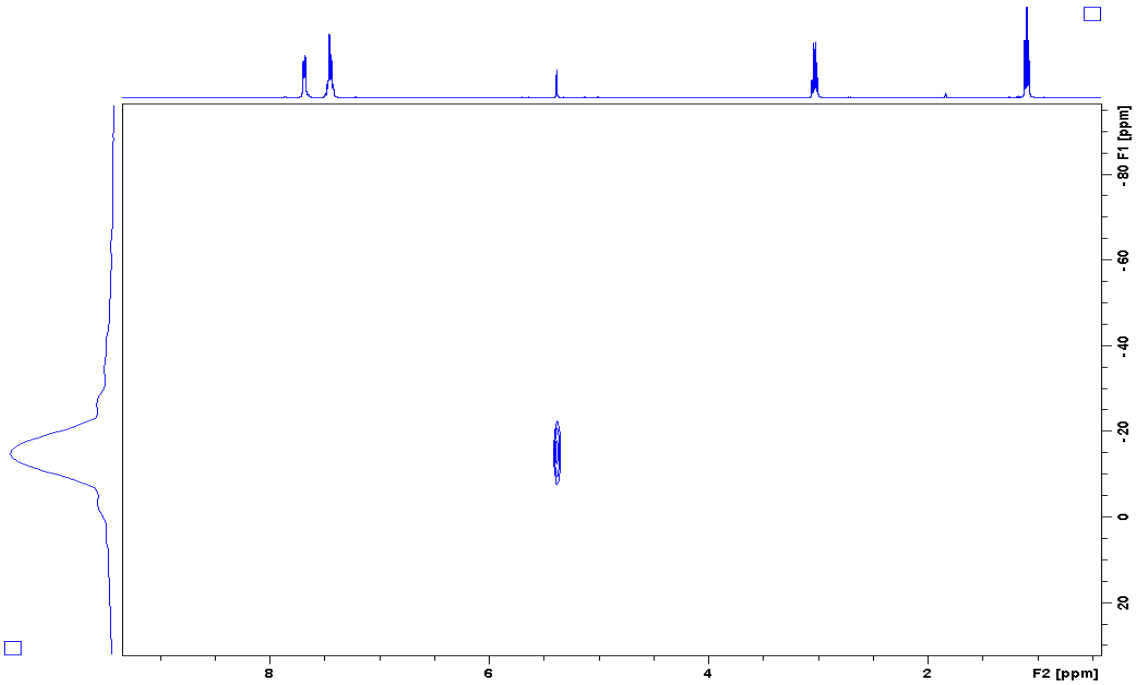

Figure S45. ^{1}H- ^{29}Si HMQC NMR of $Ph_2SiH(NEt_2)$ in CD_2Cl_2.

$Ph_2SiH[N(CH_2)_4]$

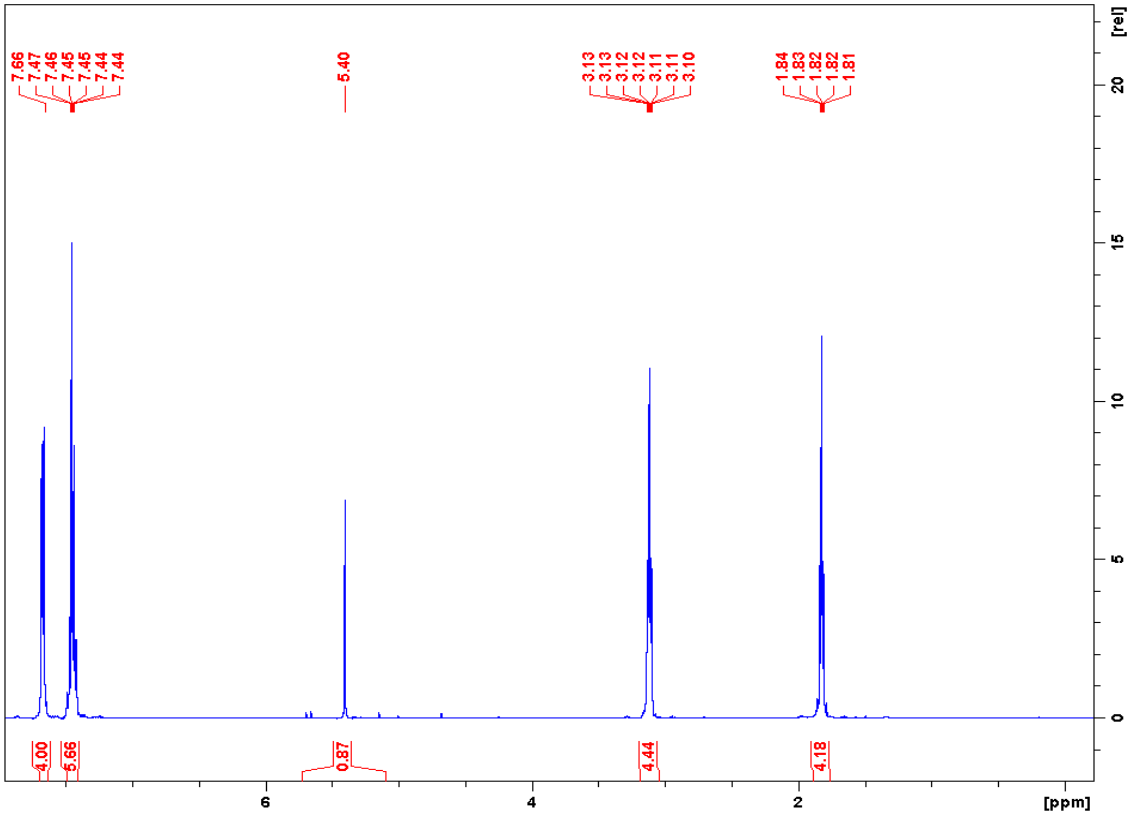

Figure S46. ^{1}H NMR (400 MHz) of $Ph_2SiH[N(CH_2)_4]$ in CD_2Cl_2.

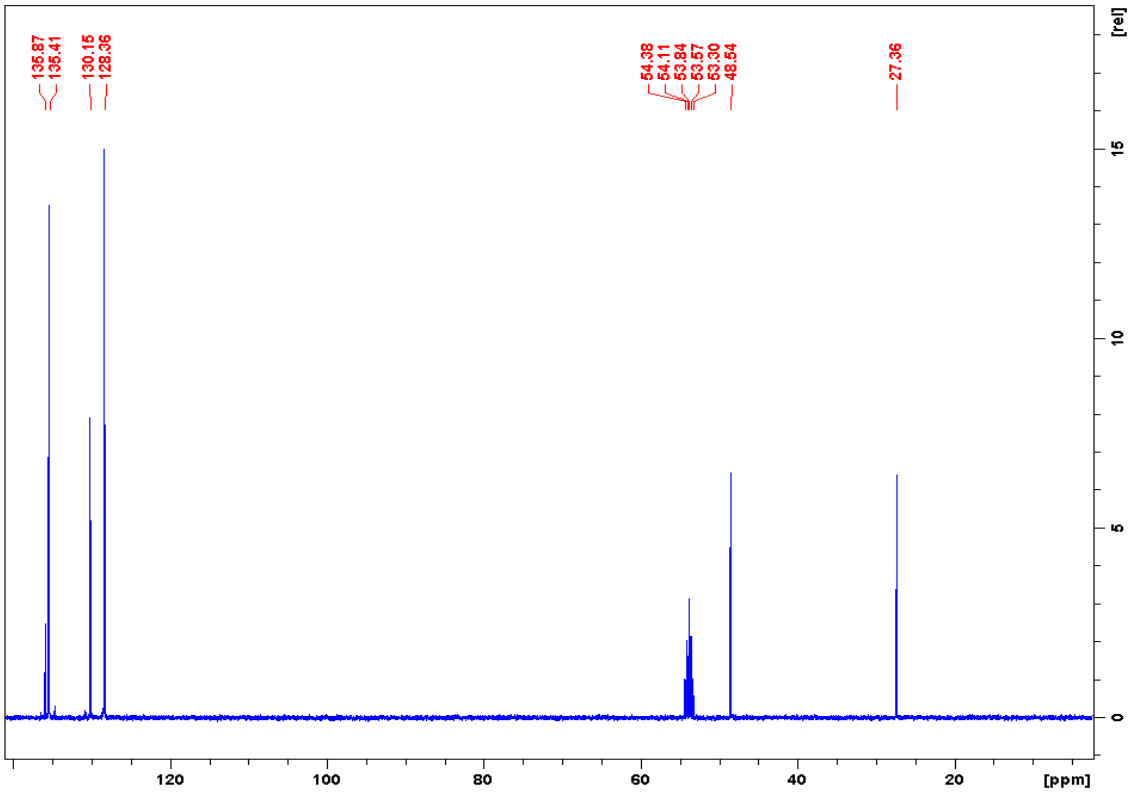

Figure S47. $^{13}C\{^{1}H\}$ NMR (100 MHz) of $Ph_2SiH[N(CH_2)_4]$ in CD_2Cl_2.

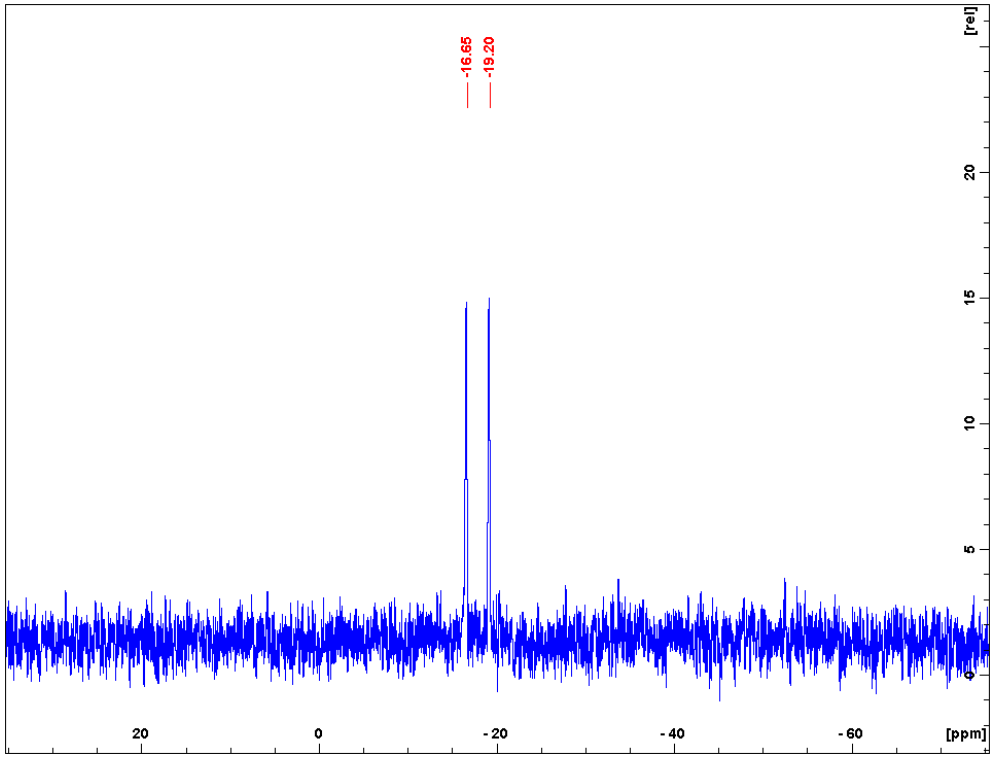

Figure S48. ^{29}Si NMR (79 MHz) of $Ph_2SiH[N(CH_2)_4]$ in CD_2Cl_2.

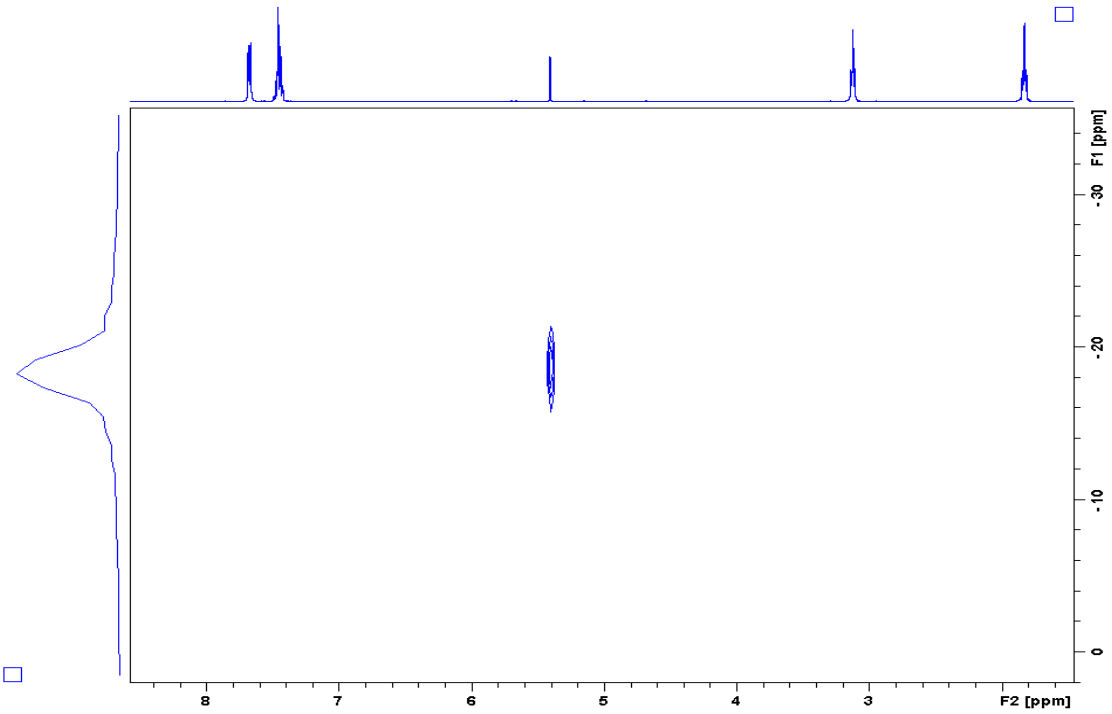

Figure S49. ^{1}H-^{29}Si HMQC NMR of $Ph_2SiH[N(CH_2)_4]$ in CD_2Cl_2.

^{n}BuSiH$_2$(NH^{t}Bu)

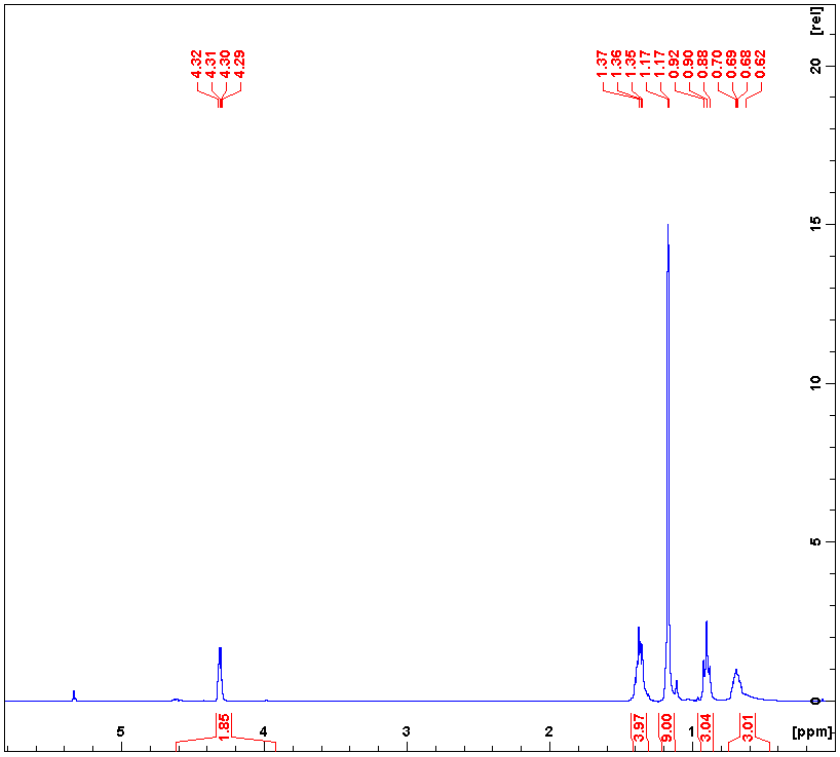

Figure S50. ^{1}H NMR (300 MHz) of ^{n}BuSiH$_2$(NH^{t}Bu) in CD_2Cl_2.

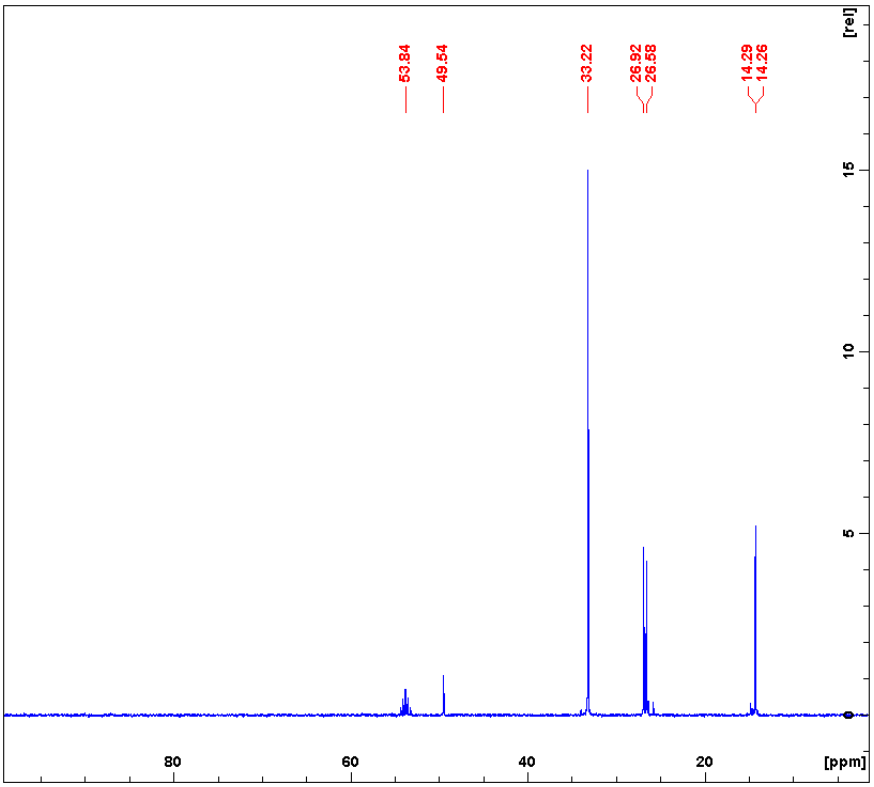

Figure S51. $^{13}C\{^{1}H\}$ NMR (100 MHz) of $^{n}BuSiH_2(NH^{t}Bu)$ in CD_2Cl_2.

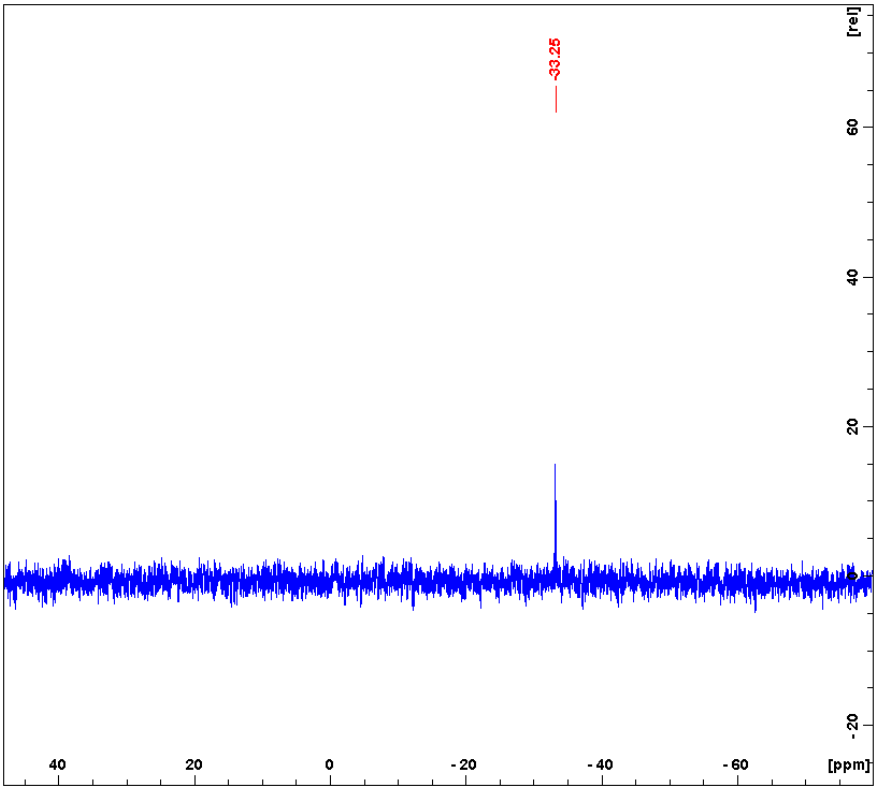

Figure S52. $^{29}Si\{^{1}H\}$ NMR (79 MHz) of $^{n}BuSiH_2(NH^{t}Bu)$ in CD_2Cl_2.

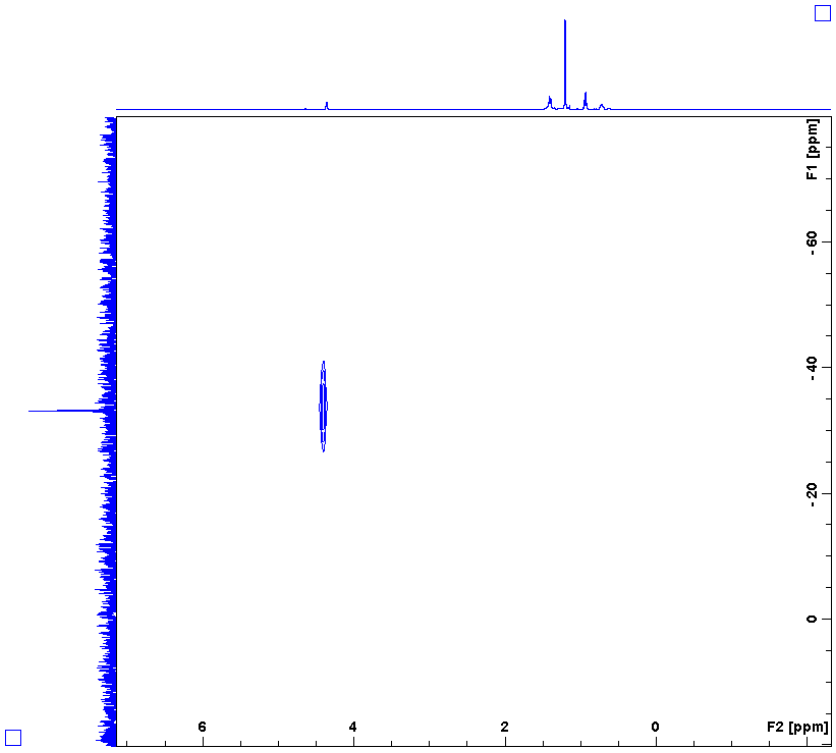

Figure S53. ^{1}H- ^{29}Si HMQC NMR of ^{n}BuSiH$_2$(NH^{t}Bu) in CD_2Cl_2.

^{n}BuSiH(NH^{t}Bu)$_2$

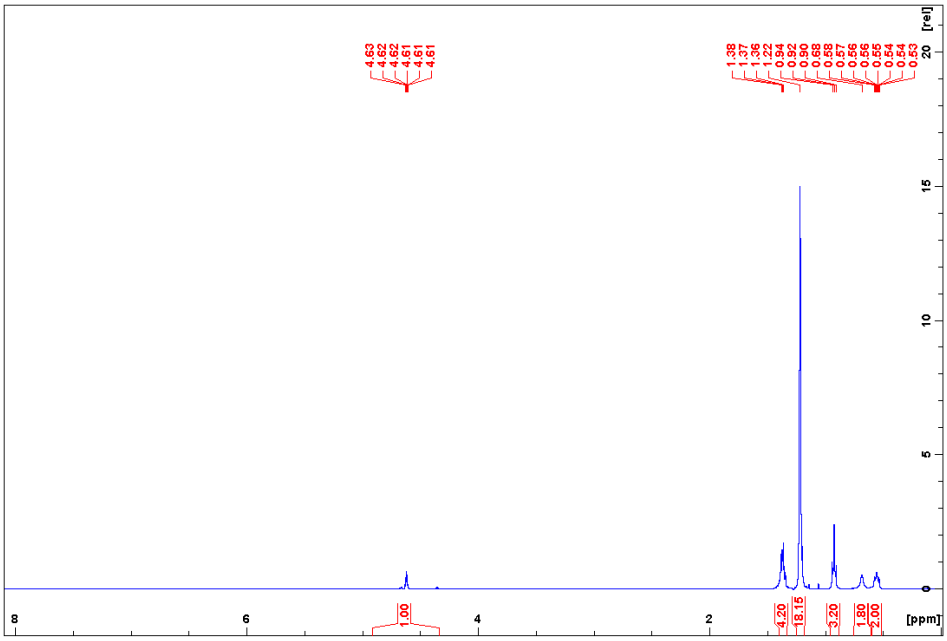

Figure S54. ^{1}H NMR (400 MHz) of ^{n}BuSiH(NH^{t}Bu)$_2$ in CD_2Cl_2.

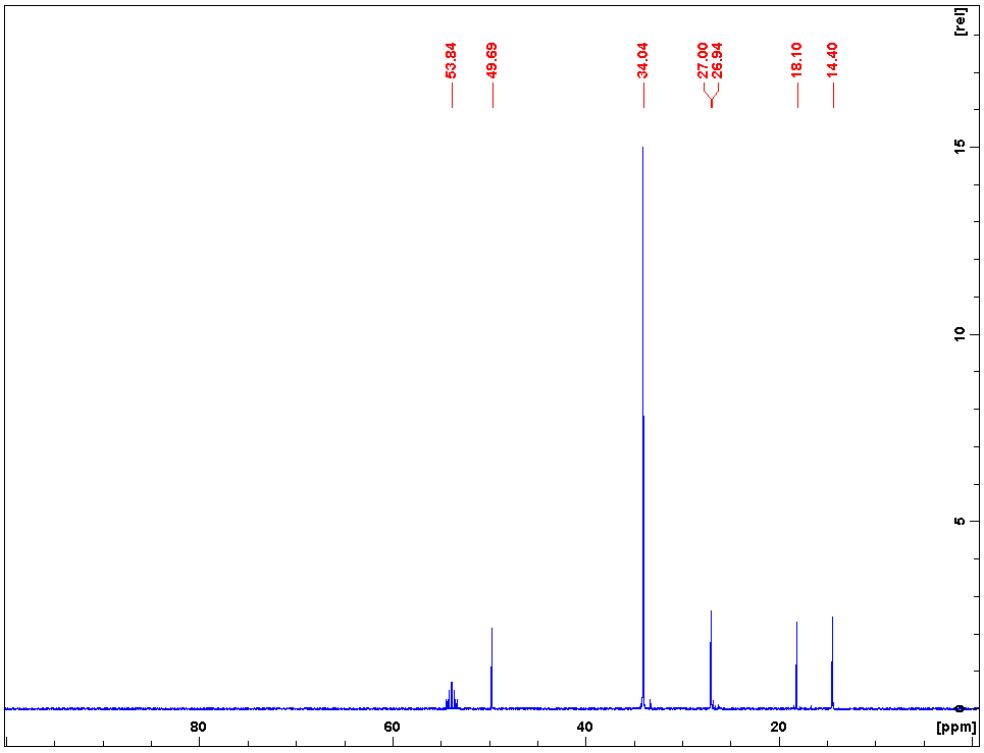

Figure S55. $^{13}C\{^{1}H\}$ NMR (100 MHz) of $^{n}BuSiH(NH^{t}Bu)_2$ in CD_2Cl_2.

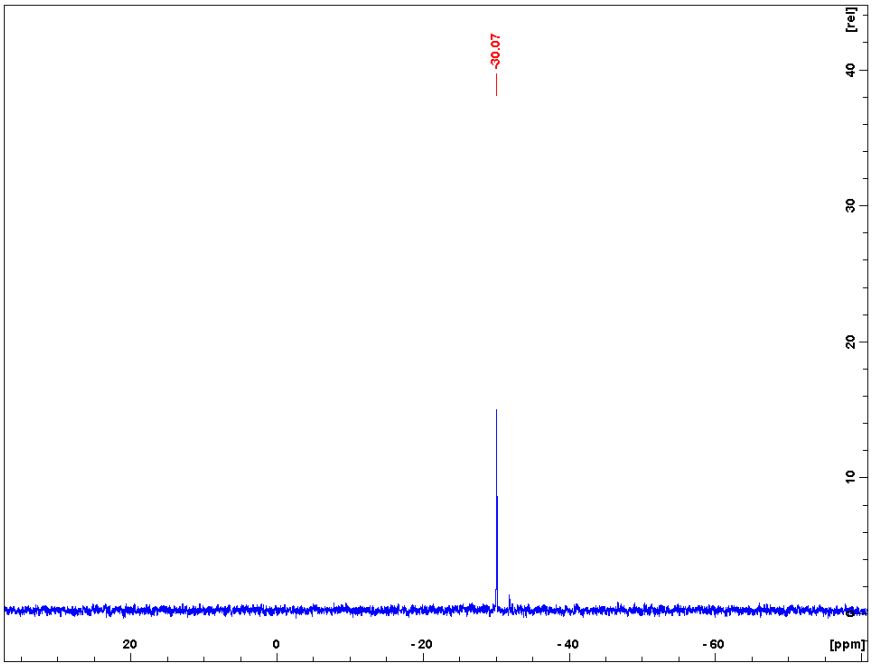

Figure S56. $^{29}Si\{^{1}H\}$ NMR (79 MHz) of $^{n}BuSiH(NH^{t}Bu)_2$ in CD_2Cl_2.

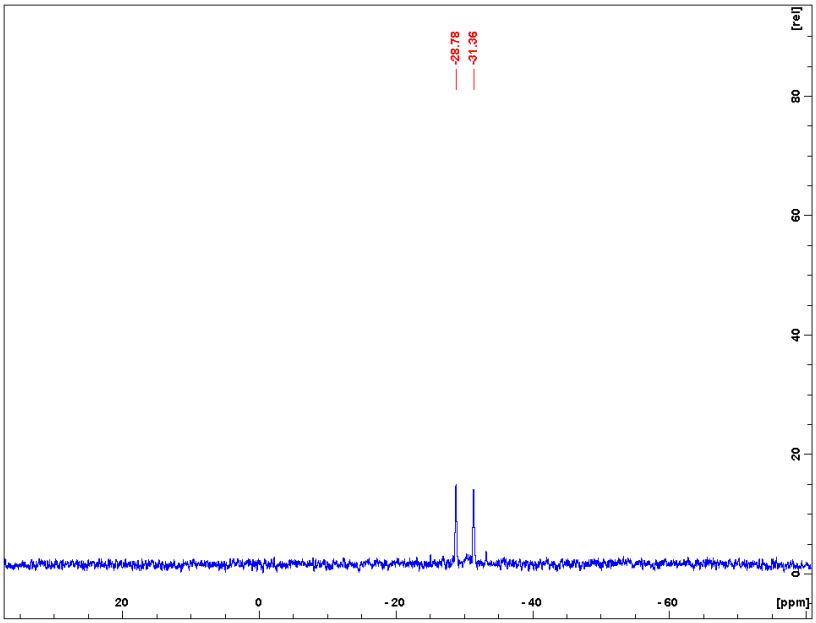

Figure S57. ^{29}Si NMR (79 MHz) of ^{n}BuSiH(NH^{t}Bu)$_2$ in CD_2Cl_2.

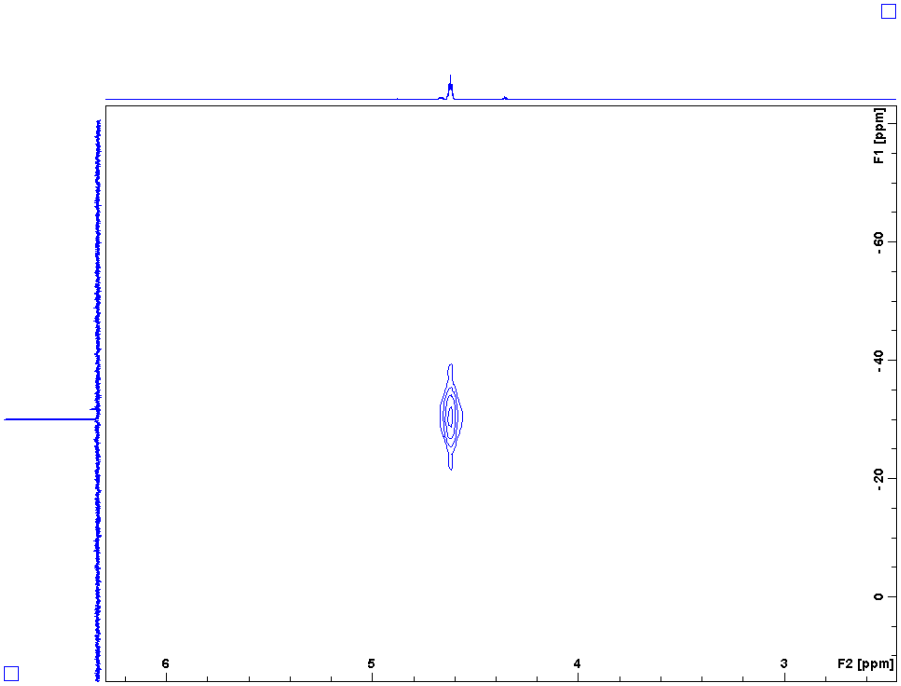

Figure S58. ^{1}H- ^{29}Si HMQC NMR of ^{n}BuSiH(NH^{t}Bu)$_2$ in CD_2Cl_2.

^{n}BuSiH$_2$(NEt$_2$)

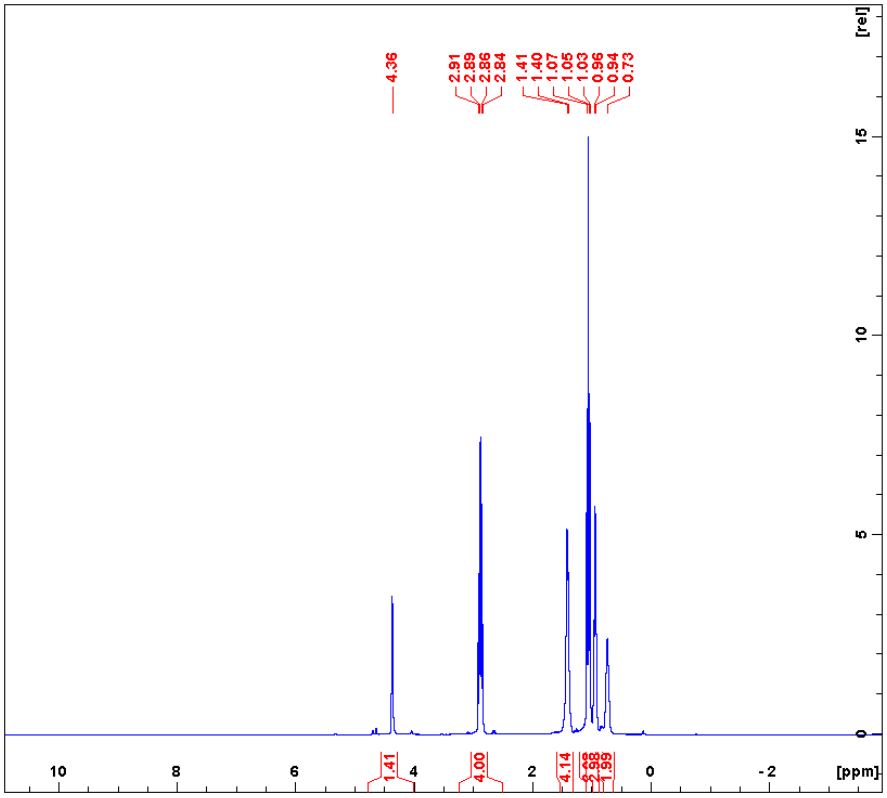

Figure S59. ^{1}H NMR (300 MHz) of ^{n}BuSiH$_2$(NEt$_2$) in CD_2Cl_2.

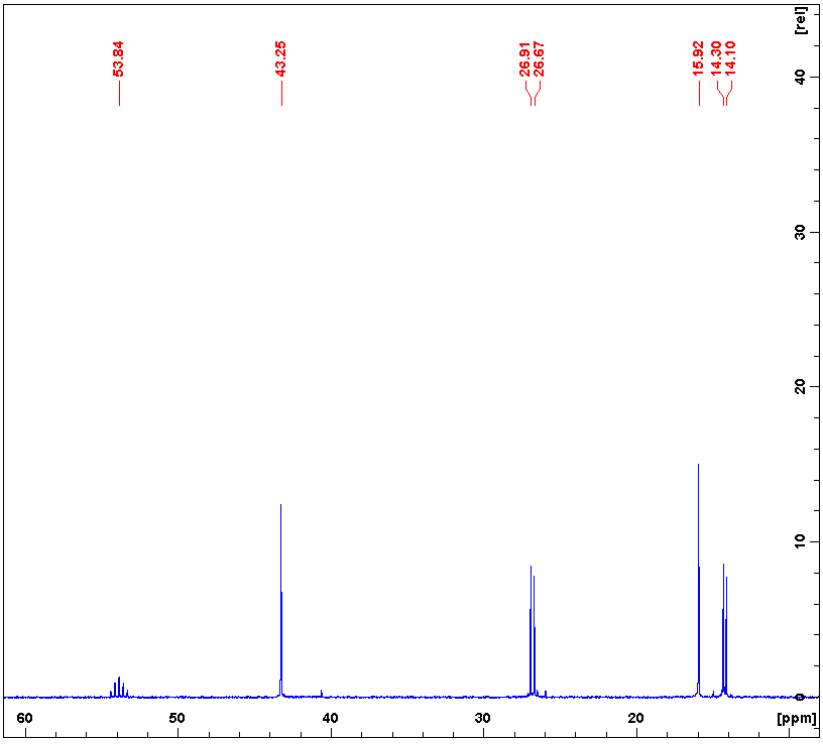

Figure S60. ^{13}C{^{1}H} NMR (100 MHz) of ^{n}BuSiH$_2$(NEt$_2$) in CD_2Cl_2.

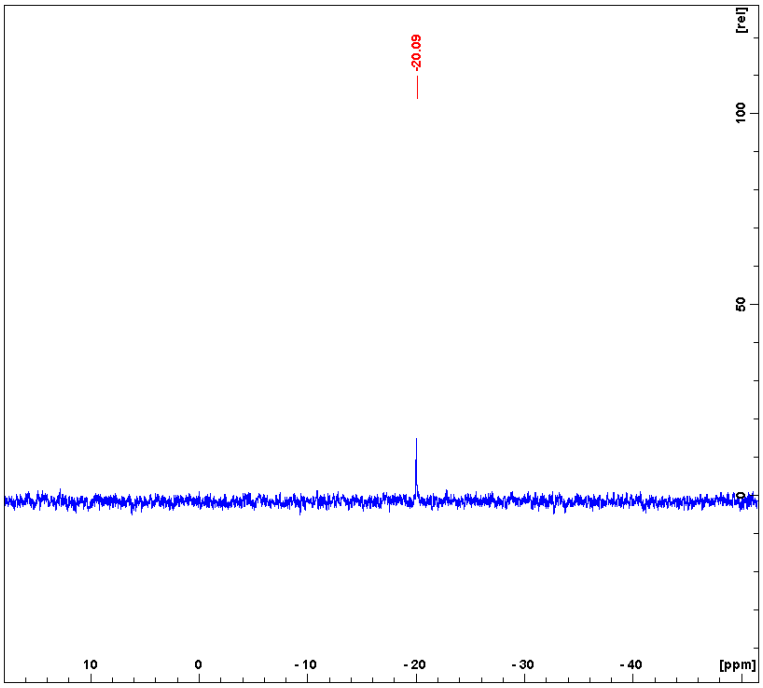

Figure S61. $^{29}Si\{^{1}H\}$ NMR (79 MHz) of $^{n}BuSiH_2(NEt_2)$ in CD_2Cl_2.

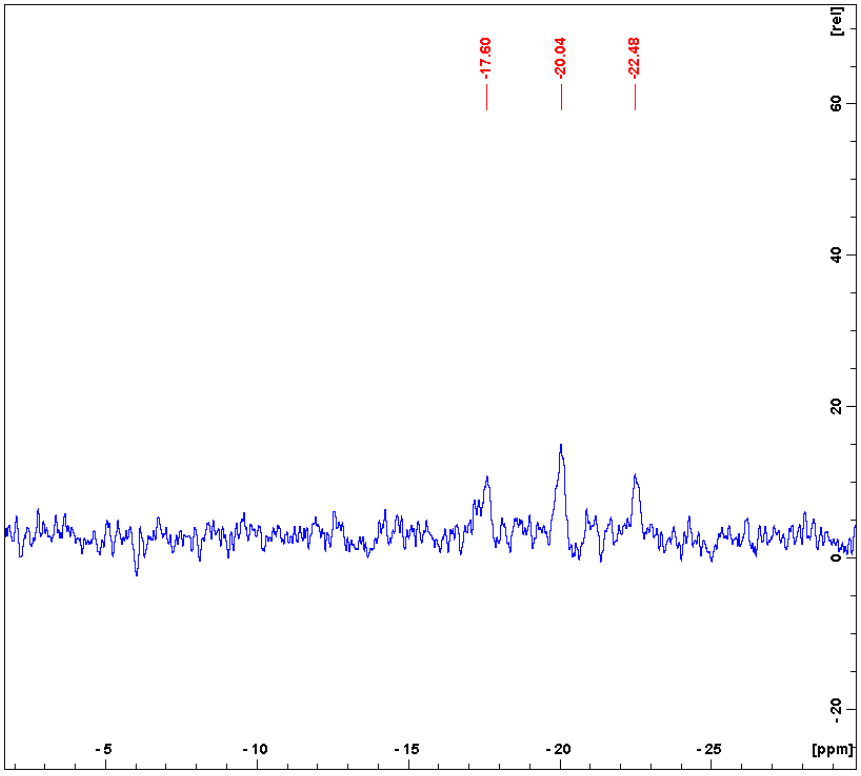

Figure S62. ^{29}Si NMR (79 MHz) of $^{n}BuSiH_2(NEt_2)$ in CD_2Cl_2.

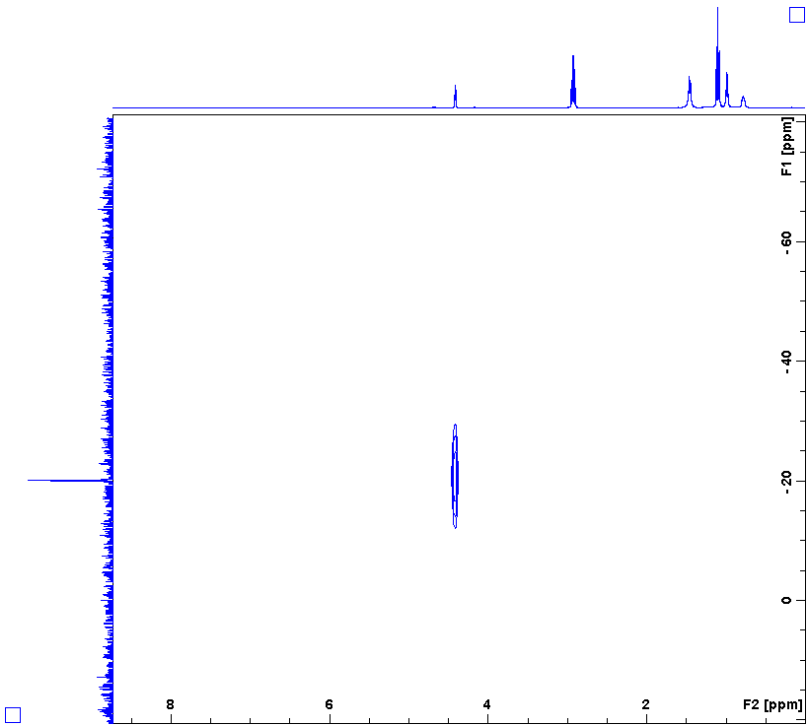

Figure S63. ^{1}H- ^{29}Si HMQC NMR of $^{n}BuSiH_2(NEt_2)$ in CD_2Cl_2.

$^{n}BuSiH(NEt_2)_2$

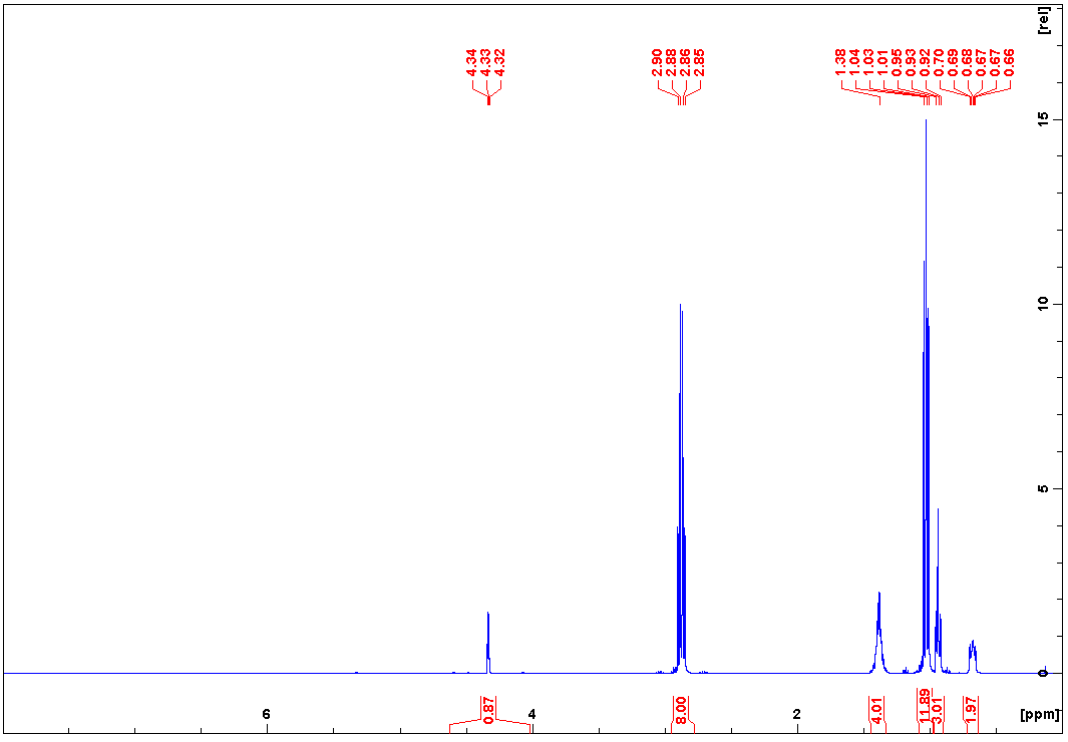

Figure S64. ^{1}H NMR (300 MHz) of $^{n}BuSiH(NEt_2)_2$ in CD_2Cl_2.

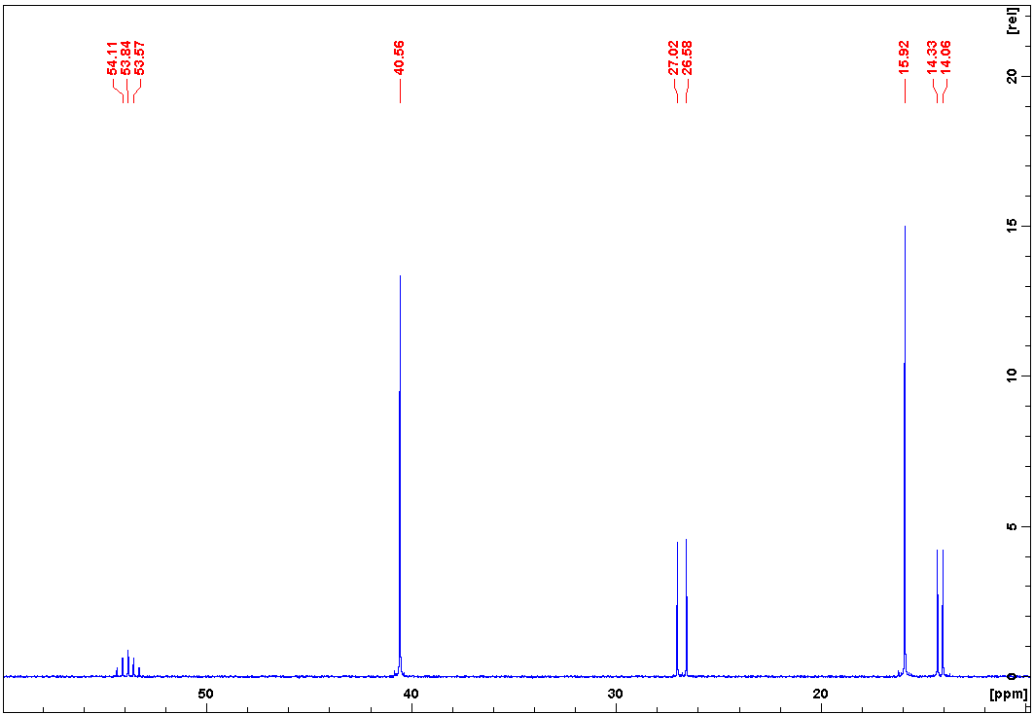

Figure S65. $^{13}C\{^{1}H\}$ NMR (100 MHz) of $^{n}BuSiH(NEt_2)_2$ in CD_2Cl_2.

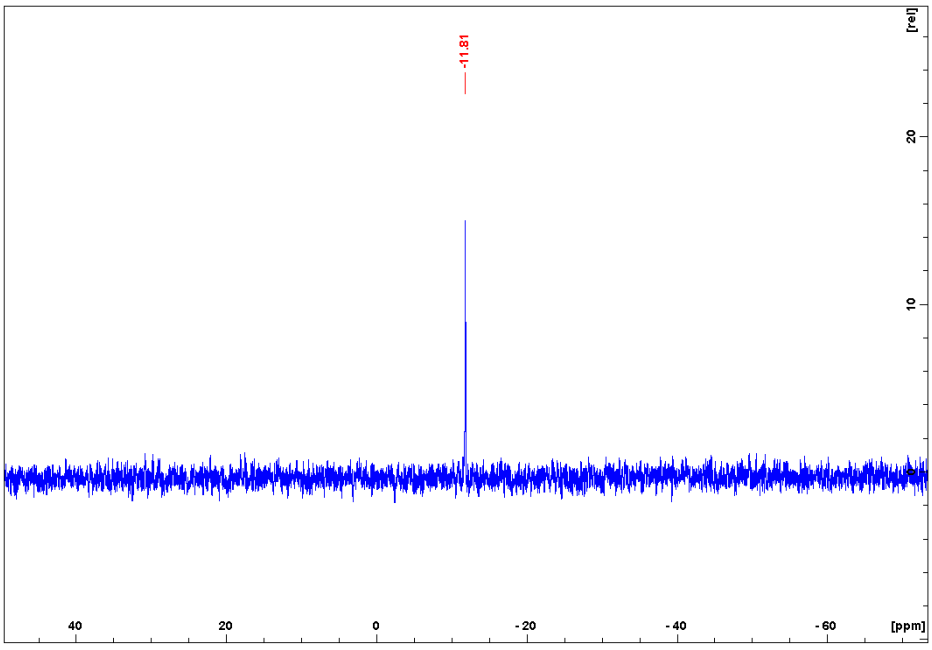

Figure S66. $^{29}Si\{^{1}H\}$ NMR (79 MHz) of $^{n}BuSiH(NEt_2)_2$ in CD_2Cl_2.

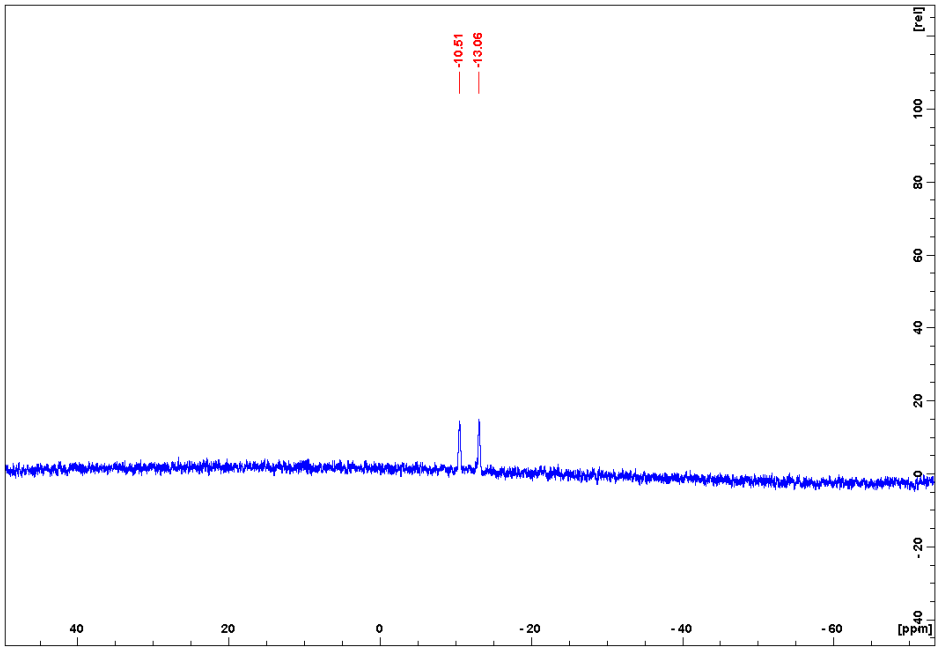

Figure S67. ^{29}Si NMR (79 MHz) of ^{n}BuSiH(NEt$_2$)$_2$ in CD_2Cl_2.

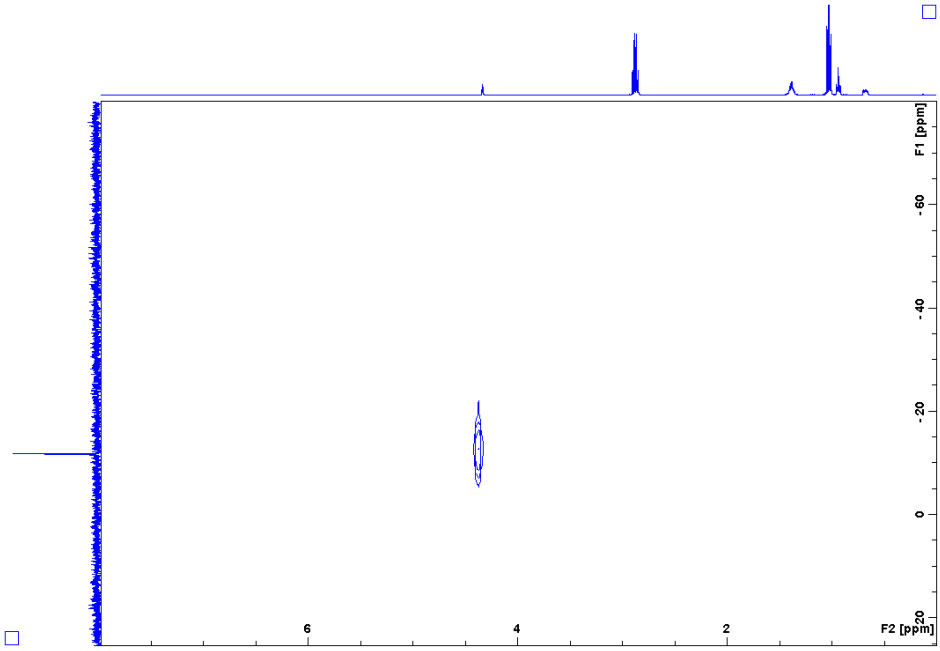

Figure S68. ^{1}H-^{29}Si HMQC NMR of ^{n}BuSiH(NEt$_2$)$_2$ in CD_2Cl_2.

^{n}BuSiH$_2$[N(CH$_2$)$_4$]

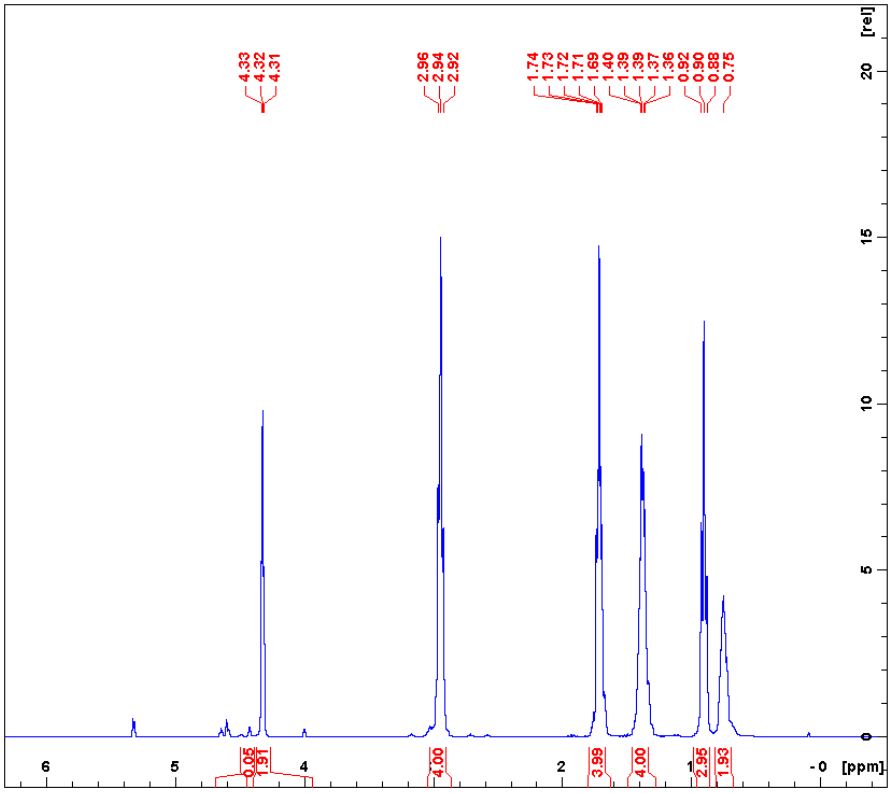

Figure S69. ^{1}H NMR (300 MHz) of ^{n}BuSiH$_2$[N(CH$_2$)$_4$] in CD$_2$Cl$_2$.

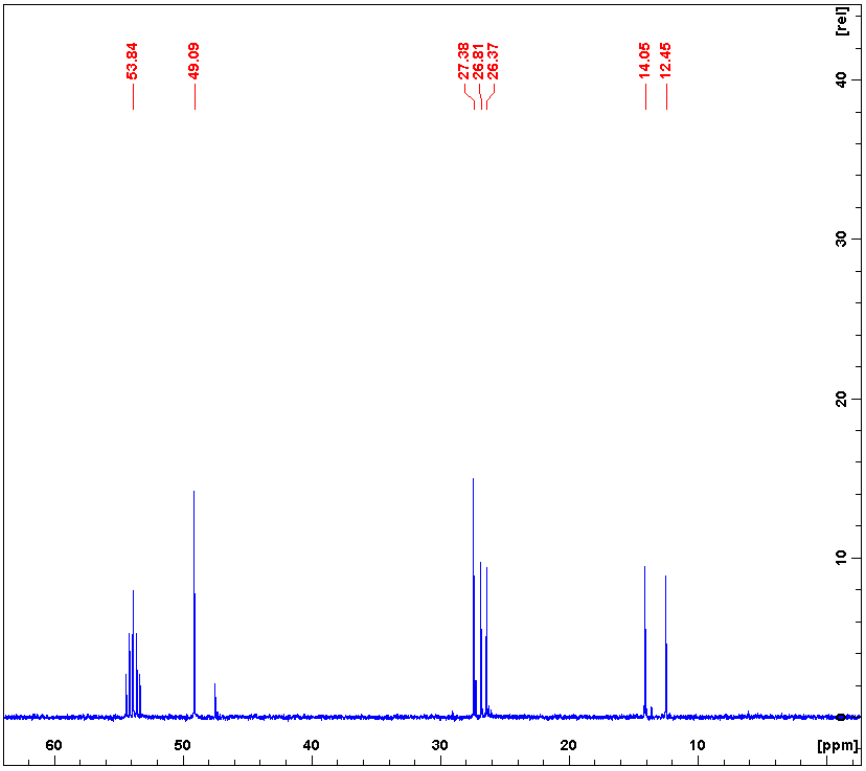

Figure S70. ^{13}C{^{1}H} NMR (100 MHz) of ^{n}BuSiH$_2$[N(CH$_2$)$_4$] in CD$_2$Cl$_2$.

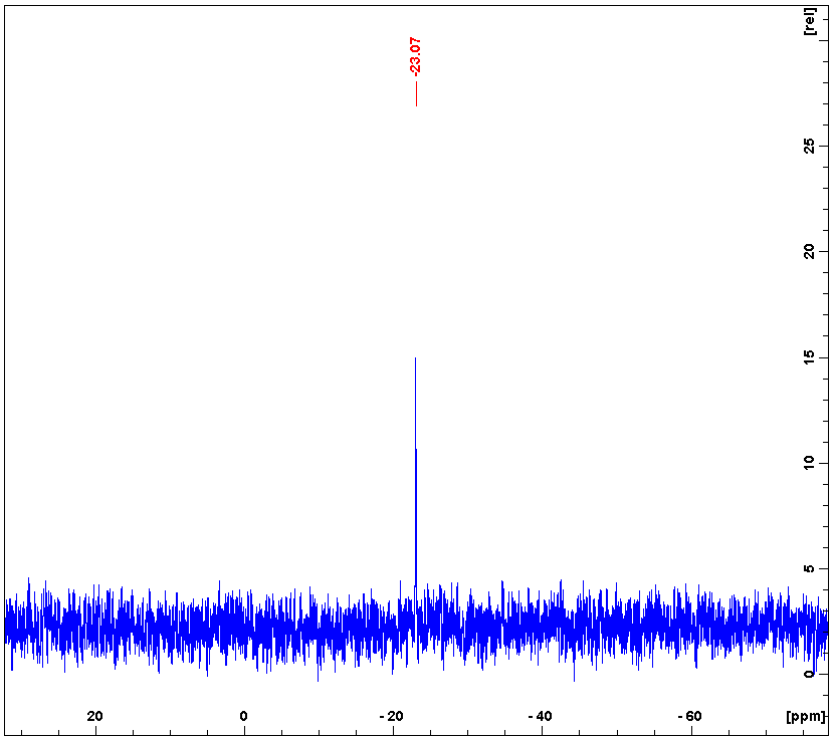

Figure S71. $^{29}Si\{^{1}H\}$ NMR (79 MHz) of $^{n}BuSiH_2[N(CH_2)_4]$ in CD_2Cl_2.

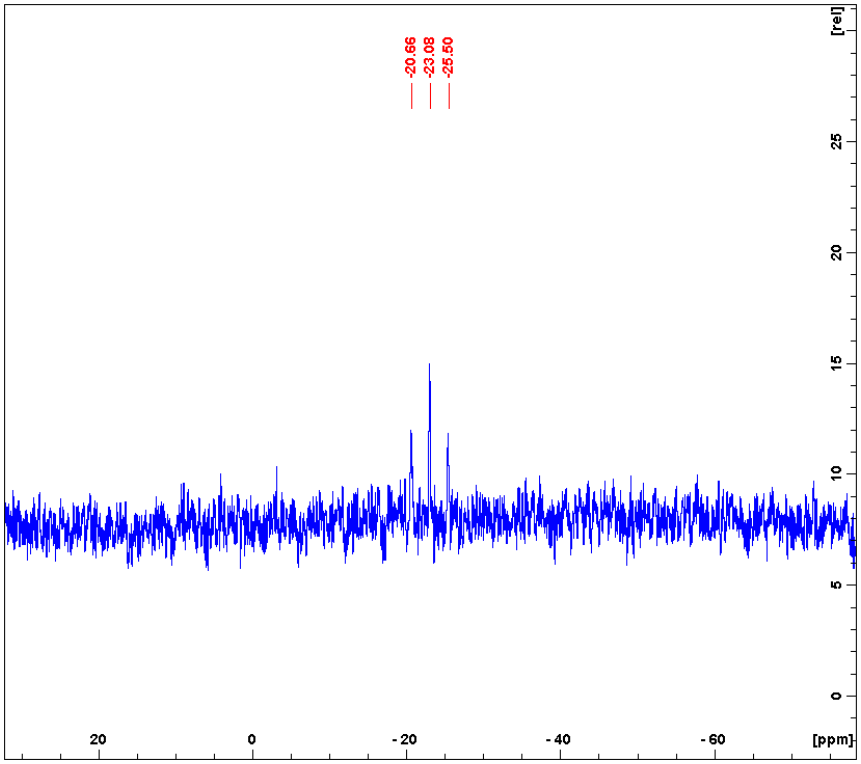

Figure S72. ^{29}Si NMR (79 MHz) of $^{n}BuSiH_2[N(CH_2)_4]$ in CD_2Cl_2.

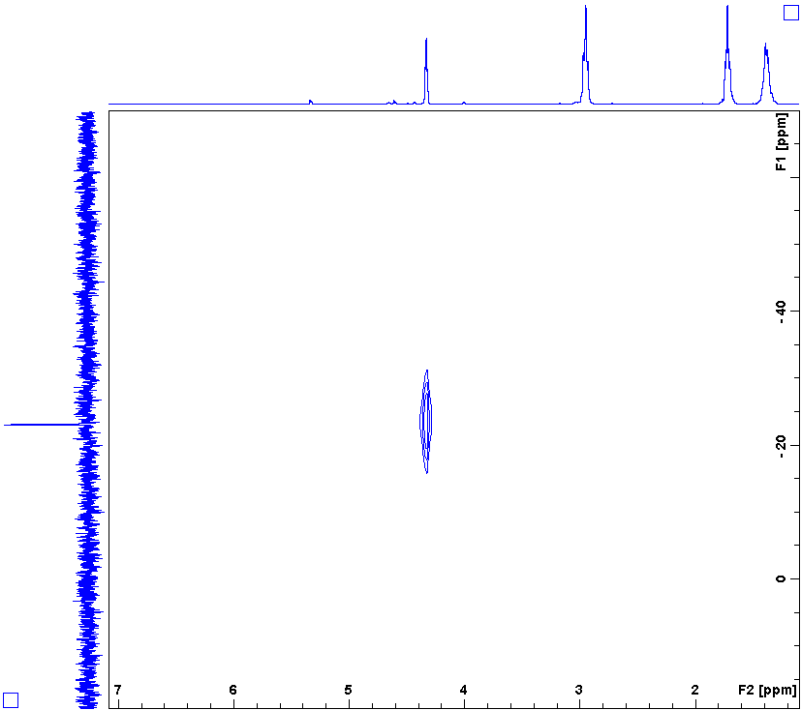

Figure S73. ^{1}H- ^{29}Si HMQC NMR of ^{n}BuSiH$_2$[N(CH$_2$)$_4$] in CD_2Cl_2.

^{n}BuSiH[N(CH$_2$)$_4$]$_2$

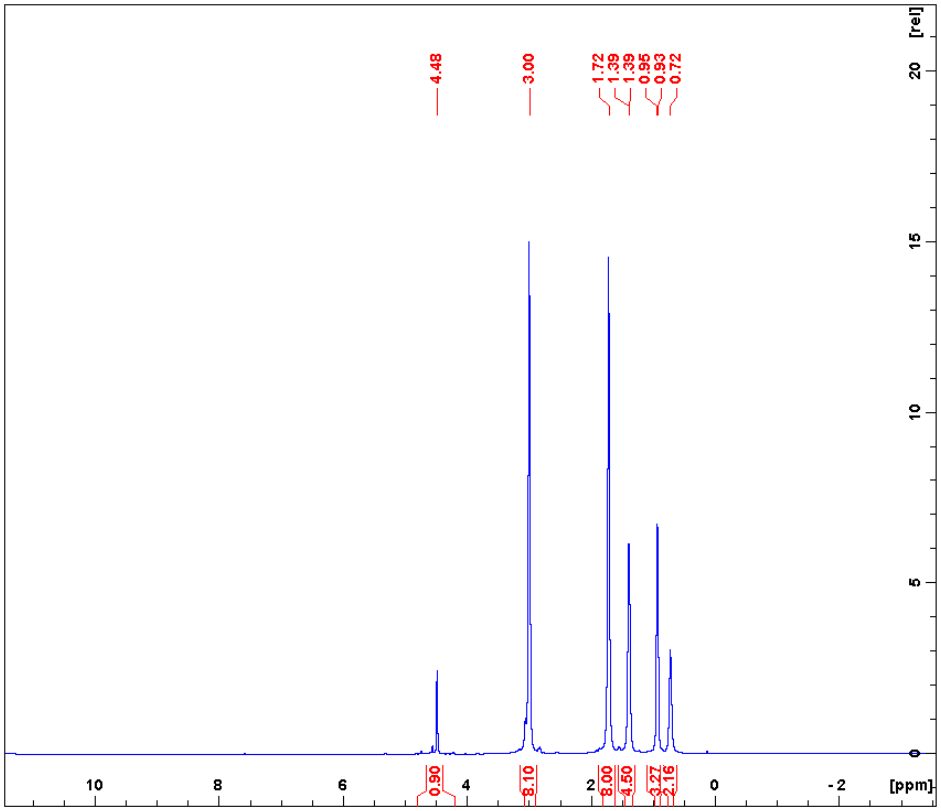

Figure S74. ^{1}H NMR (400 MHz) of ^{n}BuSiH[N(CH$_2$)$_4$]$_2$ in CD_2Cl_2.

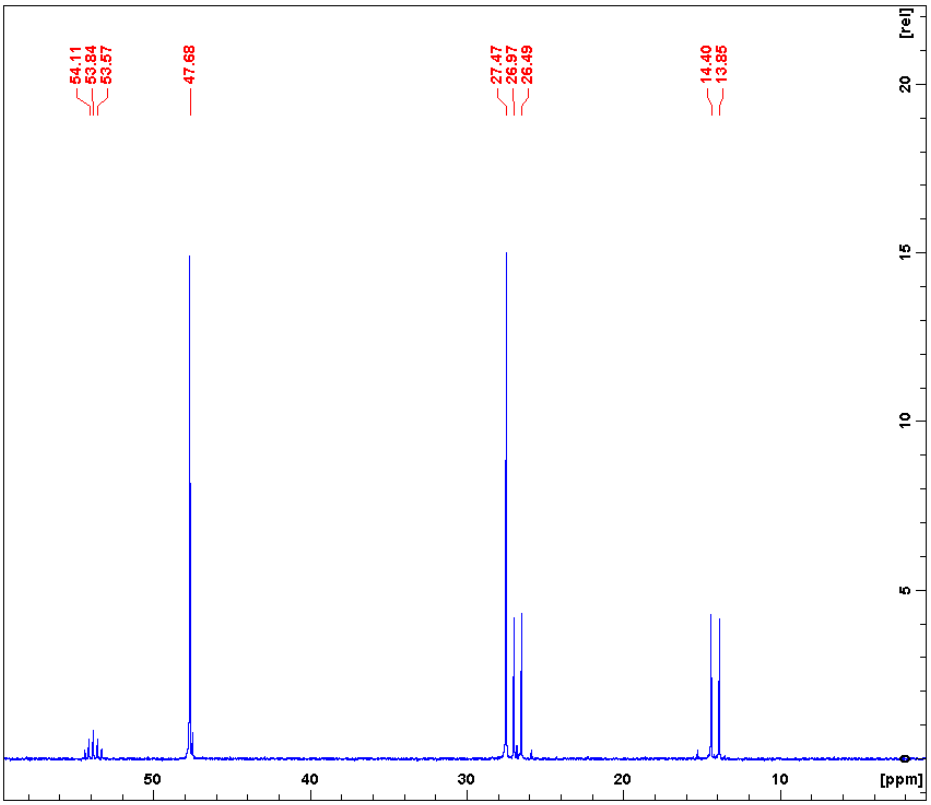

Figure S75. $^{13}C\{^{1}H\}$ NMR (100 MHz) of $^{n}BuSiH[N(CH_2)_4]_2$ in CD_2Cl_2.

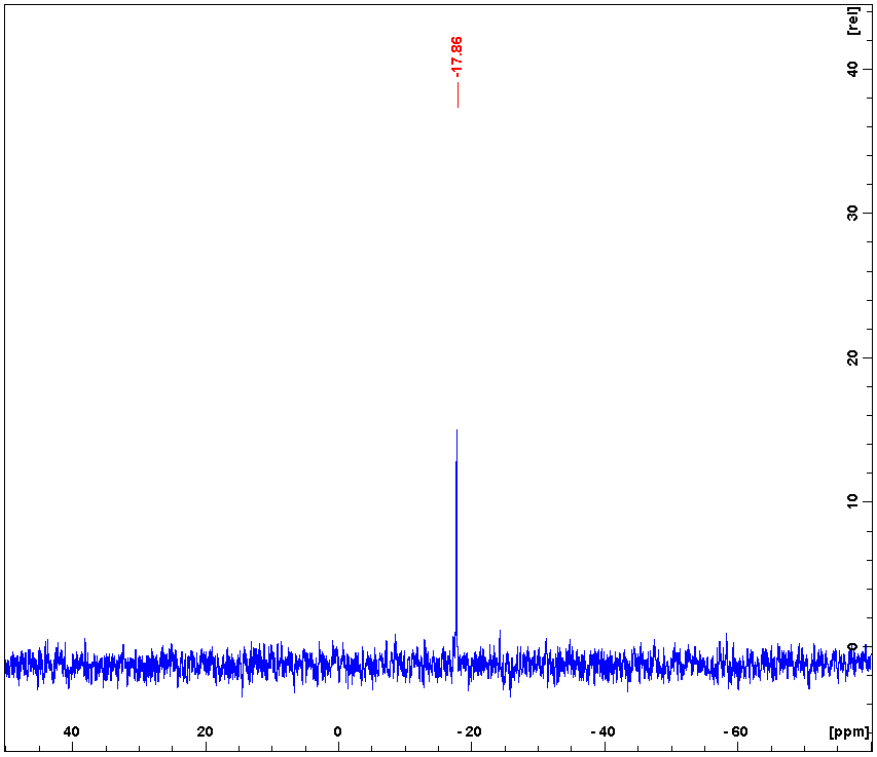

Figure S76. $^{29}Si\{^{1}H\}$ NMR (79 MHz) of $^{n}BuSiH[N(CH_2)_4]_2$ in CD_2Cl_2.

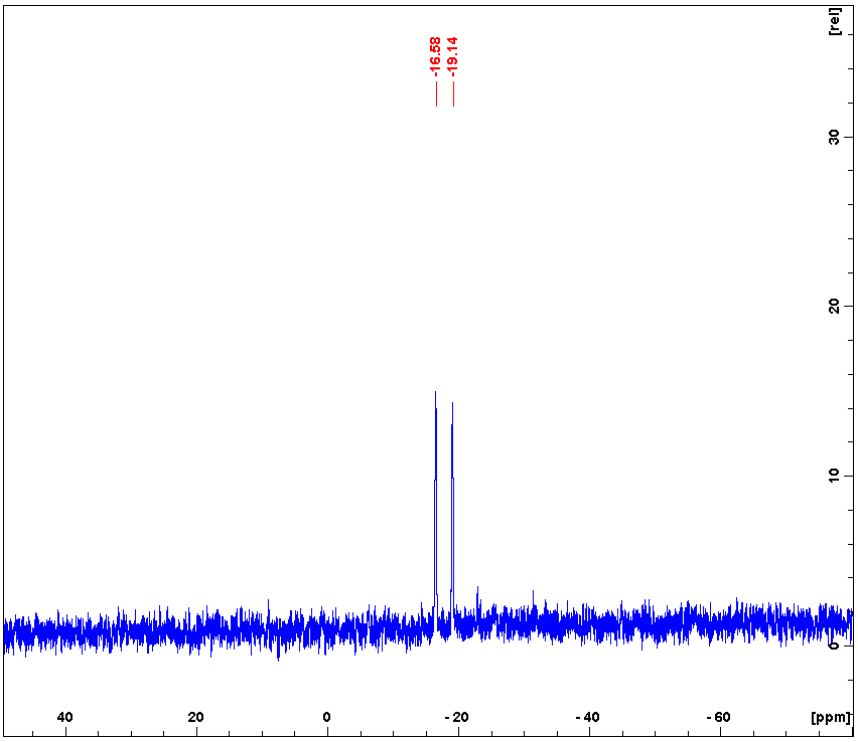

Figure S77. ^{29}Si NMR (79 MHz) of ^{n}BuSiH[N(CH$_2$)$_4$]$_2$ in CD_2Cl_2.

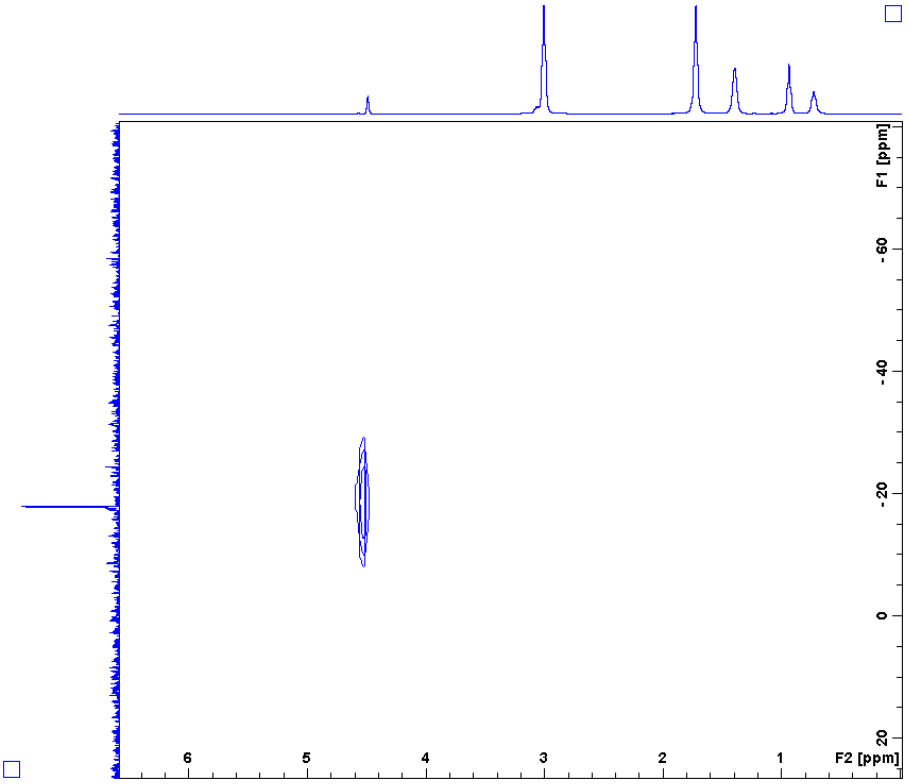

Figure S78. ^{1}H- ^{29}Si HMQC NMR of ^{n}BuSiH[N(CH$_2$)$_4$]$_2$ in CD_2Cl_2.

^{n}BuSiH$_2$(N^{i}Pr$_2$)

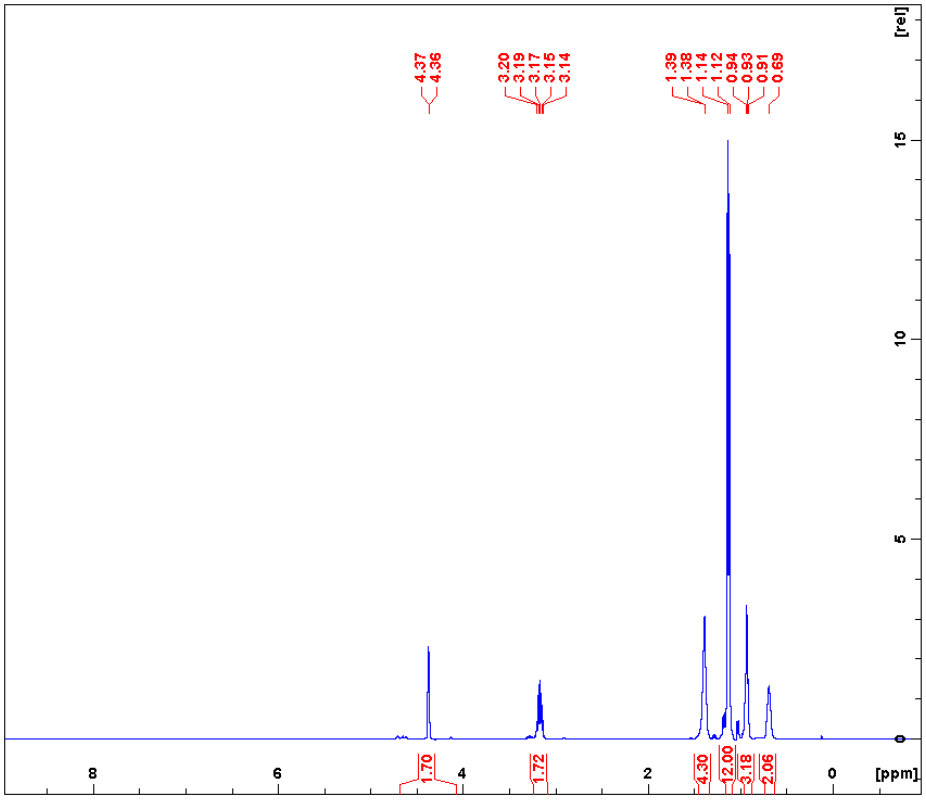

Figure S79. ^{1}H NMR (400 MHz) of ^{n}BuSiH$_2$(N^{i}Pr$_2$) in CD_2Cl_2.

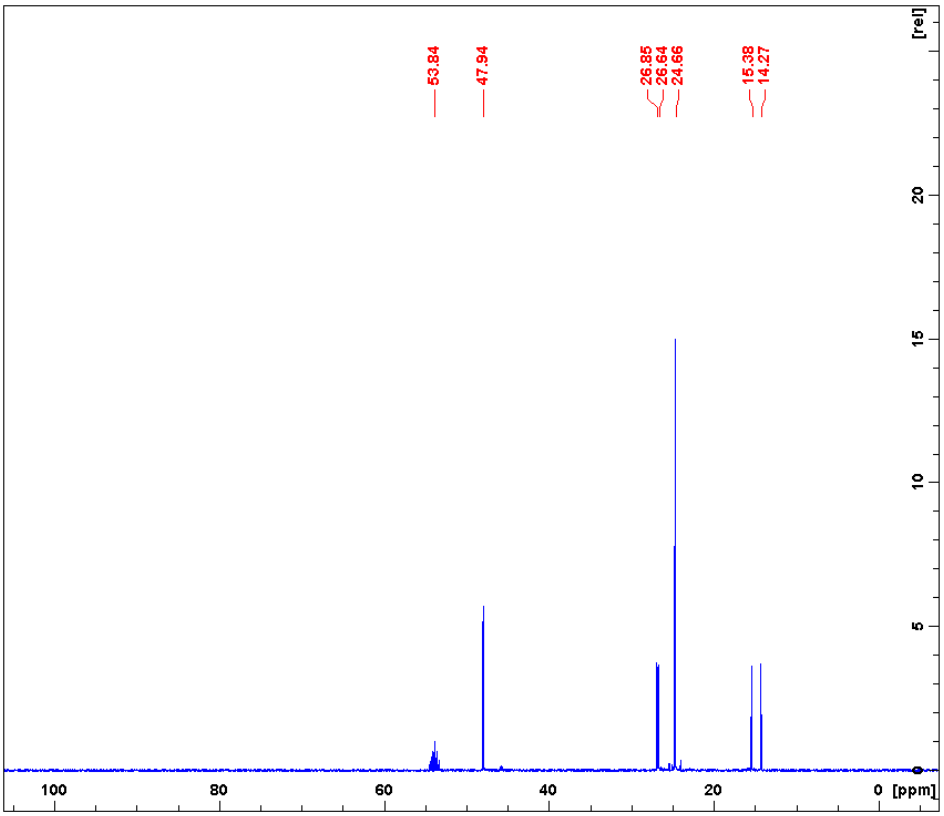

Figure S80. ^{13}C{^{1}H} NMR (100 MHz) of ^{n}BuSiH$_2$(N^{i}Pr$_2$) in CD_2Cl_2.

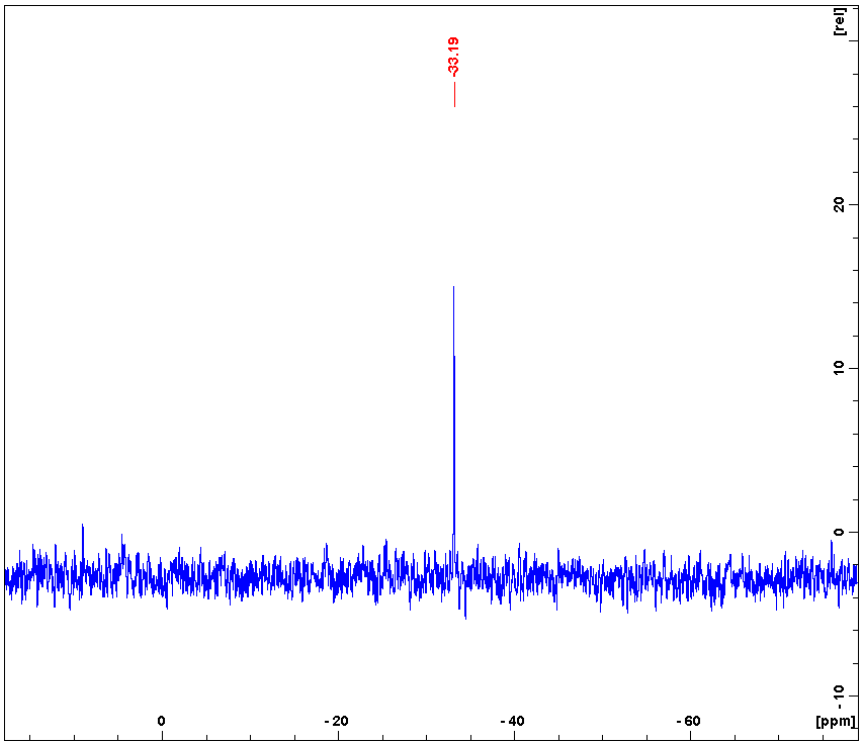

Figure S81. $^{29}Si\{^{1}H\}$ NMR (79 MHz) of $^{n}BuSiH_2(N^{i}Pr_2)$ in CD_2Cl_2.

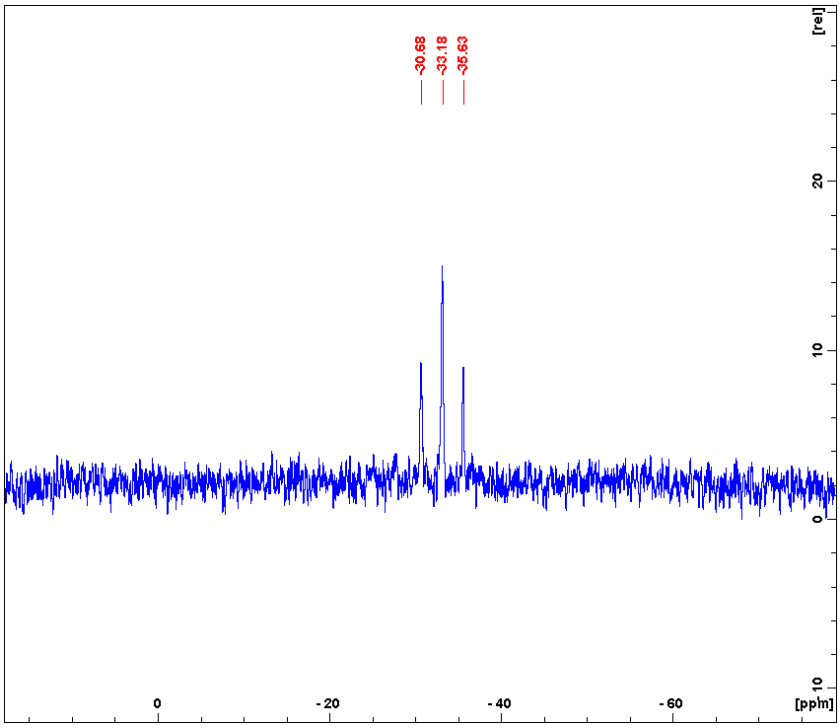

Figure S82. ^{29}Si NMR (79 MHz) of $^{n}BuSiH_2(N^{i}Pr_2)$ in CD_2Cl_2.

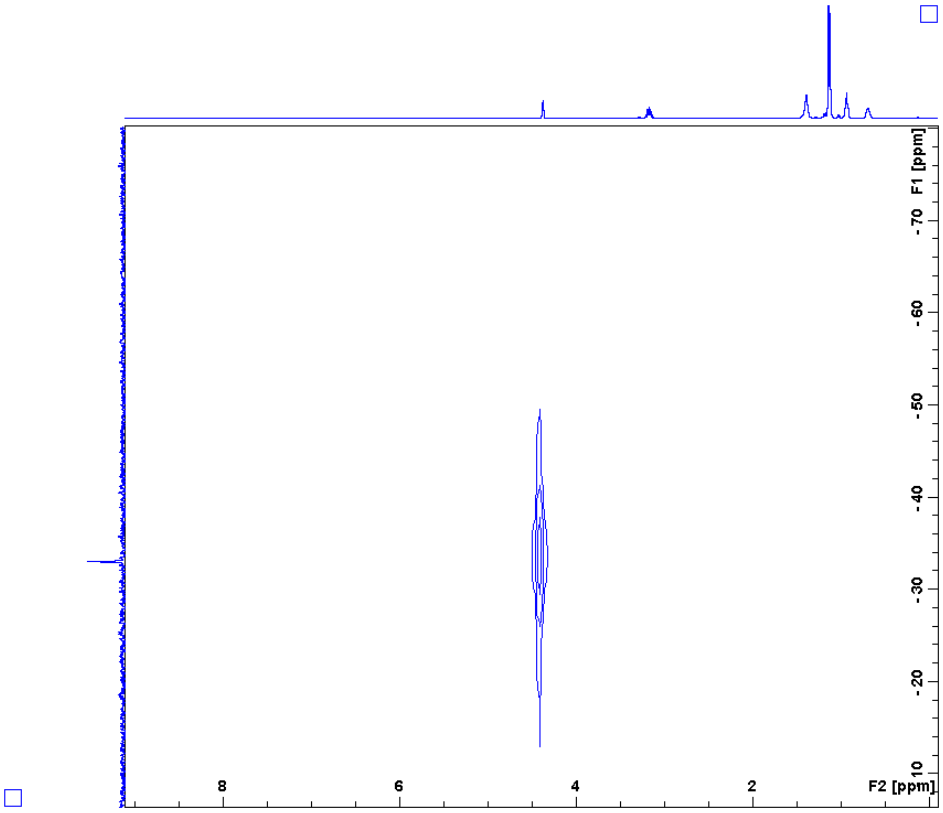

Figure S83. ^{1}H-^{29}Si HMQC NMR of ^{n}BuSiH$_2$(N^{i}Pr$_2$) in CD_2Cl_2.

$Et_2SiH(NEt)_2$

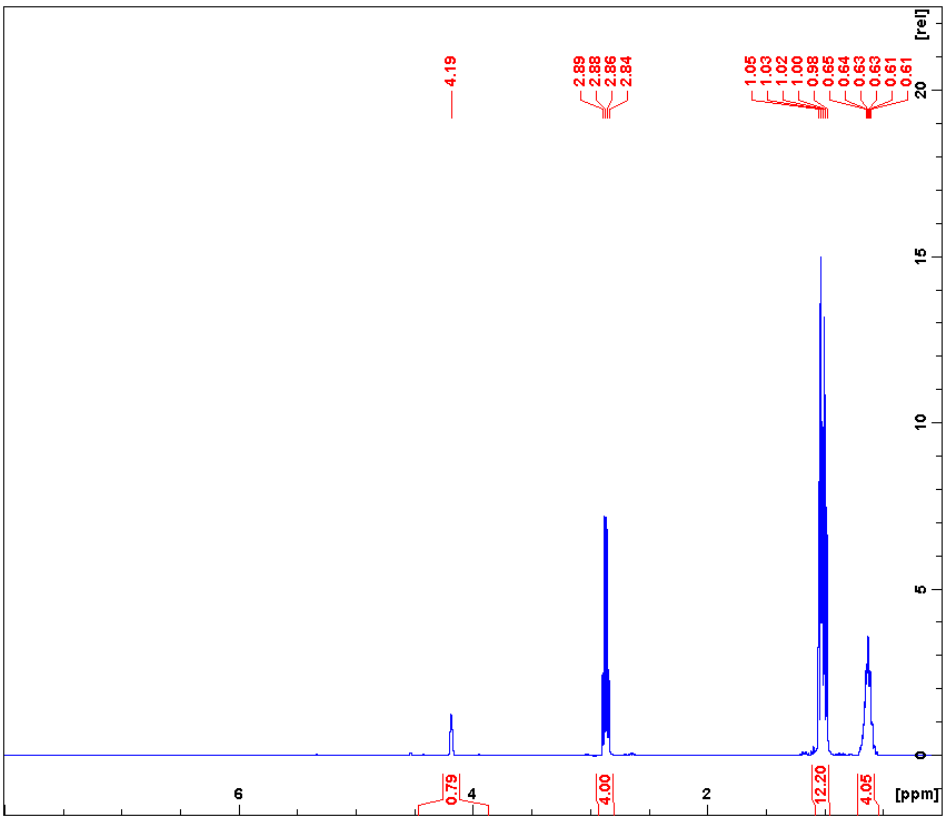

Figure S84. ^{1}H NMR (400 MHz) of $Et_2SiH(NEt)_2$ in CD_2Cl_2.

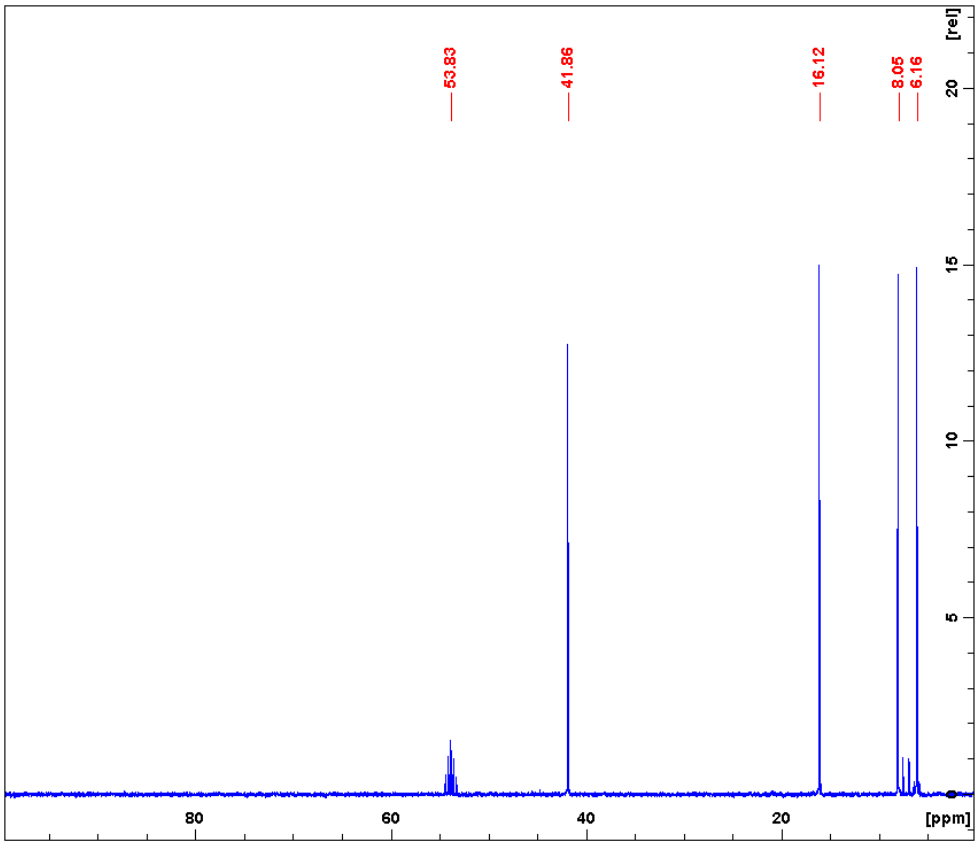

Figure S85. $^{13}C\{^{1}H\}$ NMR (100 MHz) of $Et_2SiH(NEt_2)$ in CD_2Cl_2.

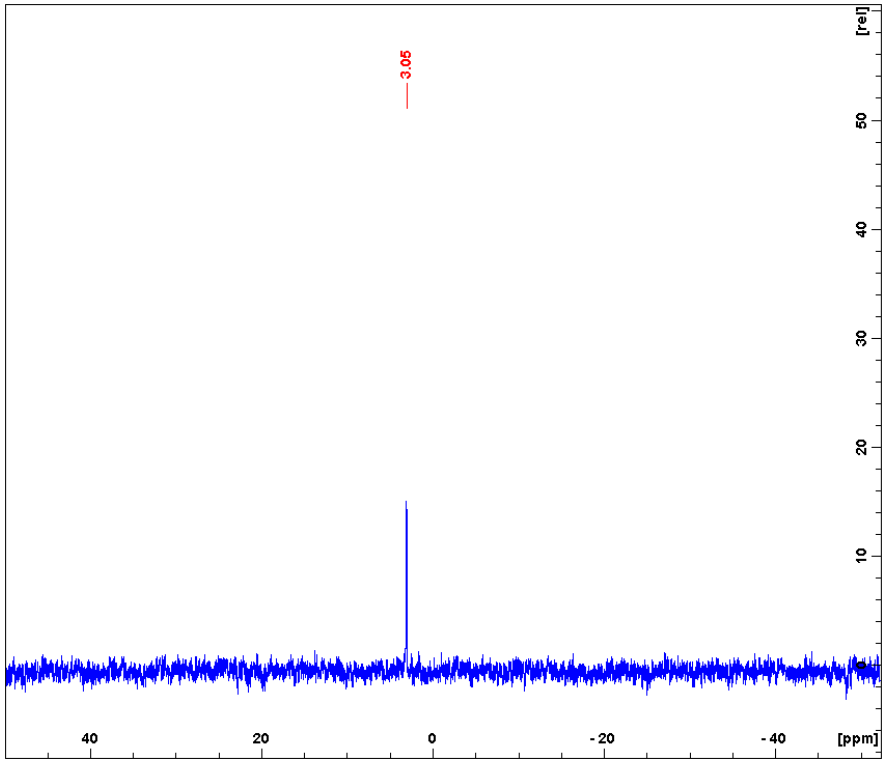

Figure S86. $^{29}Si\{^{1}H\}$ NMR (79 HMz) of $Et_2SiH(NEt_2)$ in CD_2Cl_2.

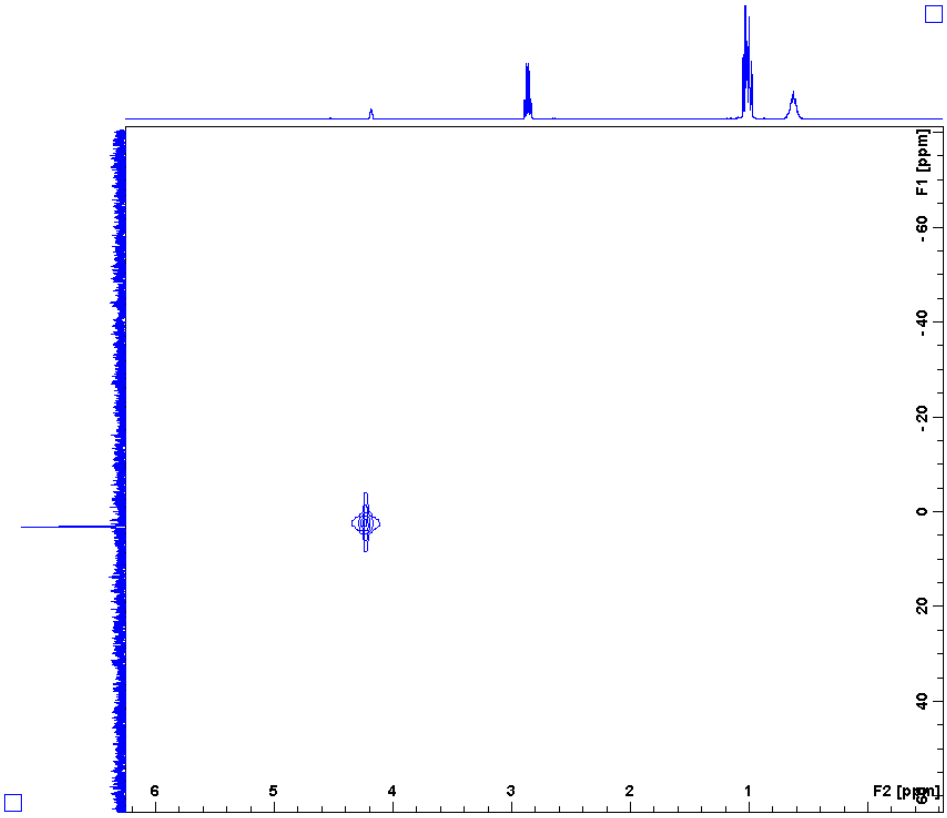

Figure S87. ^{1}H- ^{29}Si HMQC NMR of $Et_2SiH(NEt_2)$ in CD_2Cl_2.

$Et_2SiH(NH^tBu)$

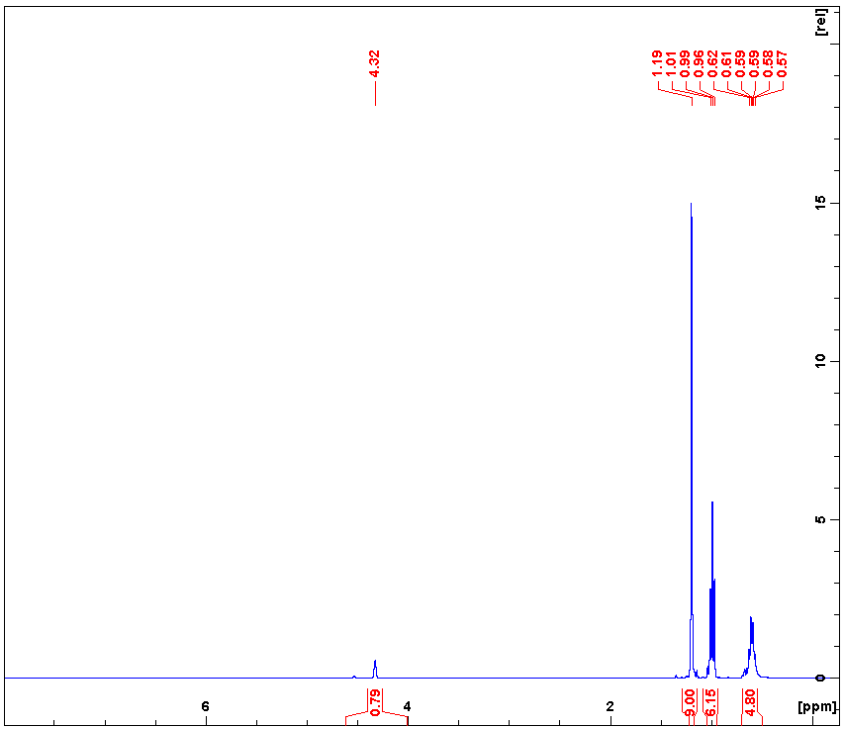

Figure S88. ^{1}H NMR (400 MHz) of $Et_2SiH(NH^tBu)$ in CD_2Cl_2.

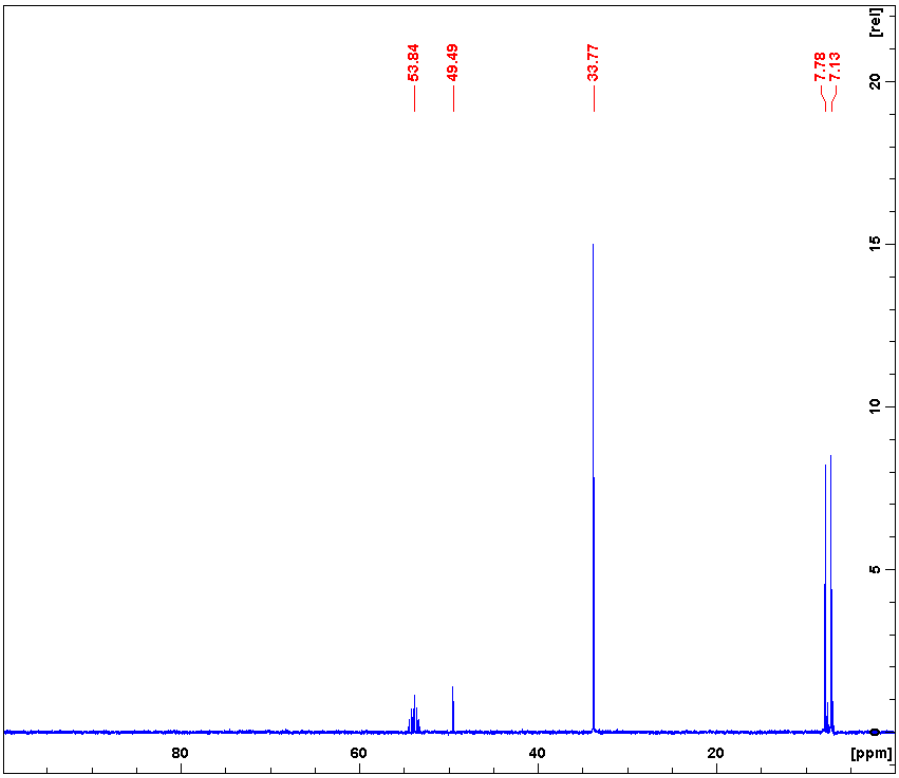

Figure S89. $^{13}C\{^{1}H\}$ NMR (100 MHz) of $Et_2SiH(NH^tBu)$ in CD_2Cl_2.

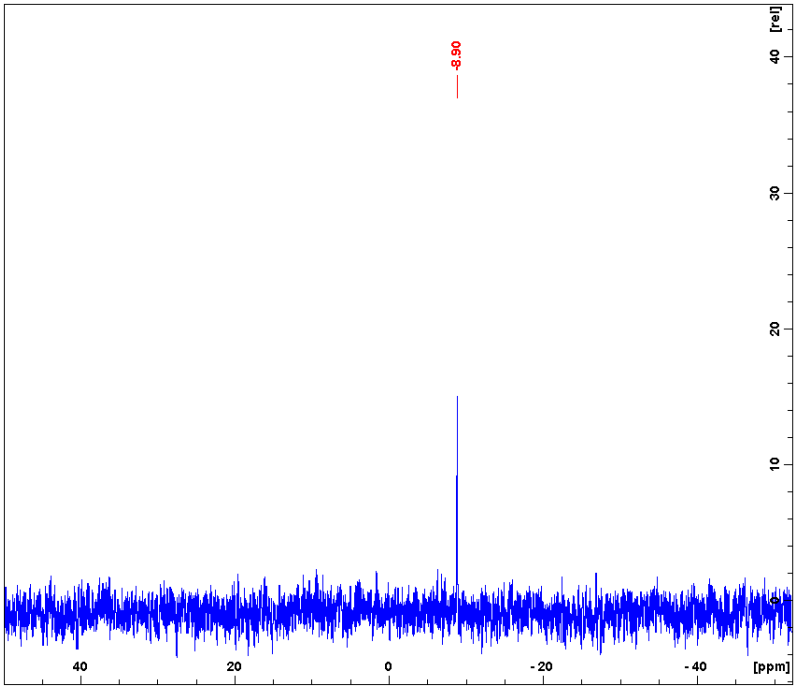

Figure S90. $^{29}Si\{^{1}H\}$ NMR (79 MHz) of $Et_2SiH(NH^tBu)$ in CD_2Cl_2.

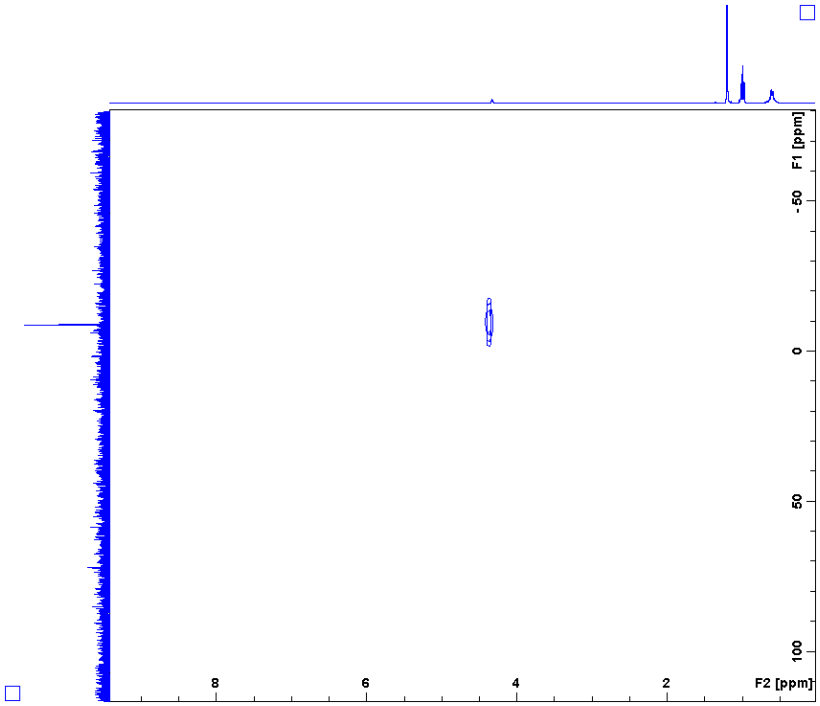

Figure S91. ^{1}H- ^{29}Si HMQC NMR of $Et_2SiH(NH^tBu)$ in CD_2Cl_2.

$Et_2SiH[N(CH_2)_4]$

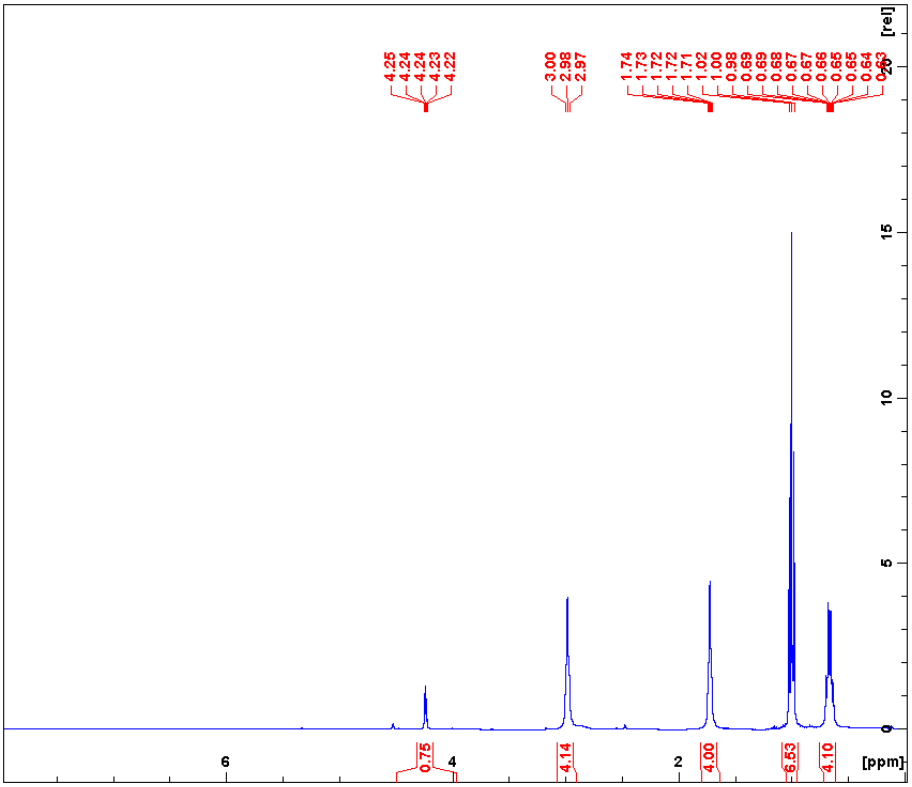

Figure S92. ^{1}H NMR (400 MHz) of $Et_2SiH[N(CH_2)_4]$ in CD_2Cl_2.

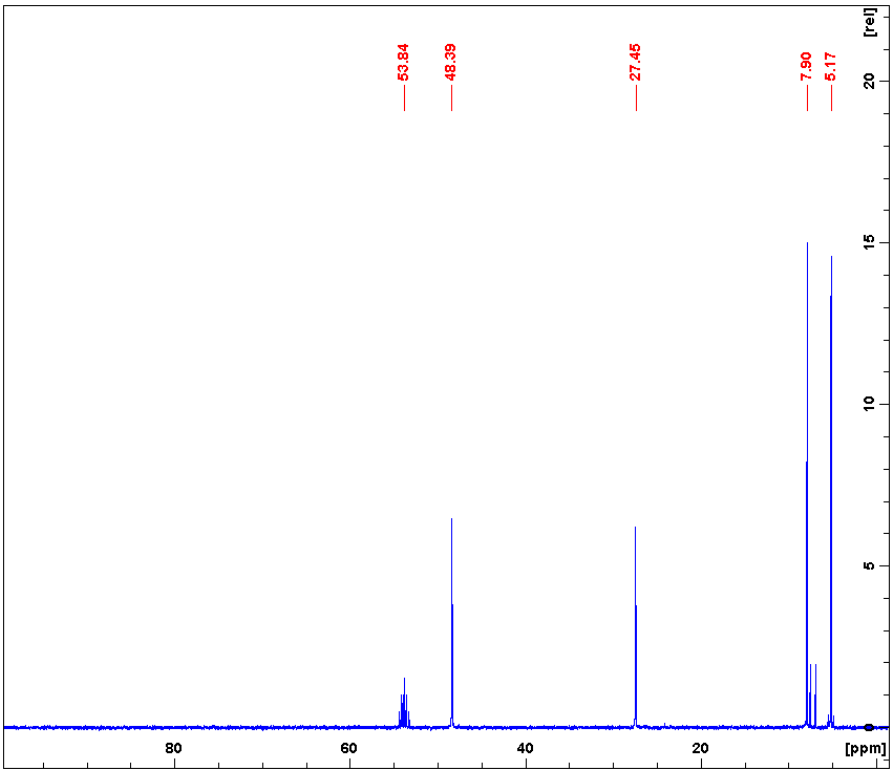

Figure S93. $^{13}C\{^{1}H\}$ NMR (100 MHz) of $Et_2SiH[N(CH_2)_4]$ in CD_2Cl_2.

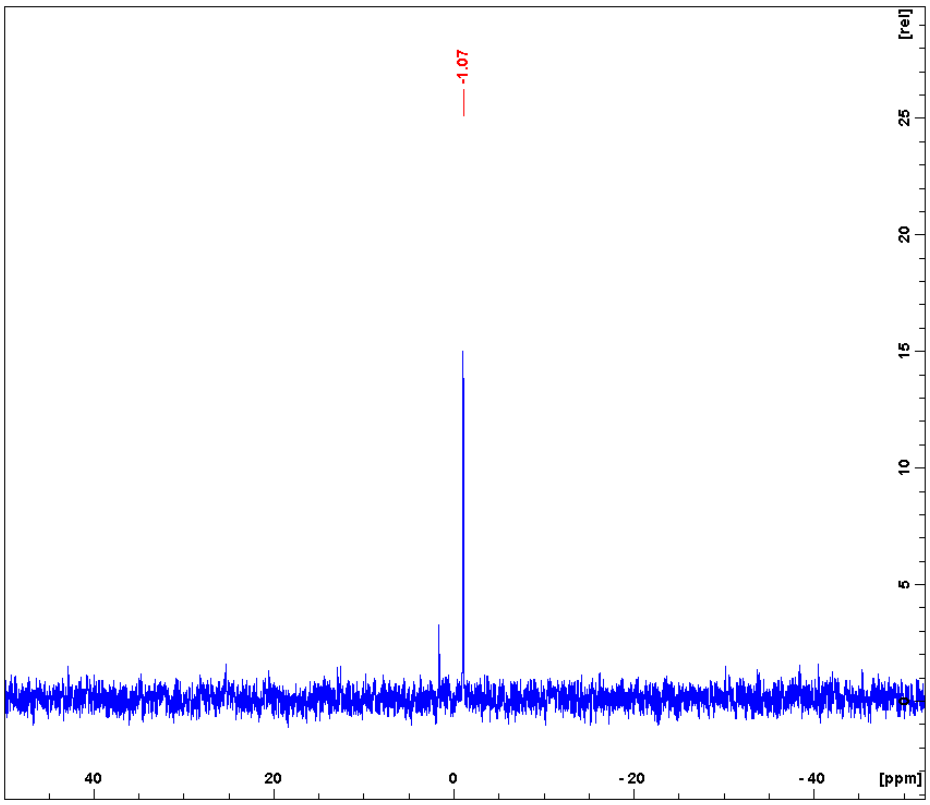

Figure S94. $^{29}Si\{^{1}H\}$ NMR (79 MHz) of $Et_2SiH[N(CH_2)_4]$ in CD_2Cl_2.

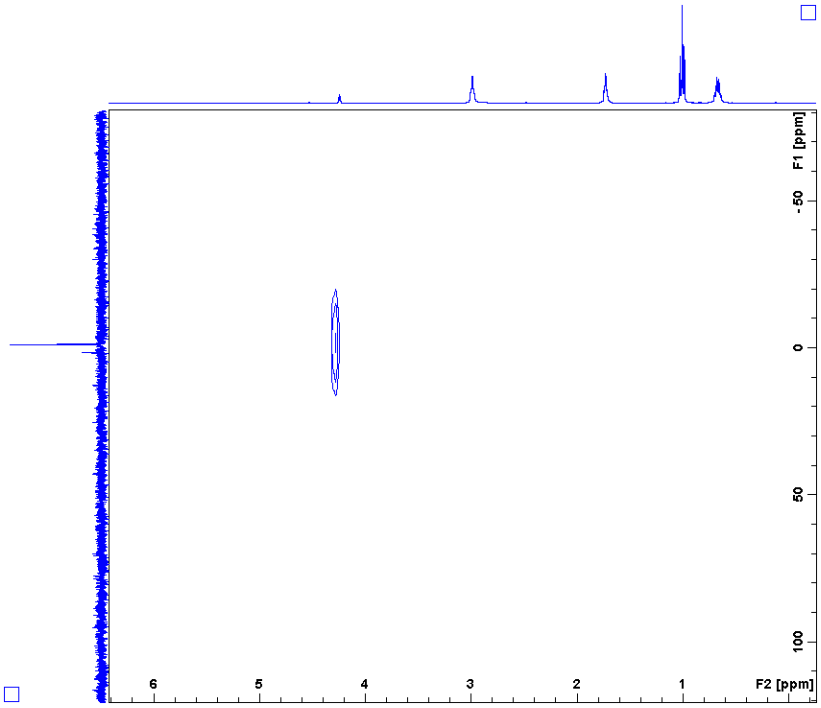

Figure S95. ^{1}H- ^{29}Si HMQC NMR of $Et_2SiH[N(CH_2)_4]$ in CD_2Cl_2.

3. Low Temperature NMR reaction of 1a, NEt_2H and Ph_2SiH_2.

50 mg (0.035 mmol) of complex **1a** and 3.7 μL of NEt_2H (0.035 mmol) were dissolved in 0.4 mL of d^8-THF in a screw-capped NMR tube. The solution was cooled to -80 °C and a cooled solution (-80 °C) of 7.8 μL Ph_2SiH_2 (0.042 mmol) in 0.2 mL of d^8-THF was transferred via cannula to the NMR tube. The solution was shaken and immediately inserted in a pre-cooled (-80 °C) NMR apparatus. ^{1}H NMR spectra were recorded at several temperatures between -70 to 25 °C, at intervals of 10 °C.

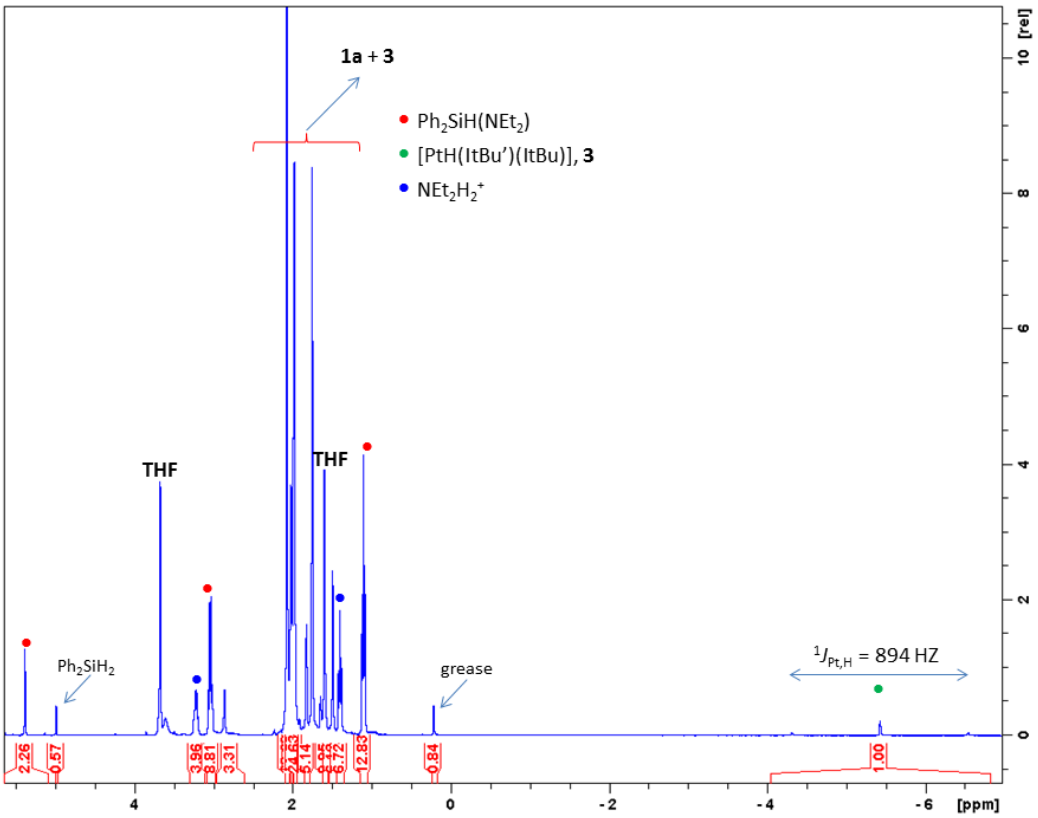

Figure S96. Portion of the ^{1}H NMR (400 MHz) spectrum of the reaction of **1a**, Ph_2SiH_2 and NEt_2H recorded at -30 °C, in d^8-THF.

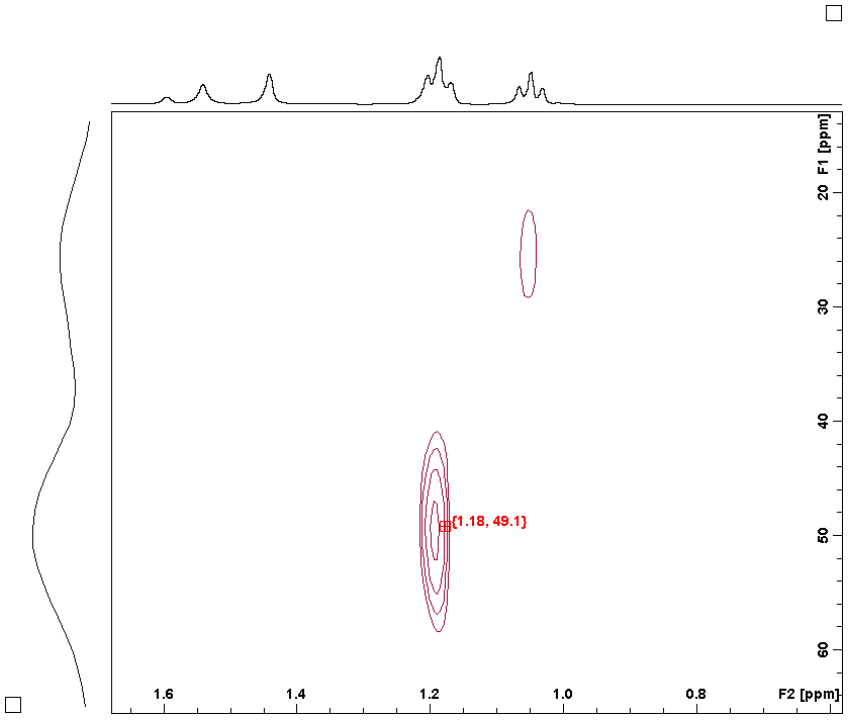

Figure S97. Portion of the ^{1}H,^{15}N -HMBC spectrum of the reaction of **1a**, Ph_2SiH_2 and NEt_2H recorded at -30 °C, in d^8-THF.

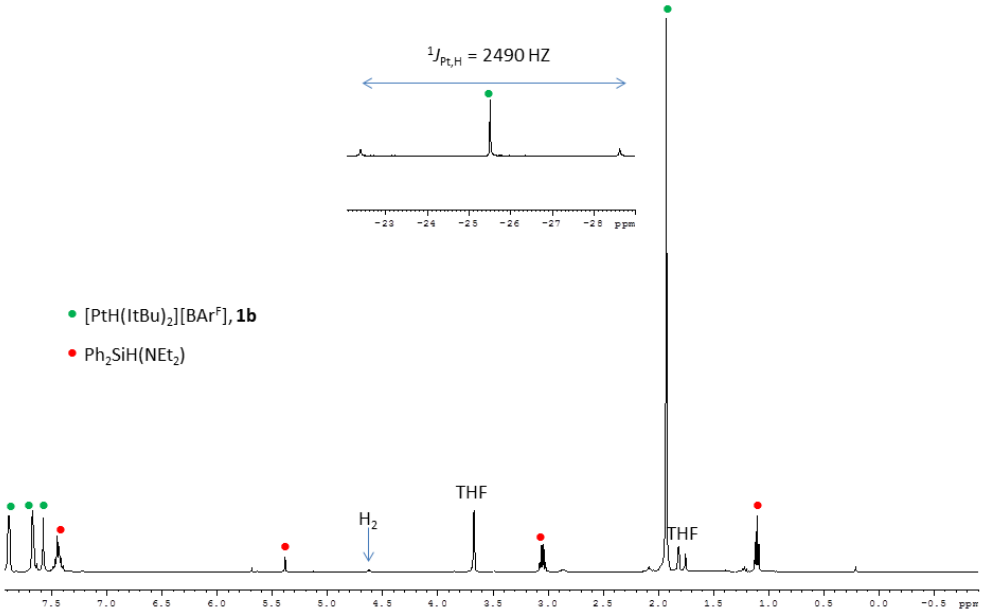

Figure S98. ^{1}H NMR (400 MHz) spectrum of the reaction of **1a**, Ph_2SiH_2 and NEt_2H recorded at 25 °C, in d^8-THF.

4. Synthesis of [NEt$_2$H$_2$][BAr^F]

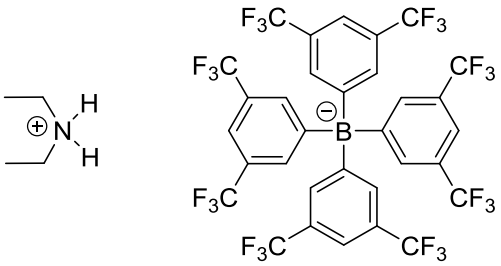

In a glovebox, a solution of Et_2NH (2.7 µL, 25.9 µmol) in CD_2Cl_2 (0.2 mL) was added to a screw-capped NMR tube containing a solution of $H(Et_2O)_2BAr_4^F$ (25 mg, 24.7 µmol) in CD_2Cl_2 (0.3 mL). After confirming by ^{1}H NMR the formation of the ammonium species, the solution was transferred via cannula to a J. Young flask. The solvent and the slight excess of amine were removed under vacuum, affording a white solid, which was redissolved in d^8-THF and analyzed by NMR to compare the spectra with those of the low-temperature experiments. The NH_2 protons were detected only at low temperatures (see below).

^{1}H-NMR (400 MHz, d^8-THF, 25 °C): δ 1.31 (t, $^3J_{HH}$ = 7.3 Hz, 6H, CH_3), 3.14 (m, , 4H, CH_2), 7.59 (s, 4H, Ph-CH_p), 7.79 (s, 8H, Ph-CH_o). ^{13}C{^{1}H}-NMR (100 MHz, CD_2Cl_2,

25 ^{0}C): δ 12.2 (*C*H$_3$), 43.0 (*C*H$_2$) ^{1}H-NMR (400 MHz, d^{8}-THF, -50 °C): δ 7.60 (bs, 2H, N*H*$_2$).

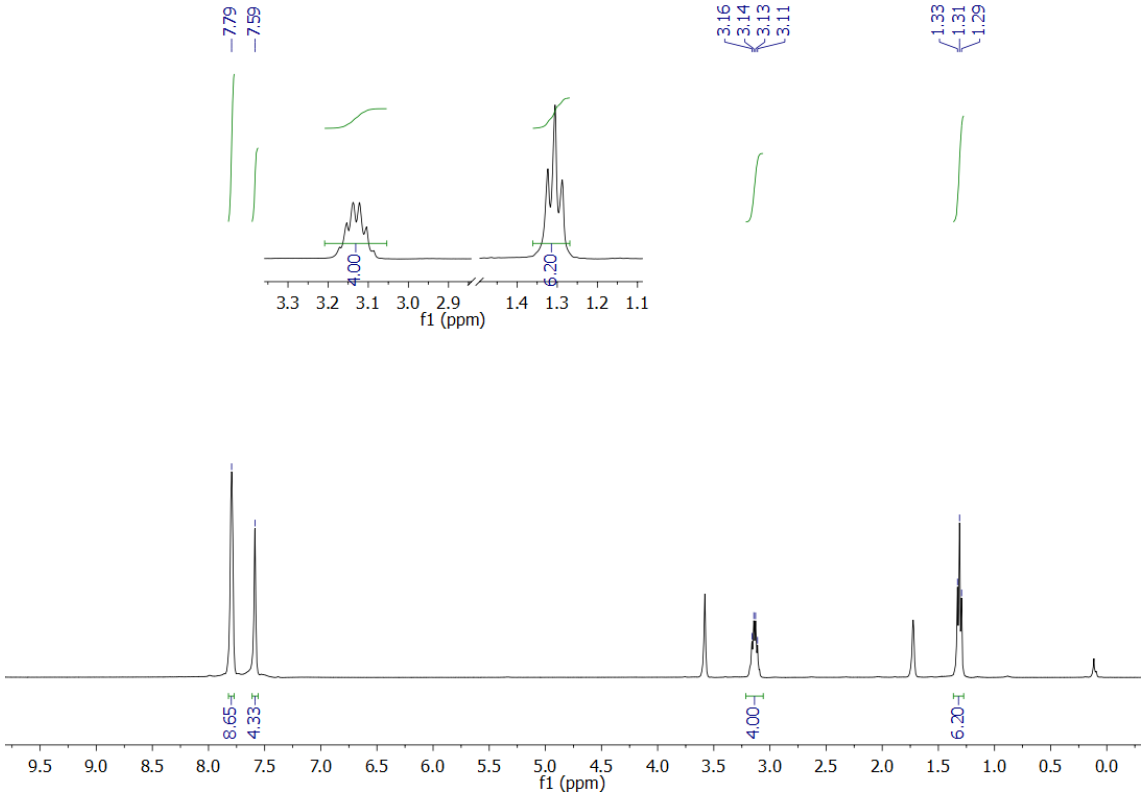

Figure S99. ^{1}H NMR (400 MHz) of [Et$_2$NH$_2$][BAr^{F}] at 25 °C.

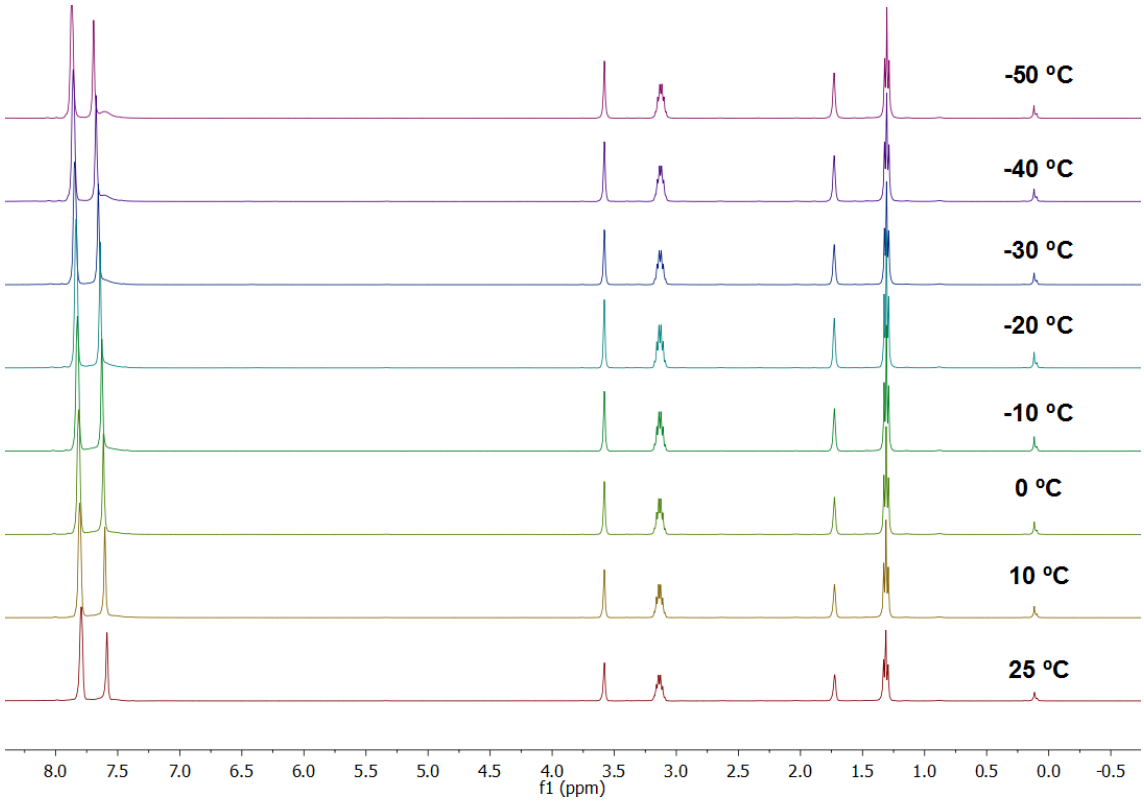

Figure S100. ^{1}H NMR (400 MHz) of [Et$_2$NH$_2$][BAr^{F}] at different temperatures.

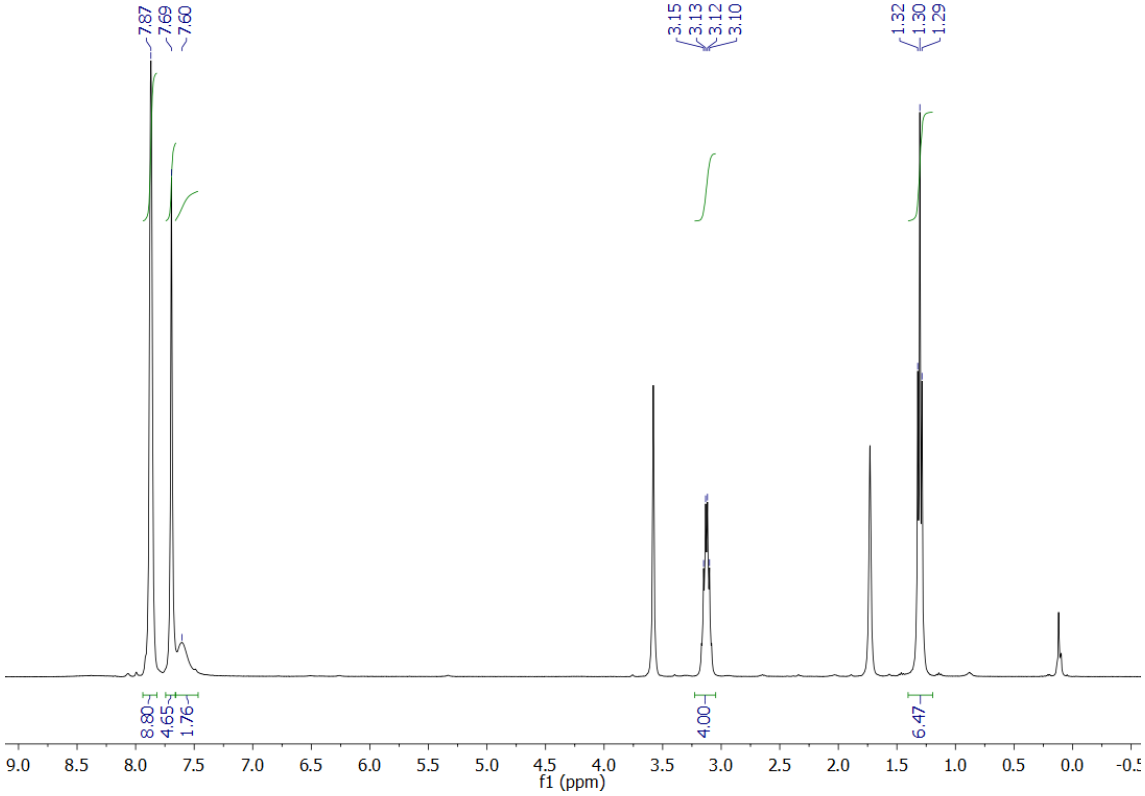

Figure S101. ^{1}H NMR (400 MHz) of $[Et_2NH_2][BAr^F]$ at -50 °C.

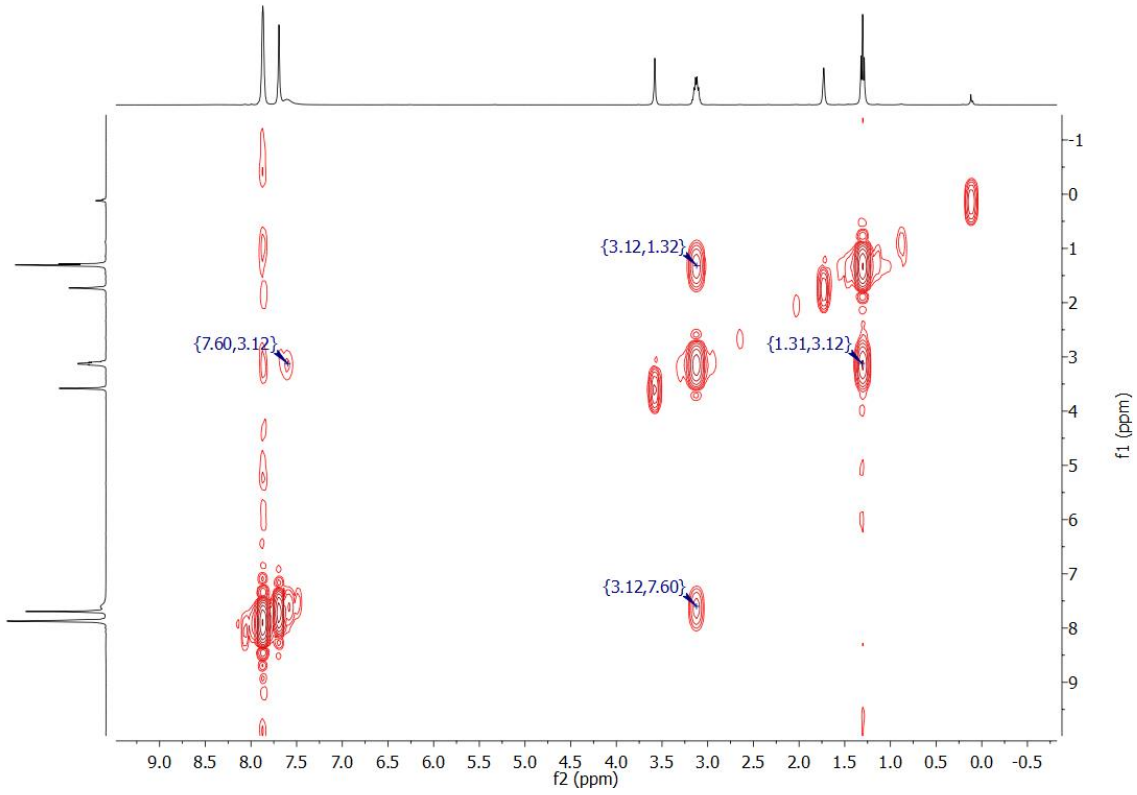

Figure S102. COSY spectrum of $[Et_2NH_2][BAr^F]$ at -50 °C. The cross-peaks between the NH_2 peak and the alkyl chains can be observed.

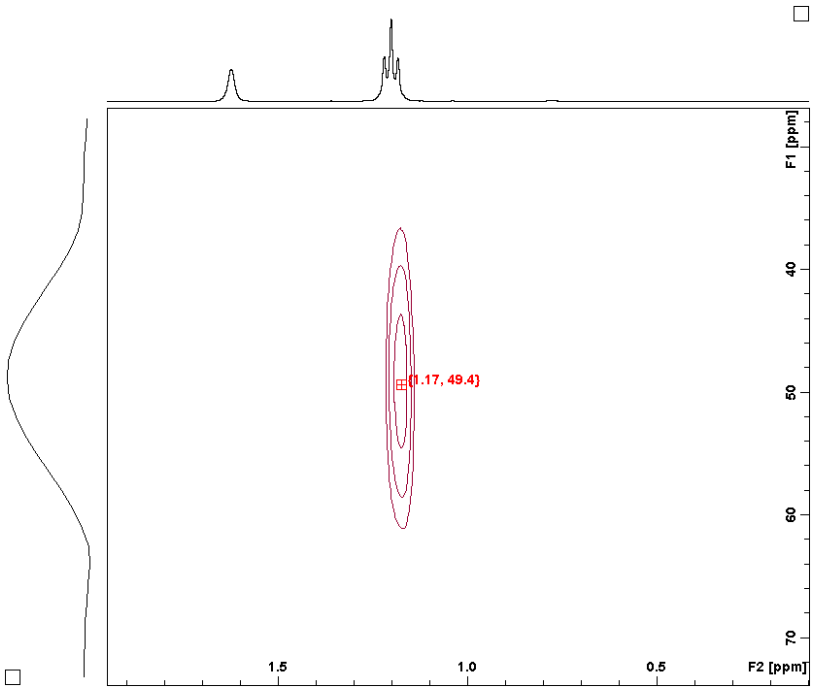

Figure S103. Portion of the $^{1}H,^{15}N$-HMBC spectrum of $[Et_2NH_2][BAr^F]$ at -30 °C.

5. H_2 Evolution graphics

Examples of H_2 evolution measured in a closed system.

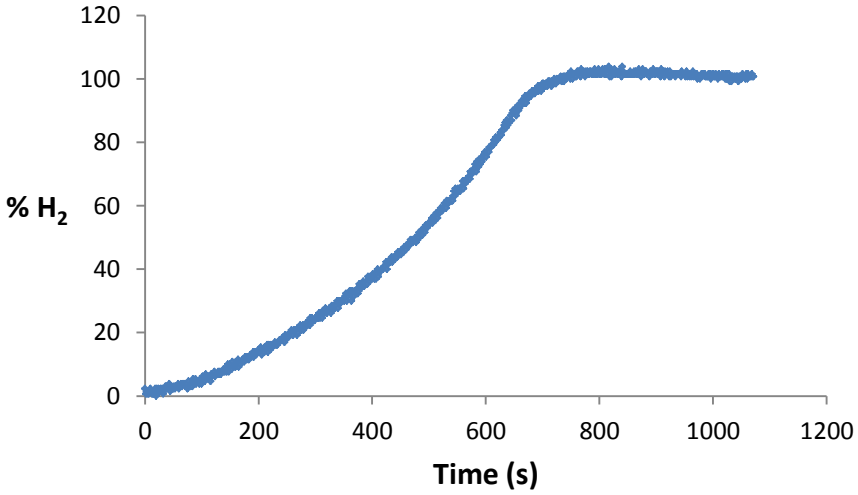

Figure S104. Monitoring of the amount of H_2 released in the catalytic dehydrogenation of $PhSiH_3$ and N^tBuH_2 (1 : 1 ratio) with 50 ppm of complex **1a** in a closed reaction vessel.

Since sigmoid-like kinetic shapes are usually associated to the formation of nanoparticles, a poisoning experiment using a large excess of Hg (1000 equiv) was

performed. Nevertheless, the reaction proceeded at the same rate with identical kinetic sigmoid profile, ruling out the formation nanoparticles or colloids during the reaction.

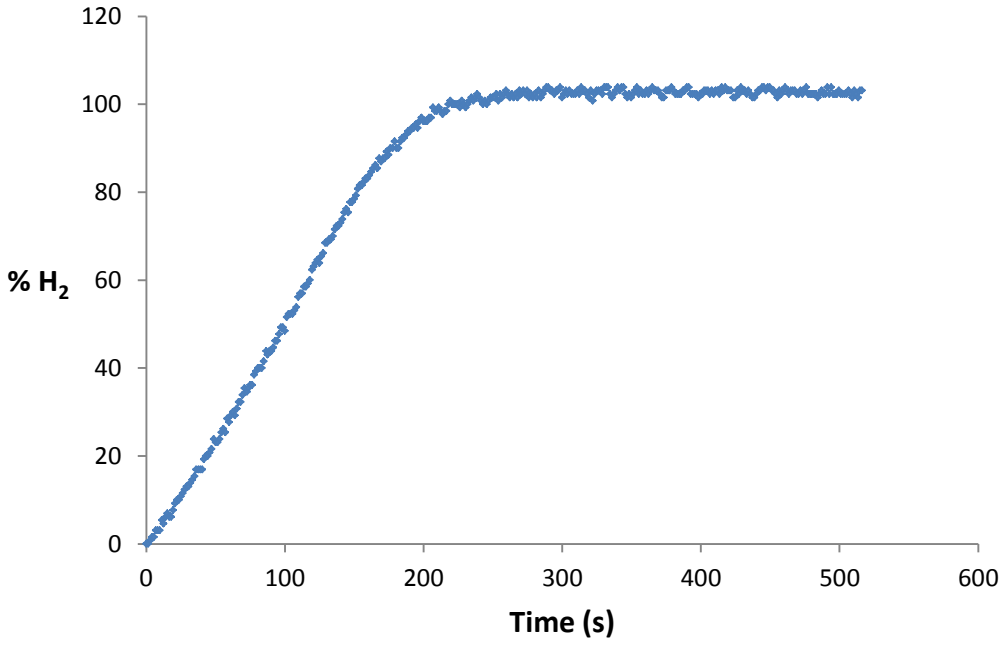

Figure S105. Monitoring of the amount of H_2 released in the catalytic dehydrogenation of $PhSiH_3$ and NEt_2H (1 : 1 ratio) with 50 ppm of complex **1a** in a closed reaction vessel.

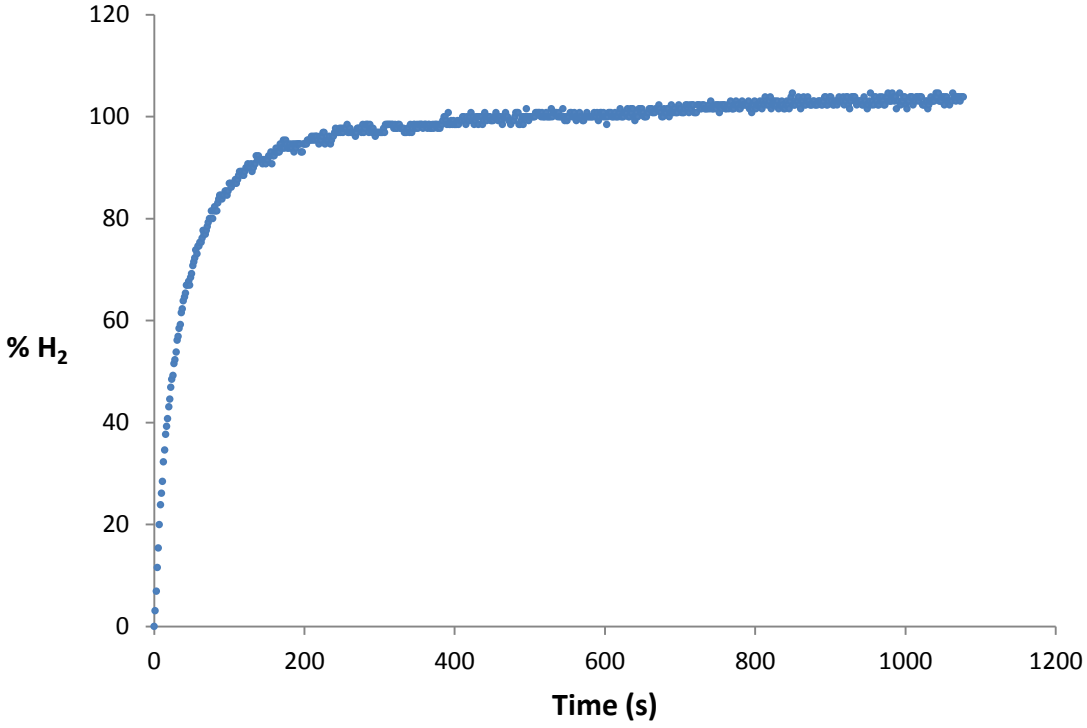

Figure S106. Monitoring of the amount of H_2 released in the catalytic dehydrogenation of $PhSiH_3$ and N^iPr_2H (1 :1 ratio) with 0.3% complex **1a** in a closed reaction vessel.

Kinetic profiles in all reactions with Ph_2SiH_2 (and Et_2SiH_2) exhibit exponential shapes This different behaviour might be related to a more efficient interaction of Ph_2SiH_2 with the metal compared to $PhSiH_3$ (calculated ΔE_{int} is 4.8 kcal·mol^{-1} higher for this silane). An analogous result has been previously observed in the interaction of ^{n}BuSiH$_3$ and Et_2SiH_2 with complexes **1a** (see ref. 9 in manuscript).

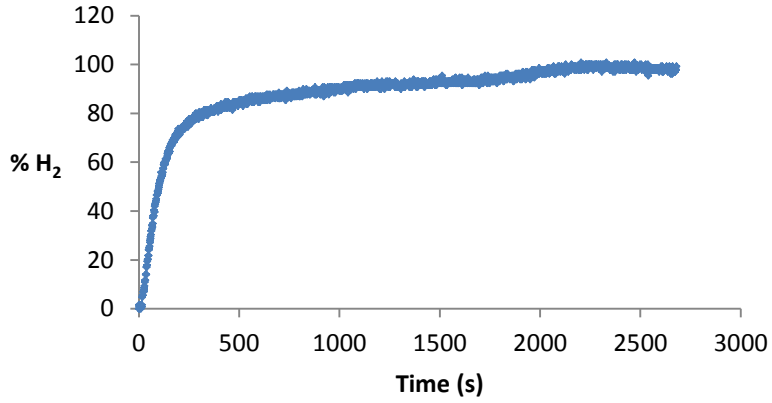

Figure S107. Monitoring of the amount of H_2 released in the catalytic dehydrogenation of Ph_2SiH_2 and N^tBuH_2 (1 : 1 ratio) with 0.1% of complex **1a** in a closed reaction vessel.

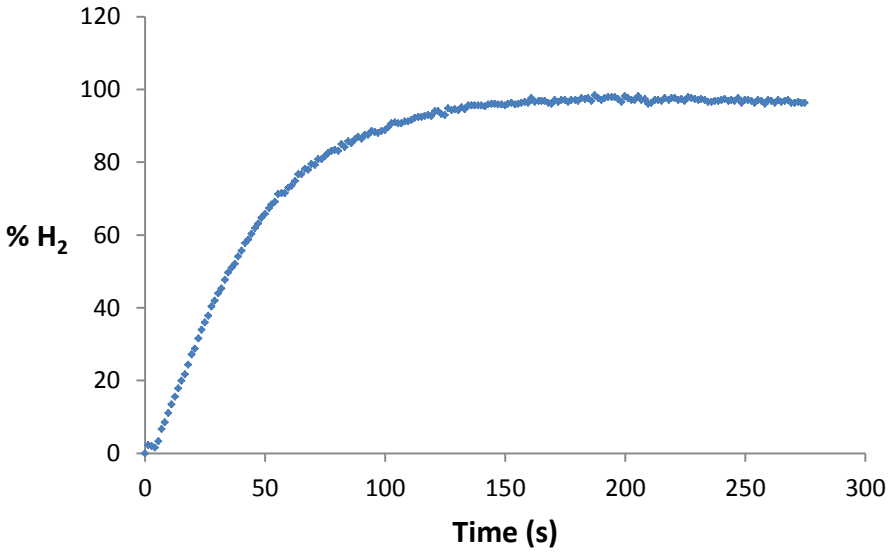

Figure S108. Monitoring of the amount of H_2 released in the catalytic dehydrogenation of Ph_2SiH_2 and NEt_2H (1 : 1 ratio) with 0.3% of complex **1a** in a closed reaction vessel.

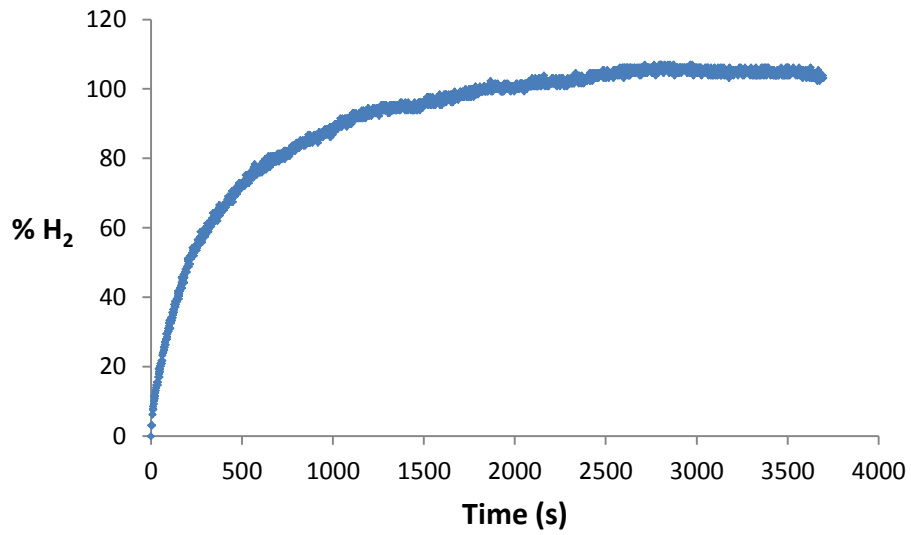

Figure S109. Monitoring of the amount of H_2 released in the catalytic dehydrogenation of Ph_2SiH_2 and $NH(CH_2CH_2)_2$ (1:1 ratio) with 0.2% of complex **1a** in a closed reaction vessel.

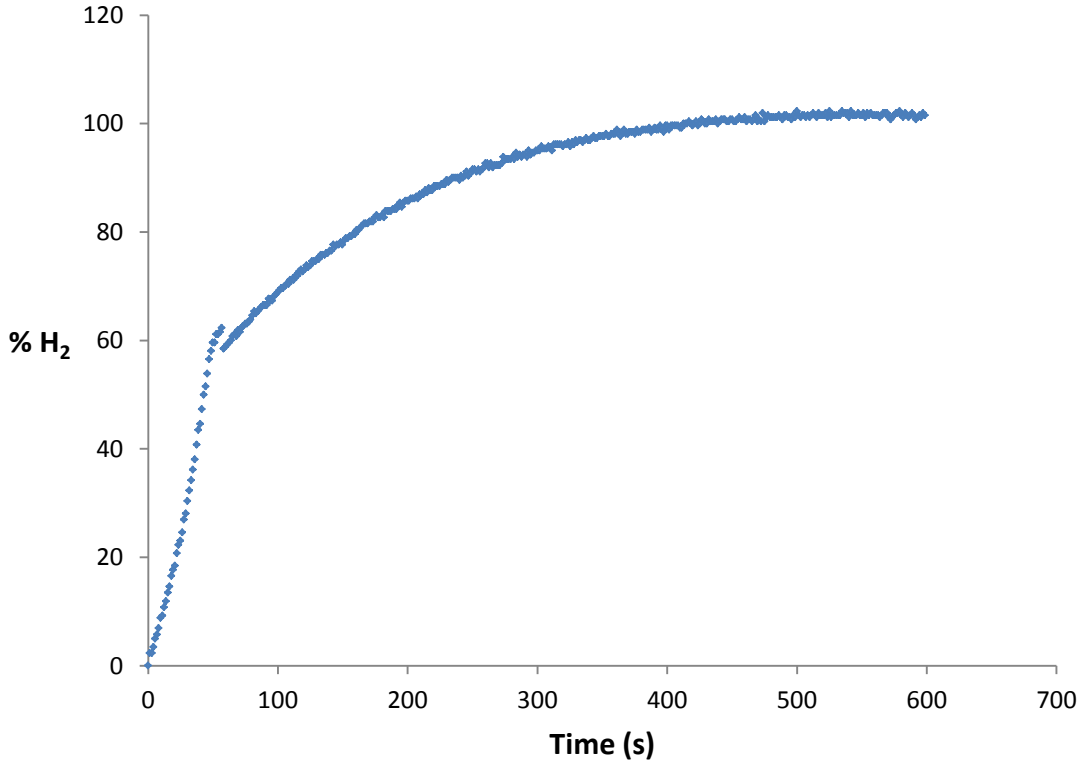

Figure S110. Monitoring of the amount of H_2 released in the catalytic dehydrogenation of $PhSiH_3$ and $NH(CH_2CH_2)_2$ (2 equiv) with 0.2 % of catalyst **1a** leading to $PhSiH[N(CH_2CH_2)_2]_2$ in a closed reaction vessel. During these processes two clearly distinguished regimens for the first and the second dehydrogenation are discernible.

Effect of the amine concentration on the rate of the catalytic dehydrocoupling.

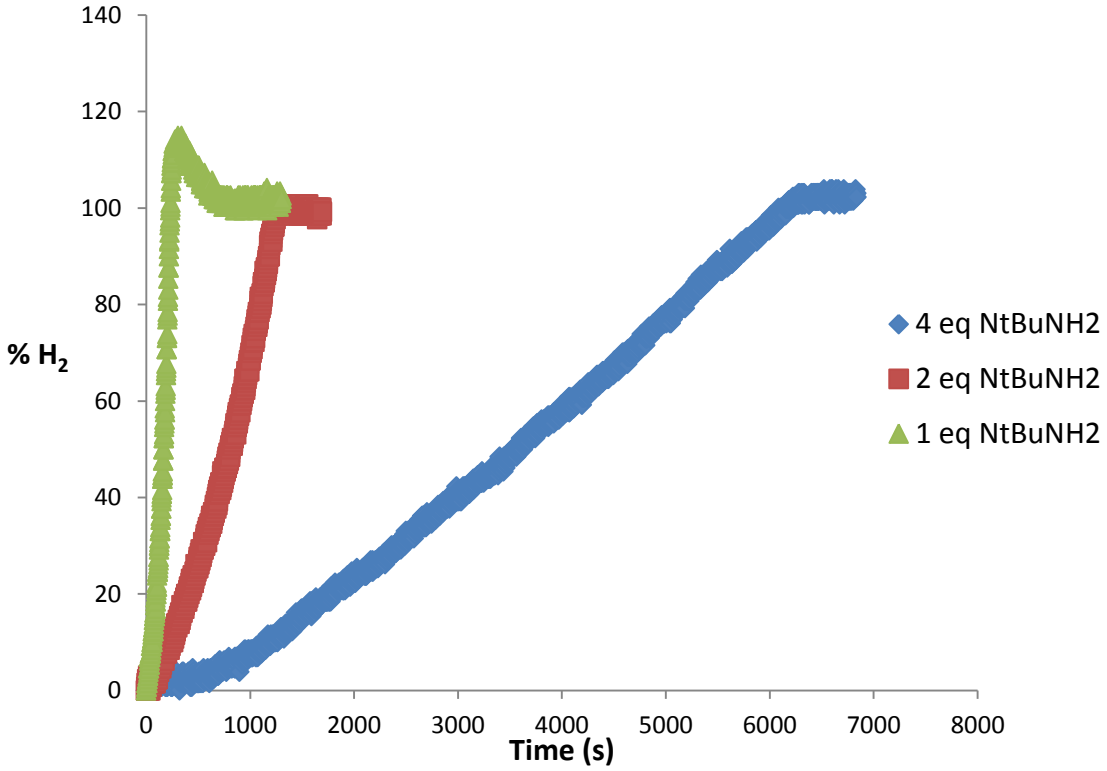

Figure S111. Effect of the concentration of N^tBuH_2 on the rate of H_2 evolution in the reaction of $PhSiH_3$ and N^tBuH_2 with 0.01 % of catalyst **1a**.

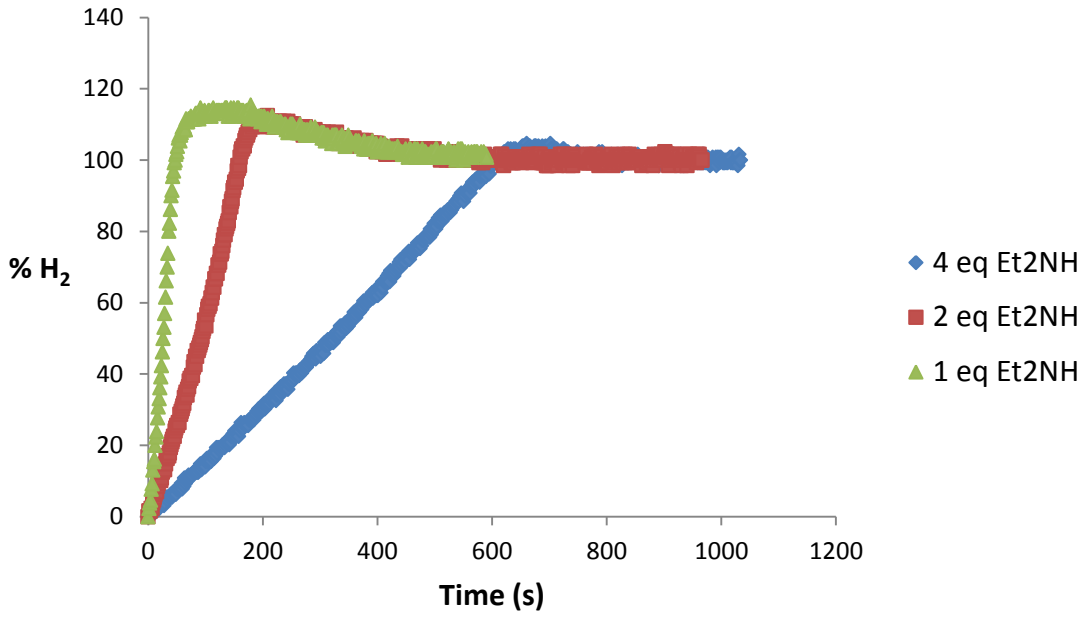

Figure S112. Effect of the concentration of NEt_2H on the rate of H_2 evolution in the reaction of $PhSiH_3$ and NEt_2H with 0.01 % of catalyst **1a**.

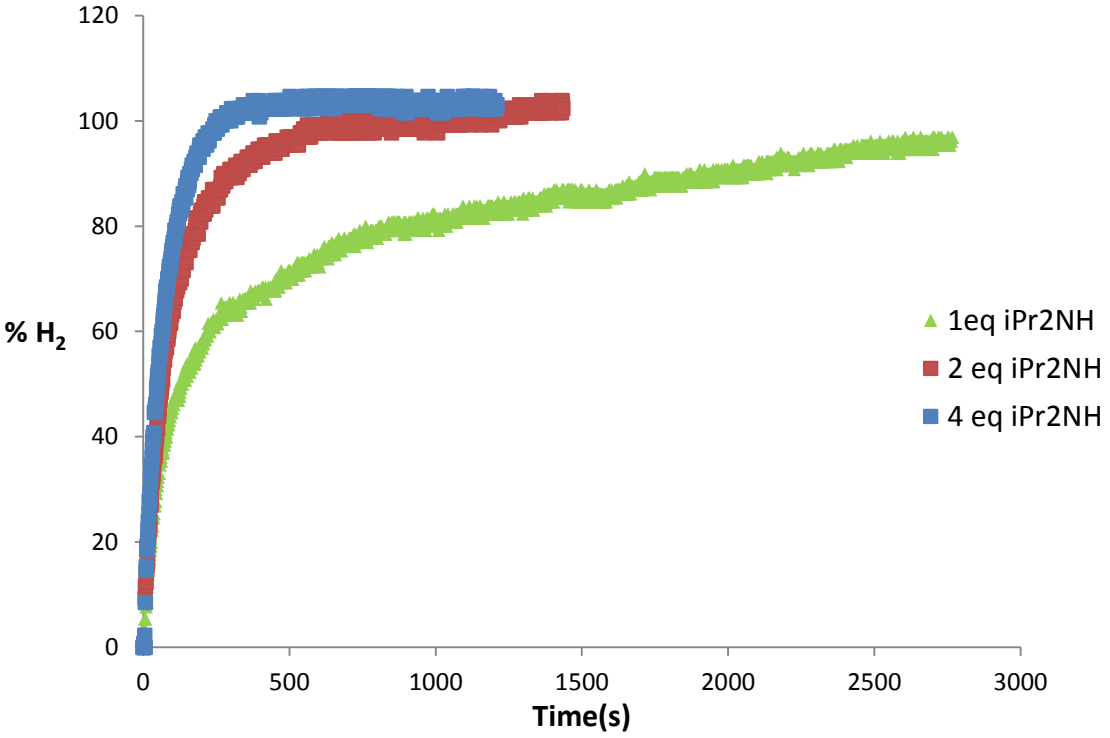

Figure S113. Effect of the concentration of N^iPr_2H on the rate of H_2 evolution in the reaction of $PhSiH_3$ and N^iPr_2H with 0.1 % of catalyst **1a**.

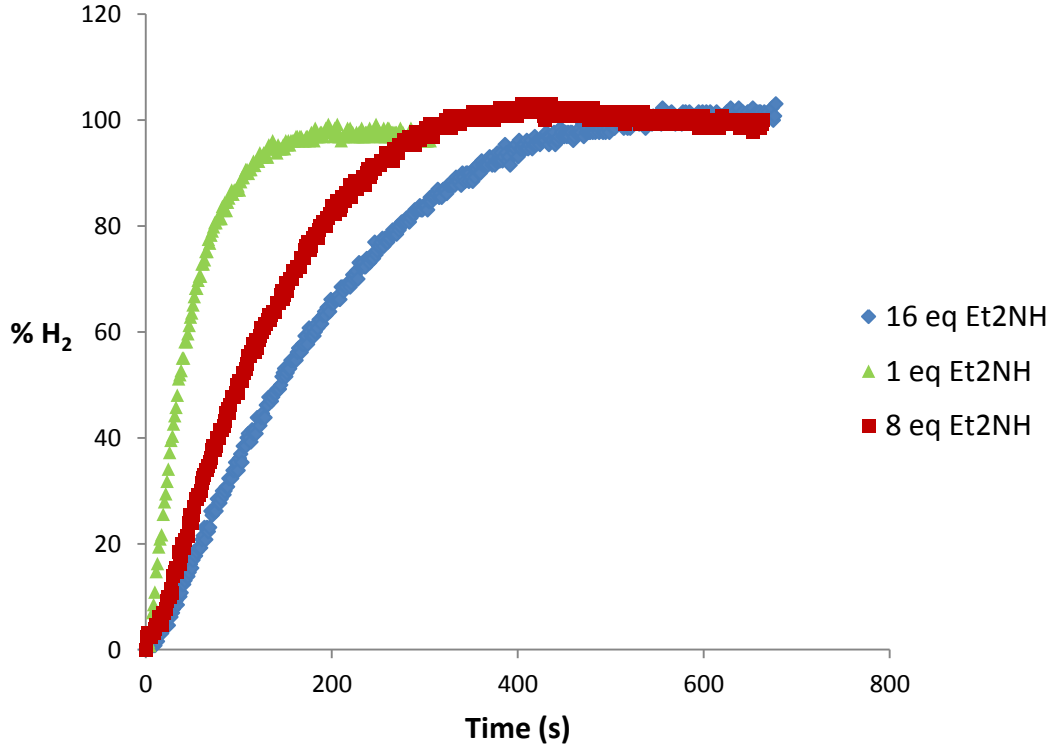

Figure S114. Effect of the concentration of NEt_2NH on the rate of H_2 evolution in the reaction of Ph_2SiH_2 and NEt_2NH with 0.3 % of catalyst **1a**.

6. Computational details

DFT calculations were performed with the Gaussian 09 package.[4] Two levels of theory were used for the calculations: in both cases Pt atoms were represented by the Stuttgart/Dresden Effective Core Potential SDD and the associated basis set as implemented in Gaussian 09,[5] and the remaining H, C, Si and N atoms were represented by means of the 6-31G(d,p) basis set.[6-8] The first level of theory (BS1) uses Truhlar's hybrid meta-GGA functional M06,[9] and in this case the geometries for all species described were optimized in the gas phase without symmetry restrictions. The solvent effects (dichloromethane) were then modelled with the SMD[10] continuum model by single point calculations on gas phase-optimized geometries and free optimizations in solution. The relative free energies in solution were calculated according to: $\Delta G^{solution} = \Delta E^{solution} + (\Delta G^{gas} - \Delta E^{gas})$, where $\Delta E^{solution}$ is the electronic energy plus the solvent entropy.[11] The second level of theory (BS2) uses the hybrid PBE0 functional,[12] with dispersion effects taken into account by adding the D3 version of Grimme's empirical dispersion.[13] In this case all geometries were optimized including dispersion and solvent (dichloromethane, SMD) effects.

Frequency calculations were performed on the optimized structures at the same level of theory (BS1 or BS2) to characterize the stationary points, as well as for obtaining the corresponding Zero-Point corrections and thermal corrections to Enthalpy and Free Energy.

6.1 Interaction energy of 1a with silanes

The bonding and interaction energies between cation **1a**$^+$ and the silanes $PhSiH_3$ and Ph_2SiH_2 have been calculated according to the scheme below[14] using BS1. The bonding interaction is decomposed in two terms: one is the energy involved in the deformation of the fragments from their isolated geometries to their geometries in the σ-complexes and the other is the interaction energy between the fragments with the geometries that they adopt in the adducts.

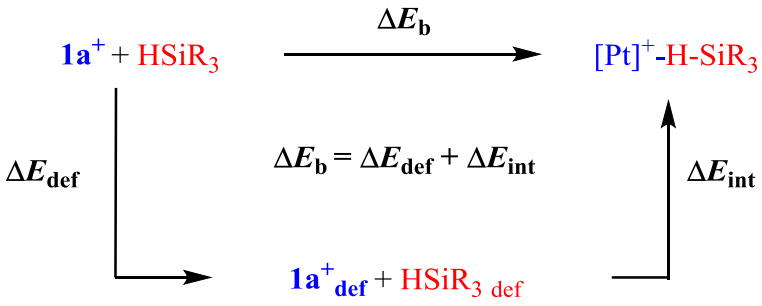

	L= $HSiH_2Ph$	L= $HSiHPh_2$	$\Delta\Delta E$
ΔE_{def} **1a**$^{+}$[a]	4.2	5.3	1.1
ΔE_{def} L ($HSiR_3$)[b]	0.8	1.2	0.4
ΔE_{int}	-18.3	-23.1	4.8
ΔE_b	-7.9	-8.8	0.9

[a] (BS1) kcal·mol^{-1}; [b] The interaction and bonding energies include basis set superposition error (BSSE, Counterpoise method) corrections. The bonding energies in parentheses have been corrected for solvation (dichloromethane) effects according to $\Delta E_b^{DCM} = \Delta E_b + \Sigma\Delta E_{solvation}$.

The interaction energy of the organometallic cation with Ph_2SiH_2 is larger than with $PhSiH_3$ by 4.8 kcal·mol^{-1} (Figure S114). This is partially offset by a higher energy needed to deform the silane and organometallic fragment in this case, resulting in a calculated bonding energy difference (including solvation effects) of 0.9 kcal·mol^{-1} between the two silane complexes, still in favour of the Ph_2SiH_2 adduct.

Calculations using the BS2 level of theory (PBE0-D3 + SDD) yield interaction energies (BSSE-corrected) ΔE_{int} = -19.97 and -25.86 kcal·mol^{-1} for **1a^{+}·H-SiH$_2$Ph** and **1a^{+}·HSiHPh$_2$** respectively, with their interaction energy difference being 5.9 kcal·mol^{-1} in favour of the Ph_2SiH_2 complex.

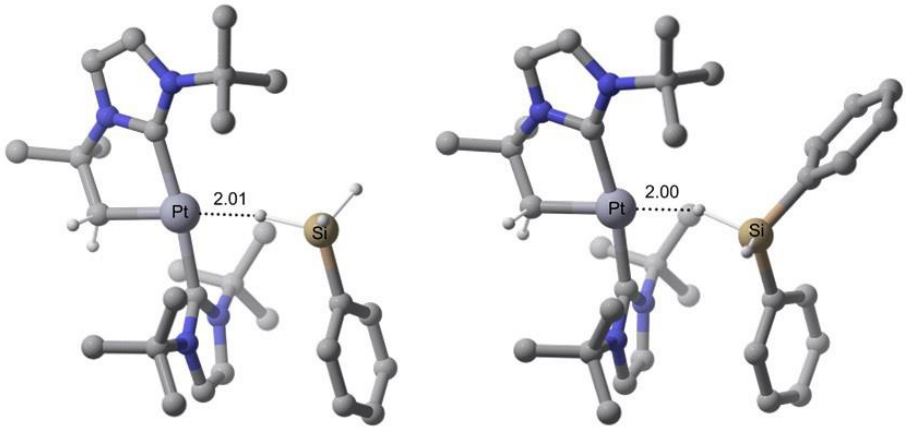

1a^{+}···H-SiH_2Ph **1a**$^{+}$···H-$SiHPh_2$

Figure S115. DFT-optimized (BS1) geometries of two silane adducts of **1a**$^{+}$ (most H atoms have been omitted for clarity).

6.2 Tables of the optimized geometries (Cartesian coordinates, in Angstroms) for the calculated species

Gas phase Energies (in Hartrees) in parenthesis:

BS1

$PhSiH_3$ E = -522.722193605

Si	-2.338970000	0.000019000	0.004673000
H	-2.837095000	-1.211864000	-0.695994000
H	-2.836308000	1.220352000	-0.681732000
H	-2.883764000	-0.008348000	1.387729000
C	-0.465979000	0.000069000	-0.007841000
C	0.254628000	-1.201029000	-0.007495000
C	0.254691000	1.201056000	-0.007507000
C	1.645211000	-1.204402000	0.002898000
H	-0.279194000	-2.151773000	-0.021646000
C	1.645340000	1.204314000	0.002904000
H	-0.279053000	2.151828000	-0.021590000
C	2.342186000	-0.000046000	0.008990000
H	2.187246000	-2.147608000	0.001314000
H	2.187399000	2.147504000	0.001323000
H	3.429878000	-0.000125000	0.013484000

Ph_2SiH_2 E= -753.599149990

Si	-0.040164000000	-1.465246000000	-0.593189000000
H	-0.139094000000	-2.717930000000	0.203974000000
H	0.008254000000	-1.801516000000	-2.042632000000
C	-1.547594000000	-0.417724000000	-0.206466000000
C	-2.705477000000	-0.988769000000	0.335432000000
C	-1.551146000000	0.958620000000	-0.468971000000
C	-3.832461000000	-0.215830000000	0.597694000000
H	-2.726815000000	-2.055257000000	0.561638000000
C	-2.674504000000	1.735994000000	-0.210463000000
H	-0.656655000000	1.433211000000	-0.875351000000
C	-3.817886000000	1.147716000000	0.322686000000
H	-4.722389000000	-0.677145000000	1.020780000000
H	-2.657953000000	2.803236000000	-0.420900000000
H	-4.696888000000	1.754318000000	0.529787000000
C	1.537722000000	-0.550132000000	-0.169761000000
C	2.249015000000	0.153203000000	-1.150154000000
C	2.016846000000	-0.514805000000	1.146236000000
C	3.396779000000	0.871689000000	-0.828804000000
H	1.903126000000	0.135045000000	-2.184599000000
C	3.164944000000	0.197808000000	1.473245000000
H	1.484790000000	-1.056627000000	1.929201000000
C	3.855596000000	0.892800000000	0.484166000000
H	3.936438000000	1.411025000000	-1.604373000000
H	3.524061000000	0.210956000000	2.500060000000
H	4.754416000000	1.450711000000	0.738031000000

Cation 1a E = -1199.28680100

C	2.022763000000	0.040261000000	-0.082399000000
C	4.143575000000	-0.580908000000	-0.530594000000
C	4.197326000000	0.597484000000	0.125347000000
C	2.328057000000	-2.119110000000	-1.426499000000
C	1.538615000000	-3.032767000000	-0.499663000000
H	0.619879000000	-2.544360000000	-0.162451000000
C	1.475576000000	-1.646284000000	-2.599850000000
C	3.526528000000	-2.887747000000	-1.970858000000
C	2.535408000000	2.307146000000	0.996817000000
C	3.808003000000	3.047299000000	1.391401000000
C	1.792241000000	3.123005000000	-0.055090000000
C	1.683097000000	2.105363000000	2.242704000000
C	-2.083843000000	0.013217000000	0.195517000000
C	-3.988228000000	-0.669169000000	1.170050000000
C	-4.317611000000	0.110813000000	0.111019000000
C	-3.048612000000	1.278396000000	-1.767961000000
C	-1.662859000000	1.895405000000	-1.916268000000
C	-4.088165000000	2.393173000000	-1.763262000000
C	-3.310902000000	0.288331000000	-2.897845000000
C	-1.696532000000	-1.521034000000	2.033184000000
C	-0.298349000000	-0.898852000000	1.846863000000
H	0.484580000000	-1.657735000000	1.962639000000
H	-0.135938000000	-0.107835000000	2.590301000000
C	-1.757776000000	-2.958619000000	1.529610000000
C	-2.103704000000	-1.449139000000	3.498437000000
N	2.896569000000	0.977036000000	0.393981000000
N	2.809484000000	-0.915941000000	-0.661615000000
N	-2.609366000000	-0.705356000000	1.209726000000
N	-3.132887000000	0.536084000000	-0.478625000000
Pt	-0.078977000000	0.056367000000	0.037129000000
H	5.058098000000	1.177258000000	0.415453000000
H	4.951563000000	-1.188531000000	-0.903294000000
H	-4.613971000000	-1.177021000000	1.890190000000
H	-5.288699000000	0.405316000000	-0.258458000000
H	3.520597000000	4.005424000000	1.835315000000
H	4.387737000000	2.499568000000	2.143451000000
H	4.447150000000	3.269266000000	0.529457000000
H	4.177482000000	-3.259072000000	-1.170965000000
H	3.152761000000	-3.759659000000	-2.516608000000
H	4.119460000000	-2.292429000000	-2.674524000000
H	2.040641000000	-0.959166000000	-3.240552000000
H	1.173052000000	-2.509672000000	-3.203564000000
H	0.563280000000	-1.141829000000	-2.253167000000
H	2.137262000000	-3.314942000000	0.375325000000
H	1.263771000000	-3.947589000000	-1.036952000000
H	-0.871768000000	1.125639000000	-2.002566000000
H	-1.626757000000	2.471500000000	-2.847897000000
H	-1.432129000000	2.571622000000	-1.085238000000
H	-2.562075000000	-0.513688000000	-2.892747000000
H	-4.303147000000	-0.167439000000	-2.803318000000
H	-3.264318000000	0.799524000000	-3.865996000000
H	-3.942863000000	3.066600000000	-0.911126000000
H	-3.997445000000	2.978691000000	-2.684159000000
H	-5.111600000000	2.004315000000	-1.731526000000
H	-1.360585000000	-1.972077000000	4.110740000000
H	-2.164968000000	-0.410432000000	3.841531000000
H	-3.070651000000	-1.935797000000	3.675399000000
H	-1.067194000000	-3.588930000000	2.102018000000
H	-2.767242000000	-3.369870000000	1.649029000000
H	-1.489450000000	-3.017683000000	0.468713000000
H	1.561250000000	3.065626000000	2.756264000000
H	0.687318000000	1.732598000000	1.985496000000
H	2.161681000000	1.402497000000	2.935460000000
H	2.405710000000	3.253749000000	-0.954229000000
H	0.850855000000	2.635459000000	-0.338617000000

H	1.552614000000	4.114128000000	0.346888000000

Cation 1a-$HSiH_2Ph$ E = -1722.03551080

C	-1.226456000000	0.972931000000	0.278715000000
C	-3.252997000000	1.833861000000	-0.210486000000
C	-3.241526000000	1.554210000000	1.106742000000
C	-1.643150000000	1.726086000000	-2.154792000000
C	-0.771511000000	2.974568000000	-2.188403000000
H	0.159526000000	2.813859000000	-1.638032000000
C	-0.922049000000	0.530673000000	-2.766901000000
C	-2.908192000000	1.970426000000	-2.973481000000
C	-1.607610000000	0.692190000000	2.820741000000
C	-2.868933000000	0.441992000000	3.646480000000
C	-0.749221000000	-0.564330000000	2.888246000000
C	-0.864343000000	1.895725000000	3.389074000000
C	2.729090000000	-0.263722000000	-0.059073000000
C	4.875269000000	0.424401000000	-0.209904000000
C	4.873296000000	-0.928776000000	-0.224906000000
C	3.109717000000	-2.772918000000	-0.126255000000
C	2.259514000000	-3.016763000000	1.115814000000
C	4.321366000000	-3.693355000000	-0.072286000000
C	2.347584000000	-3.026767000000	-1.422772000000
C	2.995640000000	2.169303000000	-0.091821000000
C	1.627486000000	2.021126000000	0.576642000000
H	0.982641000000	2.876705000000	0.339709000000
H	1.766287000000	1.984184000000	1.667087000000
C	2.908074000000	2.658290000000	-1.532481000000
C	3.883371000000	3.097367000000	0.728603000000
N	-2.001913000000	1.017106000000	1.404853000000
N	-2.021399000000	1.462809000000	-0.720825000000
N	3.558730000000	0.807340000000	-0.095819000000
N	3.553495000000	-1.345533000000	-0.124573000000
Pt	0.723610000000	0.233937000000	0.098076000000
H	-4.024836000000	1.681740000000	1.835447000000
H	-4.052065000000	2.232066000000	-0.813463000000
H	5.694059000000	1.127137000000	-0.261295000000
H	5.701844000000	-1.615409000000	-0.288766000000
H	-2.568945000000	0.099234000000	4.641628000000
H	-3.466470000000	1.347666000000	3.794161000000
H	-3.500711000000	-0.334308000000	3.197645000000
H	-3.413500000000	2.904065000000	-2.703061000000
H	-2.622964000000	2.058980000000	-4.026451000000
H	-3.616537000000	1.137433000000	-2.886619000000
H	-1.559707000000	-0.362057000000	-2.743814000000
H	-0.698488000000	0.755917000000	-3.815984000000
H	0.025739000000	0.308271000000	-2.260900000000
H	-1.300441000000	3.827121000000	-1.745452000000
H	-0.519454000000	3.228348000000	-3.224839000000
H	1.396117000000	-2.345425000000	1.160954000000
H	1.896421000000	-4.051196000000	1.118267000000
H	2.855999000000	-2.860612000000	2.022289000000
H	1.530627000000	-2.309867000000	-1.556525000000
H	3.018537000000	-2.931598000000	-2.284543000000
H	1.932185000000	-4.041963000000	-1.425502000000
H	4.923158000000	-3.525624000000	0.828366000000
H	3.965613000000	-4.728400000000	-0.044125000000
H	4.959273000000	-3.593979000000	-0.957856000000
H	3.391378000000	4.071038000000	0.831671000000
H	4.058175000000	2.692228000000	1.731803000000
H	4.852423000000	3.273393000000	0.245721000000
H	2.489526000000	3.671379000000	-1.563901000000
H	3.904939000000	2.691857000000	-1.988545000000
H	2.276722000000	1.995741000000	-2.135842000000
H	-0.596207000000	1.710044000000	4.435597000000
H	0.053881000000	2.096991000000	2.828812000000
H	-1.494977000000	2.791956000000	3.351873000000
H	-1.248351000000	-1.417032000000	2.409532000000
H	0.231258000000	-0.424180000000	2.418274000000
H	-0.582819000000	-0.818773000000	3.940965000000
H	-0.244745000000	-1.476015000000	-0.339653000000
Si	-1.216741000000	-2.621967000000	-0.594197000000
H	-0.915820000000	-3.608746000000	0.470196000000
H	-0.865595000000	-3.120160000000	-1.944286000000
C	-2.995790000000	-2.077900000000	-0.534936000000
C	-3.689072000000	-2.001731000000	0.681428000000
C	-3.695513000000	-1.784203000000	-1.714391000000
C	-5.025220000000	-1.618651000000	0.723081000000
H	-3.186509000000	-2.269441000000	1.612750000000
C	-5.032907000000	-1.402367000000	-1.677535000000
H	-3.198319000000	-1.876974000000	-2.681140000000
C	-5.696365000000	-1.312702000000	-0.457252000000
H	-5.548805000000	-1.575900000000	1.676052000000
H	-5.562749000000	-1.191007000000	-2.603777000000
H	-6.744260000000	-1.024042000000	-0.428416000000

Cation 1a-$HSiHPh_2$ E = -1952.91934097

C	-1.164372000000	-1.624215000000	-0.014550000000
C	-3.161527000000	-2.411287000000	0.680859000000
C	-3.039408000000	-2.722335000000	-0.622693000000
C	-1.763266000000	-1.356987000000	2.488626000000
C	-0.922270000000	-2.462463000000	3.113820000000
H	0.045775000000	-2.546470000000	2.611154000000
C	-1.076030000000	-0.002487000000	2.602714000000
C	-3.100967000000	-1.251088000000	3.218238000000

C	-1.341283000000	-2.488421000000	-2.457663000000
C	-2.551262000000	-2.630915000000	-3.383713000000
C	-0.484780000000	-1.348451000000	-2.990821000000
C	-0.566531000000	-3.801474000000	-2.446539000000
C	2.756304000000	-0.229077000000	-0.016006000000
C	4.891842000000	-0.807540000000	0.450567000000
C	4.908557000000	0.431027000000	-0.093341000000
C	3.184963000000	2.110763000000	-0.921804000000
C	2.276454000000	1.899403000000	-2.126609000000
C	4.411630000000	2.890882000000	-1.377452000000
C	2.500083000000	2.867161000000	0.208425000000
C	2.993011000000	-2.435415000000	1.020768000000
C	1.660799000000	-2.590483000000	0.287859000000
H	1.003257000000	-3.290410000000	0.819698000000
H	1.856967000000	-2.995833000000	-0.715453000000
C	2.833993000000	-2.272317000000	2.527880000000
C	3.902231000000	-3.619227000000	0.713253000000
N	-1.824169000000	-2.221133000000	-1.055790000000
N	-2.015888000000	-1.730517000000	1.051695000000
N	3.572210000000	-1.194840000000	0.476728000000
N	3.597447000000	0.776810000000	-0.386566000000
Pt	0.746494000000	-0.773533000000	-0.034057000000
H	-3.735546000000	-3.230950000000	-1.269375000000
H	-3.981826000000	-2.601811000000	1.352990000000
H	5.700101000000	-1.432837000000	0.800740000000
H	5.744047000000	1.078561000000	-0.305901000000
H	-2.191269000000	-2.695533000000	-4.415345000000
H	-3.125642000000	-3.544040000000	-3.196741000000
H	-3.224550000000	-1.767344000000	-3.317955000000
H	-3.593655000000	-2.220838000000	3.347165000000
H	-2.914738000000	-0.858339000000	4.222793000000
H	-3.782580000000	-0.561296000000	2.704465000000
H	-1.699401000000	0.774312000000	2.143031000000
H	-0.955803000000	0.237929000000	3.665447000000
H	-0.082536000000	0.010138000000	2.137003000000
H	-1.437804000000	-3.427998000000	3.043533000000
H	-0.743970000000	-2.245870000000	4.173745000000
H	1.411827000000	1.275047000000	-1.884748000000
H	1.912952000000	2.869707000000	-2.486421000000
H	2.825033000000	1.412433000000	-2.941686000000
H	1.646456000000	2.305992000000	0.601585000000
H	3.205369000000	3.037638000000	1.030750000000
H	2.135582000000	3.839134000000	-0.145552000000
H	4.981156000000	2.352685000000	-2.144197000000
H	4.070830000000	3.833165000000	-1.819032000000
H	5.076662000000	3.149375000000	-0.545634000000
H	3.390939000000	-4.546628000000	0.994903000000
H	4.141233000000	-3.669812000000	-0.355055000000
H	4.838607000000	-3.581551000000	1.283338000000
H	2.399775000000	-3.180216000000	2.963614000000
H	3.809794000000	-2.106654000000	3.000736000000
H	2.187708000000	-1.419479000000	2.764748000000
H	-0.243461000000	-4.052897000000	-3.463372000000
H	0.320658000000	-3.736625000000	-1.809802000000
H	-1.196100000000	-4.620033000000	-2.077748000000
H	-1.031041000000	-0.396424000000	-2.976143000000
H	0.450044000000	-1.225250000000	-2.430900000000
H	-0.226422000000	-1.569133000000	-4.032653000000
H	-0.191998000000	0.978376000000	-0.219879000000
Si	-1.205674000000	1.967962000000	-0.817671000000
H	-0.979683000000	1.938281000000	-2.284083000000
C	-2.952267000000	1.431079000000	-0.438677000000
C	-3.634480000000	0.598270000000	-1.335291000000
C	-3.631390000000	1.863751000000	0.709071000000
C	-4.939045000000	0.186801000000	-1.084863000000
H	-3.140902000000	0.273269000000	-2.252743000000
C	-4.935739000000	1.452712000000	0.966338000000
H	-3.146017000000	2.550686000000	1.403614000000
C	-5.588166000000	0.607221000000	0.071952000000
H	-5.452187000000	-0.457323000000	-1.796581000000
H	-5.450642000000	1.806054000000	1.856875000000
H	-6.610864000000	0.293755000000	0.267594000000
C	-0.773018000000	3.636832000000	-0.116888000000
C	-0.637332000000	3.852552000000	1.262566000000
C	-0.569192000000	4.718069000000	-0.984137000000
C	-0.312392000000	5.109249000000	1.759153000000
H	-0.765657000000	3.023905000000	1.962276000000
C	-0.241902000000	5.977765000000	-0.490125000000
H	-0.665777000000	4.576756000000	-2.061063000000
C	-0.113609000000	6.172617000000	0.881361000000
H	-0.210117000000	5.261461000000	2.830915000000
H	-0.088958000000	6.807340000000	-1.176056000000
H	0.142269000000	7.155601000000	1.269128000000

BS2

Cation 1a-$HSiH_2Ph$ E = -1721.51017978

C	-1.203247000	1.001298000	0.309807000
C	-3.165273000	2.030970000	-0.097386000
C	-3.259805000	1.445675000	1.114579000
C	-1.415108000	2.335948000	-1.877110000
C	-0.529805000	3.531116000	-1.535881000
H	0.353877000	3.205692000	-0.988652000
C	-0.643580000	1.306410000	-2.695533000
C	-2.606917000	2.808885000	-2.711447000
C	-1.765991000	0.165091000	2.677159000
C	-3.082960000	-0.165680000	3.382731000
C	-0.988642000	-1.134464000	2.501852000

C	-0.972661000	1.164106000	3.516824000
C	2.666006000	-0.330518000	-0.011227000
C	4.844720000	0.249334000	0.103368000
C	4.781918000	-1.082691000	-0.142253000
C	2.950299000	-2.807773000	-0.475770000
C	2.009150000	-3.220590000	0.655461000
C	4.121027000	-3.786488000	-0.511131000
C	2.274531000	-2.799654000	-1.846057000
C	3.039873000	2.043125000	0.392207000
C	1.630026000	1.842758000	0.960949000
H	1.045032000	2.761061000	0.865756000
H	1.718206000	1.605933000	2.028597000
C	3.040999000	2.760356000	-0.956376000
C	3.917053000	2.788546000	1.394133000
N	-2.060615000	0.808575000	1.355968000
N	-1.908971000	1.747674000	-0.591196000
N	3.545466000	0.679757000	0.188155000
N	3.444541000	-1.430387000	-0.204615000
Pt	0.699853000	0.231936000	0.107965000
H	-4.092117000	1.422940000	1.795729000
H	-3.902604000	2.597525000	-0.638372000
H	5.694061000	0.902716000	0.225886000
H	5.579152000	-1.795220000	-0.269534000
H	-2.849174000	-0.732828000	4.287520000
H	-3.629376000	0.728156000	3.696159000
H	-3.731922000	-0.783481000	2.754197000
H	-3.123147000	3.662549000	-2.262777000
H	-2.229759000	3.134910000	-3.684290000
H	-3.328177000	2.003395000	-2.883528000
H	-1.285968000	0.472405000	-2.990115000
H	-0.273704000	1.787671000	-3.605983000
H	0.216567000	0.913498000	-2.138664000
H	-1.077722000	4.255626000	-0.924672000
H	-0.203685000	4.028468000	-2.454439000
H	1.170844000	-2.531614000	0.765717000
H	1.614452000	-4.221615000	0.459168000
H	2.555070000	-3.244869000	1.604527000
H	1.504279000	-2.028363000	-1.901845000
H	3.010180000	-2.585709000	-2.628307000
H	1.824272000	-3.774572000	-2.053553000
H	4.667305000	-3.806158000	0.436982000
H	3.718433000	-4.787931000	-0.685947000
H	4.818322000	-3.565374000	-1.324472000
H	3.458857000	3.756829000	1.616215000
H	4.009373000	2.227516000	2.329267000
H	4.919119000	2.979502000	0.996027000
H	2.666503000	3.782052000	-0.842045000
H	4.057086000	2.812677000	-1.361187000
H	2.405793000	2.231063000	-1.672728000
H	-0.794540000	0.752191000	4.514896000
H	-0.007843000	1.379208000	3.054545000
H	-1.526077000	2.102618000	3.624322000
H	-1.548605000	-1.846218000	1.890187000
H	-0.010748000	-0.959554000	2.038153000
H	-0.825919000	-1.580459000	3.487783000
H	-0.185555000	-1.312525000	-0.536083000
Si	-1.142723000	-2.226231000	-1.318532000
H	-0.715956000	-3.584667000	-0.902485000
H	-0.864569000	-1.970477000	-2.751295000
C	-2.930141000	-1.931226000	-0.891643000
C	-3.527759000	-2.624870000	0.173698000
C	-3.722131000	-1.050570000	-1.644780000
C	-4.868460000	-2.423918000	0.492392000
H	-2.945483000	-3.334182000	0.757996000
C	-5.063206000	-0.850184000	-1.327971000
H	-3.294555000	-0.519216000	-2.490968000
C	-5.635461000	-1.531334000	-0.255454000
H	-5.316157000	-2.968304000	1.319284000
H	-5.661648000	-0.163181000	-1.919975000
H	-6.681834000	-1.374730000	-0.007834000

Cation 1a-$HSiHPh_2$ E = -1952.32012674

C	-0.998012000000	-1.686200000000	-0.041510000000
C	-2.919526000000	-2.679858000000	0.588990000000
C	-2.734714000000	-2.953245000000	-0.718533000000
C	-1.693849000000	-1.518994000000	2.437658000000
C	-0.830440000000	-2.589731000000	3.100127000000
H	0.169910000000	-2.599206000000	2.666716000000
C	-1.060934000000	-0.141552000000	2.587873000000
C	-3.069428000000	-1.477117000000	3.108249000000
C	-1.012303000000	-2.524653000000	-2.485869000000
C	-2.161640000000	-2.826566000000	-3.451514000000
C	-0.301201000000	-1.274205000000	-2.988691000000
C	-0.054936000000	-3.714038000000	-2.448327000000
C	2.741733000000	0.002860000000	0.011961000000
C	4.897091000000	-0.377055000000	0.572657000000
C	4.845851000000	0.791890000000	-0.111928000000
C	3.048617000000	2.228999000000	-1.170335000000
C	2.172742000000	1.802857000000	-2.345383000000
C	4.235954000000	3.020486000000	-1.712896000000
C	2.293369000000	3.081449000000	-0.155784000000
C	3.097091000000	-2.067021000000	1.247836000000
C	1.836277000000	-2.392564000000	0.439825000000
H	1.214935000000	-3.117162000000	0.972875000000
H	2.146226000000	-2.843146000000	-0.511241000000
C	2.806120000000	-1.781938000000	2.719724000000
C	4.121237000000	-3.190595000000	1.116628000000
N	-1.565466000000	-2.331953000000	-1.105565000000

N	-1.861624000000	-1.894025000000	0.996551000000
N	3.607748000000	-0.839427000000	0.625832000000
N	3.525282000000	1.012510000000	-0.458047000000
Pt	0.802928000000	-0.685985000000	-0.023851000000
H	-3.356822000000	-3.517052000000	-1.391382000000
H	-3.729588000000	-2.964785000000	1.237085000000
H	5.733390000000	-0.904393000000	1.003712000000
H	5.642078000000	1.464955000000	-0.379937000000
H	-1.756940000000	-2.839195000000	-4.466899000000
H	-2.617856000000	-3.804818000000	-3.277256000000
H	-2.937402000000	-2.056058000000	-3.406056000000
H	-3.517539000000	-2.468400000000	3.217163000000
H	-2.944680000000	-1.069791000000	4.115096000000
H	-3.759397000000	-0.828469000000	2.560106000000
H	-1.697341000000	0.625524000000	2.140814000000
H	-0.954299000000	0.077735000000	3.654515000000
H	-0.069537000000	-0.097846000000	2.122210000000
H	-1.278610000000	-3.580613000000	2.973532000000
H	-0.741026000000	-2.384982000000	4.171541000000
H	1.338418000000	1.179354000000	-2.023261000000
H	1.772679000000	2.690961000000	-2.843393000000
H	2.761407000000	1.232153000000	-3.071350000000
H	1.475510000000	2.517064000000	0.292355000000
H	2.967523000000	3.400064000000	0.646180000000
H	1.878593000000	3.972403000000	-0.634925000000
H	4.846661000000	2.421683000000	-2.396018000000
H	3.843056000000	3.873699000000	-2.272646000000
H	4.871183000000	3.416421000000	-0.914936000000
H	3.670639000000	-4.123787000000	1.467176000000
H	4.427029000000	-3.325006000000	0.074372000000
H	5.012069000000	-3.002972000000	1.725333000000
H	2.445537000000	-2.688091000000	3.215532000000
H	3.715773000000	-1.451792000000	3.232224000000
H	2.045762000000	-1.001548000000	2.816343000000
H	0.313553000000	-3.925108000000	-3.456883000000
H	0.801393000000	-3.505500000000	-1.805461000000
H	-0.564501000000	-4.607544000000	-2.073456000000
H	-0.981541000000	-0.419765000000	-3.032921000000
H	0.554373000000	-1.012185000000	-2.355169000000
H	0.068904000000	-1.467829000000	-3.999991000000
H	-0.185710000000	0.931909000000	-0.176729000000
Si	-1.305643000000	1.817412000000	-0.782453000000
H	-1.045209000000	1.872967000000	-2.241239000000
C	-3.019599000000	1.143180000000	-0.470301000000
C	-3.641341000000	0.304479000000	-1.407733000000
C	-3.754547000000	1.540238000000	0.658644000000
C	-4.944519000000	-0.145951000000	-1.210542000000
H	-3.110909000000	0.002768000000	-2.306880000000
C	-5.056972000000	1.089724000000	0.858696000000
H	-3.312390000000	2.218328000000	1.384868000000
C	-5.651741000000	0.241153000000	-0.074207000000
H	-5.408599000000	-0.796994000000	-1.946470000000
H	-5.610151000000	1.407561000000	1.738280000000
H	-6.669162000000	-0.108402000000	0.078925000000
C	-1.069344000000	3.496131000000	-0.002745000000
C	-0.838452000000	3.651242000000	1.373320000000
C	-1.135153000000	4.643833000000	-0.806638000000
C	-0.679811000000	4.917769000000	1.928955000000
H	-0.767137000000	2.777276000000	2.017349000000
C	-0.976608000000	5.912195000000	-0.251009000000
H	-1.305817000000	4.551355000000	-1.877298000000
C	-0.747715000000	6.049317000000	1.116517000000
H	-0.498239000000	5.022770000000	2.995199000000
H	-1.027388000000	6.792187000000	-0.886465000000
H	-0.619509000000	7.037569000000	1.549809000000

7. References

[1] Rivada-Wheelaghan, O.; Donnadieu, B.; Maya, C.; Conejero, S. *Chem. Eur. J.* **2010**, *16*, 10323−10326.

[2] Rivada-Wheelaghan, O.; Roselló-Merino, M.; Ortuño. M. A.; Vidossich, P.; Gutiérrez-Puebla, E.; Lledós, A.; Conejero, S. *Inorg. Chem.* **2014**, *53*, 4527−4268.

[3] www.manonthemoontech.com

[4] Gaussian 09, Revision D. 01, Frisch, M. J.; Trucks, G. W.; Schlegel, H. B.; Scuseria, G. E.; Robb, M. A.; Cheeseman, J. R.; Scalmani, G.; Barone, V.; Mennucci, B.; Petersson, G. A.; Nakatsuji, H.; Caricato, M.; Li, X.; Hratchian, H. P.; Izmaylov, A. F.; Bloino, J.; Zheng, G.; Sonnenberg, J. L.; Hada, M.; Ehara, M.;

Toyota, K.; Fukuda, R.; Hasegawa, J.; Ishida, M.; Nakajima, T.; Honda, Y.; Kitao, O.; Nakai, H.; Vreven, T.; Montgomery Jr., J. A.; Peralta, J. E.; Ogliaro, F.; Bearpark, M.; Heyd, J. J.; Brothers, E.; Kudin, K. N.; Staroverov, V. N.; Keith, T.; Kobayashi, R.; Normand, J.; Raghavachari, K.; Rendell, A.; Burant, J. C.; Iyengar, S. S.; Tomasi, J.; Cossi, M.; Rega, N.; Millam, J. M.; Klene, M.; Knox, J. E.; Cross, J. B.; Bakken, V.; Adamo, C.; Jaramillo, J.; Gomperts, R.; Stratmann, R. E.; Yazyev, O.; Austin, A. J.; Cammi, R.; Pomelli, C.; Ochterski, J. W.; Martin, R. L.; Morokuma, K.; Zakrzewski, V. G.; Voth, G. A.; Salvador, P.; Dannenberg, J. J.; Dapprich, S.; Daniels, A. D.; Farkas, O.; Foresman, J. B.; Ortiz, J. V.; Cioslowski, J.; Fox, D. J. In Gaussian, Inc. Wallingford CT, 2013.

[5] Zhao, Y.; Truhlar, D. *Theor. Chem. Acc.* **2008**, *120*, 215−241.

[6] Andrae, D. U. H.; Dolg, M.; Stoll, H.; Preul, H. *Theor. Chim. Acc.* **1990**, *77*, 123−141.

[7] Hehre, W. J.; Ditchfield, R.; Pople, J. A. *J. Phys. Chem.* **1972**, *56*, 2257−2261.

[8] Hariharan, P. C.; Pople, J. A. *Theor. Chim. Acta.* **1973**, *28*, 213−222.

[9] Francl, M. M.; Pietro, W. J.; Hehre, W. J.; Binkley, J. S.; Gordon, M. S.; DeFrees, D. J.; Pople, J. A. *J. Chem. Phys.* **1982**, *77*, 3654−3665.

[10] Marenich, A. V.; Cramer, C. J.; Truhlar, D. G. *J. Phys. Chem. B* **2009**, *113*, 6378− 6396.

[11] Braga, A. A. C.; Ujaque, G.; Maseras, F. *Organometallics* **2006**, *25*, 3647−3658.

[12] Adamo, C.; Barone, V. *J. Chem. Phys.* **1999**, *110*, 6158−6170.

[13] Grimme, S.; Antony, J.; Ehrlich, S.; Krieg, H. *J. Chem. Phys.* **2010**, *132*, 154104.

[14] Conejero, S.; López-Serrano, J.; Paneque, M.; Petronilho, A.; Poveda, M. L.; Vattier, F.; Álvarez, E.; Carmona, E. *Chem. Eur. J.* **2012**, *18*, 4644−4664.